

The ability of intermediate-band Strömgen photometry to correctly identify dwarf, subgiant, and giant stars and provide stellar metallicities and surface gravities[★]

A. S. Árnadóttir¹, S. Feltzing¹, and I. Lundström¹

Lund Observatory, Department of Astronomy and Theoretical Physics, Lund University, Box 43, SE-221 00 Lund, Sweden
e-mail: anna, sofia, ingemar, @astro.lu.se

Received 25 October 2009; Accepted 10 Feb 2010

ABSTRACT

Context. Several large scale photometric and spectroscopic surveys are being undertaken to provide a more detailed picture of the Milky Way. Given the necessity of generalisation in the determination of, e.g., stellar parameters when tens and hundred of thousands of stars are considered it remains important to provide independent, detailed studies to verify the methods used in the surveys.

Aims. Our first aim is to critically evaluate available calibrations for deriving $[M/H]$ from Strömgen photometry. Secondly, we develop the standard sequences for dwarf stars to reflect their inherent metallicity dependence. Finally, we test how well metallicities derived from *ugriz* photometry reproduce metallicities derived from the well-tested system of Strömgen photometry.

Methods. We evaluate available metallicity calibrations based on Strömgen *uvby* photometry for dwarf stars using a catalogue of stars with both *uvby* photometry and spectroscopically determined iron abundances ($[Fe/H]$). The catalogue was created for this project. Using this catalogue we also evaluate available calibrations that determine $\log g$. A larger catalogue, in which metallicity is determined directly from *uvby* photometry, is used to trace metallicity-dependent standard sequences for dwarf stars. We also perform comparisons, for both dwarf and giant stars, of metallicities derived from *ugriz* photometry with metallicities derived from Strömgen photometry.

Results. We provide a homogenised catalogue of 451 dwarf stars with $0.3 < (b - y)_0 < 1.0$. All stars in the catalogue have *uvby* photometry and $[Fe/H]$ determined from spectra with high resolution and high signal-to-noise ratios (S/N). Using this catalogue, we test how well various photometric metallicity calibrations reproduce the spectroscopically determined $[Fe/H]$. Using the preferred metallicity calibration for dwarf stars, we derive new standard sequences in the $c_{1,0}$ versus $(b - y)_0$ plane and in the $c_{1,0}$ versus $(v - y)_0$ plane for dwarf stars with $0.40 < (b - y)_0 < 0.95$ and $1.10 < (v - y)_0 < 2.38$.

Conclusions. We recommend the calibrations by Ramírez & Meléndez (2005) for deriving metallicities from Strömgen photometry and find that intermediate band photometry, such as Strömgen photometry, more accurately than broad band photometry reproduces spectroscopically determined $[Fe/H]$. Strömgen photometry is also better at differentiating between dwarf and giant stars. We conclude that additional investigations of the differences between metallicities derived from *ugriz* photometry and intermediate-band photometry, such as Strömgen photometry, are required.

Key words. Stars: abundances, Stars: fundamental parameters (classification, colours, luminosities, metallicities), Stars: late-type

1. Introduction

The photometric system introduced by Bengt Strömgen (Strömgen 1963, 1964) provides a means of reliably estimating stellar parameters for stars with a wide range of spectral classes. For instance, metallicities can be determined for many types of stars. In particular, the system can accurately identify stars at different evolutionary stages (see discussion in, e.g., Strömgen 1963). This makes it possible to determine the distances of stars with no parallax measurements. If reddening is not known, the system must, however, be complemented with $H\beta$ photometry.

The advent of CCD photometry has meant that larger and deeper areas of sky can be scanned to determine the properties of stars in the field and from them infer the properties of the stellar populations in the Milky Way. For broad-band photometry, this approach has been very successful, e.g., Gilmore & Reid (1983), who inferred the existence of the thick disk and, e.g.,

Ibata et al. (2001) and Ferguson et al. (2005), who studied the stellar structures in the Andromeda galaxy. Arguably the most important large study of this kind is the Sloan Digital Sky Survey (SDSS) (York et al. 2000), which provides deep photometry of stars for roughly half the sky.

However, in contrast, the usage of narrow and medium band photometry for Galactic studies was for a much longer time severely hampered by the relative inefficiency of the CCDs, which required too long exposure times to make these techniques competitive. This combined with relatively small fields of view (mainly due to small filters on the cameras equipped with suitable filters) meant that only very small portions of the sky could be usefully studied. Additionally, the size of telescopes that have cameras with Strömgen filters and relatively low efficiency in the blue also hampered observations in the *u* filter (e.g., von Hippel 1992). All of this meant that systems, such as that designed by Strömgen, were mainly applied to the study of globular and open clusters (two fairly recent examples are provided by Grundahl et al. 2002; Twarog et al. 2003) or to individual stars (e.g., Olsen 1994b, 1995; Schuster & Nissen 1989a;

[★] Appendices A and B are only available in electronic form at the <http://www.aanda.org>. The table in Appendix B will be available through CDS.

Schuster et al. 2004, 2006). Recent attempts to use Strömgren photometry to study the properties of the Milky Way stellar disks away from the solar neighbourhood are few. Interesting examples being von Hippel & Bothun (1993) and Jönch-Sørensen (1995).

Advancements in technology have meant that we now also have access to larger CCD areas on telescopes equipped with large *uvby*-filters, enabling an efficient study of stellar properties across larger areas of the sky.

We have published two studies based on Strömgren photometry of the red giant branches of dwarf spheroidal galaxies in the Local Group using the Wide Field Camera (WFC) on the Isaac Newton Telescope on La Palma (Faria et al. 2007; Adén et al. 2009a). This camera is equipped with large filters that allow an, almost, unvignetted field of view of half by half a degree. However, far more can be achieved with this dataset. It provides the largest database of Strömgren photometry for Milky Way disk stars without any kinematic or colour biases. The stars are situated at distances between 0.5 and 4 kpc away from the Sun and in the directions of the four dwarf spheroidal galaxies Draco, Sextans, Hercules, and Ursa Major II. We intend to apply this unique dataset to explore the properties of the Milky Way disk(s) in some detail.

As part of a series of papers on the properties of the Milky Way disks using Strömgren photometry, we have undertaken a critical evaluation of the available calibrations for metallicity and $\log g$ determinations for dwarf and sub-giant stars. We have also determined new standard sequences (compare, e.g., Olsen 1984) to improve the identification of dwarf and giant stars in the distant disk and halo. We also provide a basic comparison of metallicities derived using Strömgren photometry and metallicities derived for dwarf and giant stars from SDSS *ugriz* photometry using the calibration in Ivezić et al. (2008).

The paper is organised as follows. Section 2 provides a short introduction to the Strömgren photometric system and background to the work presented here, Sect. 3 details the catalogues we compile to test the metallicity calibrations available for dwarf stars, which is described in Sect. 4 where we also compare the Strömgren metallicities with those derived by the SDSS project (DR7 Abazajian et al. 2009). Section 5 considers the system's ability to distinguish between giant and dwarf stars of similar colour. We also provide new, metallicity-dependent stellar sequences for dwarf stars in this section. These new sequences are compared to model predictions (e.g., isochrones) in Sect. 6. Section 7 summarises our findings and provides a few suggestions for future work.

2. A short introduction to the Strömgren photometric system

The Strömgren system consists of the four medium-width filters *u*, *v*, *b*, and *y* (hereafter collectively denoted as *uvby*), where the *y* magnitude is calibrated to be the same as the *V* magnitude in the *UBV* system (e.g., Johnson & Morgan 1953, see also Olsen (1984) and Fig. 1). The filters are centred on 350, 410, 470, and 550 nm and their half-widths are 38, 20, 10, and 20 nm, respectively (e.g., Golay 1974, page 180). In addition, the system relies on the three colour indices (differences) that are constructed in the following way (compare, e.g., Strömgren 1963)

$$\begin{aligned} & (b - y) \\ m_1 & \equiv (v - b) - (b - y) \\ c_1 & \equiv (u - v) - (v - b). \end{aligned}$$

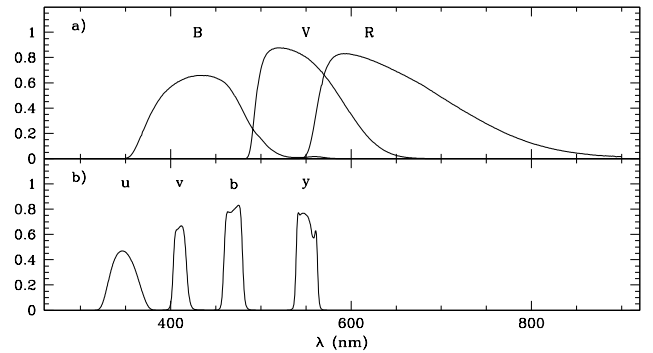


Fig. 1. Filter throughput curves for broad-band and Strömgren filters. Filter curves are from the database of filters used with the wide-field camera on the Isaac Newton Telescope. The database is available at <http://catserver.ing.iac.es/filter/>. **a)** Harris *B*, *V*, and *R* filters, and **b)** Strömgren *u*, *v*, *b*, and *y* filters.

These indices are designed to measure important properties of the stars and were first introduced by Bengt Strömgren in a series of papers, including Strömgren (1963) and Strömgren (1964). Work on the system continued by establishing standard stars (e.g., Crawford & Barnes 1970; Grønbech et al. 1976; Olsen 1983; Perry et al. 1987; Olsen 1993). However, as discussed in Clausen et al. (1997), the establishment of standard fields akin to those available for *UVBRI* photometry (Landolt 1992) have only very recently been attempted. An additional problem is that the primary standards are too bright for most available combinations of cameras with *uvby* filters and telescopes. Although Clausen et al. (1997), Cousins (1987), and Schuster & Nissen (1988) provide secondary fainter standards, the situation for both standard fields and secondary standards that can be used with large telescopes remains unsatisfactory.

There are two main sets of established standard stars for the *uvby* system, those of Bond (1980) and Olsen (1993). There are some non-negligible differences between the two sets and Olsen (1995) provides a detailed discussion of this subject. He concludes that the main difference concerns the c_1 index and is caused mainly by the *u*-filter. Hence, if we wish to compare results based on the two sets of standards we need to apply corrections (compare, e.g., Fig. 15 in Faria et al. 2007). We adopt observations calibrated to the system established by Olsen (1993).

The system was originally designed to study earlier types of stars (A2 to G2, Strömgren 1963). Later work has, however, shown that the system and its properties can be extended to later types of stars. Particularly important extensions of the application of the system have been presented by Bond (1970) (for metal-poor giants), Gustafsson & Ardeberg (1978) (for red horizontal branch stars), Olsen (1984) (for G and K dwarf stars), Schuster & Nissen (1989b) (for metal-poor stars), Anthony-Twarog & Twarog (1994) (for giants), and Twarog et al. (2007) (for G and K dwarf stars). The theoretical foundations of these extension can be found in, e.g., Bell & Gustafsson (1978) and Gustafsson & Bell (1979), and more recently Önehag et al. (2009). Applications to yellow super-giants have also been successful (see, e.g., Arellano Ferro & Mendoza V. 1993).

The colour-index ($b-y$) is relatively unaffected by blanketing effects and can thus be used to measure the stellar temperature (if the reddening is known). Recent examples of colour-temperature calibrations are given for dwarf stars by Alonso et al. (1996),

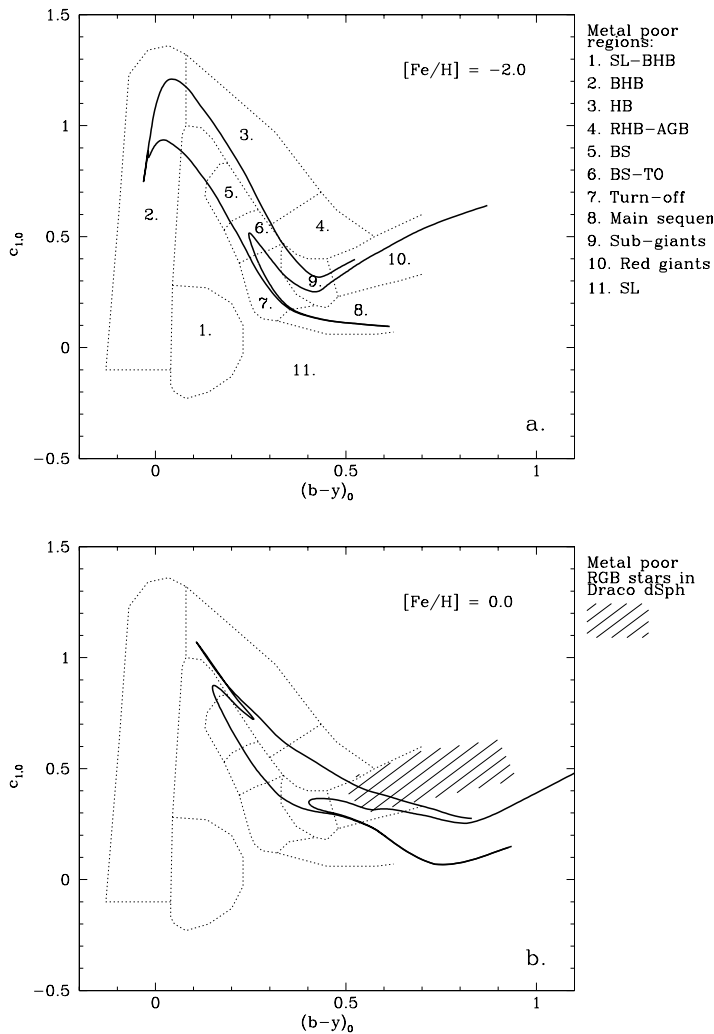


Fig. 2. Illustration of the *uvby* system’s ability to identify stars at different evolutionary stages. The classification scheme by Schuster et al. (2004) is indicated by dotted lines. Evolutionary stages are identified in panel a. as: 1. SL-BHB: sub-luminous – blue horizontal branch transition, 2. BHB: blue horizontal branch, 3. HB: horizontal branch, 4. RHB-AGB: red horizontal branch – asymptotic giant branch transition, 5. BS: blue-straggler stars, 6. BS-TO: blue-straggler – turn-off transition, 7. Turn-off: turn-off stars, 8. main sequence, 9. sub-giants, 10. red giants, and, 11. SL: sub-luminous stars. Two isochrones by Vandenberg et al. (2006) using the temperature-colour transformation by Clem et al. (2004) (age = 1Gyr and 10Gyrs). The metallicities of the isochrones are indicated in the panels. The region occupied by metal-poor red giants in the Draco dwarf spheroidal galaxy (Faria et al. 2007) is indicated by a hashed area in panel b.

and for giant stars by Alonso et al. (1999). Ramírez & Meléndez (2005b) provide calibrations for both giant and dwarf stars.

In contrast, the m_1 index is designed specifically to measure the amount of blanketing in a region around 410 nm (e.g., Crawford 1975) or as originally stated by Strömgren (1963) is “a colour difference that is a measure of the total intensity of the metal lines in the v -band”. It is thus sensitive to the total amount of metals present in the stellar atmosphere. However, it was soon recognised that these metallicity lines in population I

stars are strong enough to depend mainly on microturbulence (ξ_t) and less on metallicity. It was later shown that ξ_t is not a free parameter and hence the dependence still prevails (see, e.g., discussion in Gustafsson & Nissen 1972). Because of the properties of the m_1 index it can be used to derive metallicities for a variety of late-type stars (e.g., F to K and V to III). Recent examples of metallicity calibrations include for giants Hilker (2000) and Calamida et al. (2007), and for dwarf stars Olsen (1984), Schuster & Nissen (1989b), and Holmberg et al. (2007) (see Sect. 4 for a more complete list). The calibrations for giant stars include only linear terms in the different indices and none include c_1 . For dwarf stars, the relations are more complex and less straightforward, including dependencies also, e.g., on the c_1 index and quadratic terms. The reliability of the metallicity calibrations for dwarf stars is one of the main topics of this paper.

Finally, the c_1 index is designed to measure the Balmer discontinuity (Strömgren 1963). For early-type stars, B and A, the c_1 index is a measure of the temperature but for later type stars (F and G stars) it provides a measure of the surface gravity. Hence, for stars with spectral class later than roughly A, already by design this system is able to identify different types of stars in a reliable way. This was, in fact, the main advantage of the system as it was used in early applications. Note that the identification works equally well if the reddening is known or if all stars can be assumed to suffer from the same amount of reddening. For stars with spectral type later than A, it was possible, by measuring $(b-y)$ and c_1 and comparing to standard sequences, to determine an absolute magnitude for the star once it had been classified (e.g., Strömgren 1963). It thus became important to develop standard sequences in the c_1 vs. $(b-y)$ diagram so that stars could be reliably classified according to spectral class and evolutionary stage. We return to the issue of standard sequences for late-type dwarf stars later in this paper.

The ability to classify stars at different evolutionary stages using the *uvby* system has been elaborated upon. For metal-poor stars, Schuster et al. (2004) developed a finely tuned classification scheme to identify main sequence, turn-off, blue stragglers, red giant, horizontal branch and asymptotic branch stars (see Fig. 2). Adén et al. (2009a) used this classification scheme to successfully trace the faint ($V \sim 21.1$) horizontal branch of the Hercules dwarf spheroidal galaxy.

The scheme developed in Schuster et al. (2004) extends only to about $(b-y)_0^1$ of 0.4 for dwarf stars and about 0.6 for giants. However, the ability of the *uvby* system to distinguish different evolutionary stages (for all metallicities) improves as we move to redder colours. A simple illustration of this is given in Fig. 2. In this figure, we reproduce the classification scheme of Schuster et al. (2004) and overlay two sets of isochrones by Vandenberg et al. (2006), which use the temperature-colour transformation by Clem et al. (2004) (but see Faria et al. 2007, for a critical discussion of the reliability of the intermediate metallicity isochrones based on this temperature-colour transformation).

Finally, *uvby* photometry is often complemented with observations in additional filters. In particular, many studies have been

¹ The subscript 0 indicates that the photometry has been dereddened. In the following, we explicitly indicate which photometry has been dereddened and which has not. All metallicity and other calibrations are based on the star’s “true” colours, i.e., the dereddened photometry. However, the separation of dwarf and giant stars with the help of the c_1 index (see, e.g., Fig. 2) is effective using photometry that has not been dereddened as long as both types of stars are represented and all stars are affected by the same amount of reddening. This is, for example, the case for the dwarf spheroidal galaxies.

performed using the β index (e.g., Schuster et al. 1996). For late-type stars, this index provides a temperature estimate that is essentially independent of reddening. However, the two filters included in this index are both narrow or very narrow, hence for large-scale studies of fainter stars observing times become prohibitively long. Here we are therefore not concerned with the β index.

Other studies have also developed systems that use additional information, e.g., Ca II H and K photometry (see, e.g., Anthony-Twarog & Twarog 1998). For the same reasons given for the β index, we do not address these systems but rather consider only *uvby*, where, in terms of observing time, *u* is by far the most expensive filter.

3. Two catalogues

Before testing available metallicity and $\log g$ calibrations and deriving new standard relations we will first detail how we selected the stars used to perform these tasks. Below we describe the construction of two catalogues for dwarf stars, one with *uvby* photometry only and one with both *uvby* photometry and iron abundances determined from high-resolution spectroscopy.

3.1. Reddening

For both catalogues we need to decide whether the photometry for the stars should be dereddened or not and which reddening map to use. We only consider stars that have parallaxes in the Hipparcos catalogue (Perryman et al. 1997; van Leeuwen 2007) and use the same method to deredden the photometry in the two catalogues. In brief, we assume that the dust in the Galactic disk can be modelled as a thin exponential disk with a scale-height of 125 pc (following, e.g., Bonifacio et al. 2000; Beers et al. 2002). Since most of the stars are nearby, they are inside this dust disk. We reduce the extinction accordingly using

$$E(B - V)_{star} = [1 - \exp(-|d \sin b|/h)] \cdot E(B - V)_{LOS}, \quad (1)$$

where $E(B - V)_{LOS}$ is the full colour-excess along the line of sight (LOS) taken from the dust maps by Schlegel et al. (1998), d is the distance (here we use the parallaxes from the new reduction of the Hipparcos catalogue of van Leeuwen 2007), b is the galactic latitude, and h is the scale-height of the thin dust disk (taken to be 125 pc, see above).

Following, for instance, Nordström et al. (2004) we assume that stars with $E(B - V)$ below 0.02 are un-reddened and do not apply any dereddening to the photometry for these stars. We discuss the implications of this in Sect. 4.1.

Several studies have noted that the dust maps of Schlegel et al. (1998) overpredict $E(B - V)$ when $E(B - V) > 0.15$ (see, e.g., Arce & Goodman 1999; Beers et al. 2002; Yasuda et al. 2007). Our catalogues are dominated by nearby stars with low $E(B - V)$. For the spectroscopic catalogue discussed in Sect. 3.3 and used to test the metallicity calibration in Sect. 4.1, only two stars have $E(B - V) > 0.15$. In the photometric catalogue used to trace dwarf-star sequences in Sect. 5, there are 38 of 3645 stars that have $E(B - V) > 0.15$. Since so few stars are affected by a possible overprediction of the reddening we chose not to apply any corrections to the reddening values found from the map by Schlegel et al. (1998).

To deredden the *uvby* photometry we use the relation for $A_\lambda/E(B - V)$ from Table 6 (Col. 8) in Appendix B of Schlegel et al. (1998). For individual magnitudes, this amount

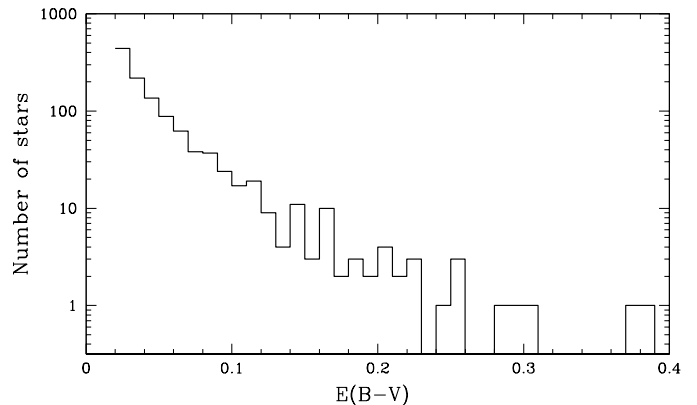


Fig. 3. Distribution of $E(B - V)$ for our photometric catalogue (see Sect. 3.2). There are 2502 stars with $E(B - V) < 0.02$, which are not shown.

to $x_0 = x - E(B - V) \cdot k_x$, where x is any of *uvby* and $k_x = 5.231, 4.552, 4.049$, and 3.277 for *uvby*, respectively, and the subscript 0 corresponds to the dereddened photometry.

3.2. The photometric catalogue

The three studies by Olsen (1993), Olsen (1994a), and Olsen (1994b) represent one of the largest homogeneous catalogues of high quality *uvby* photometry for nearby dwarf stars that also includes spectral classification of the stars. The stars were classified into three main groups: sub-giant stars (or the BAF group), giant stars (or the GKIII group), and dwarf stars (or the GKV group). For our final catalogue, we only include stars classified as dwarf stars by Olsen (the GKV group). Whenever a star has an entry in more than one of the three studies we adopt the most recent set of measurements.

Dereddening was performed as described in Sect 3.1. The majority of the stars in Olsen (1993), Olsen (1994a), and Olsen (1994b) have parallaxes from Hipparcos (ESA 1997; Perryman et al. 1997; van Leeuwen 2007). Stars that have no parallax from Hipparcos were simply discarded from the photometric catalogue. Known binary stars were excluded using the SIMBAD database. The resulting catalogue consists of 3645 dwarf stars. Figure 4 a shows the distribution of the stars in the HR-diagram.

3.3. The spectroscopic catalogue

To test the available metallicity and $\log g$ calibrations for dwarf stars, we need a homogeneous catalogue of stars, which have both *uvby* photometry and spectroscopically determined $[\text{Fe}/\text{H}]^2$ and $\log g$. The $[\text{Fe}/\text{H}]$ should preferably have been derived using parallaxes, but ionisation equilibrium might also be acceptable (compare discussion in Bensby et al. 2005).

Because we place special emphasis on the redder dwarf stars, we started our search by looking in the General Catalogue of Photometric Data (Mermilliod et al. 1997) for stars with ($b -$

² We adopt the usual notation where $[\text{Fe}/\text{H}] \equiv \log(N_{\text{Fe}}/N_{\text{H}})_* - \log(N_{\text{Fe}}/N_{\text{H}})_\odot$ and use $[\text{Fe}/\text{H}]$ exclusively for iron abundances determined from high-resolution spectroscopy. Metallicities determined from photometric calibrations will be either called just that or denoted $[M/\text{H}]$.

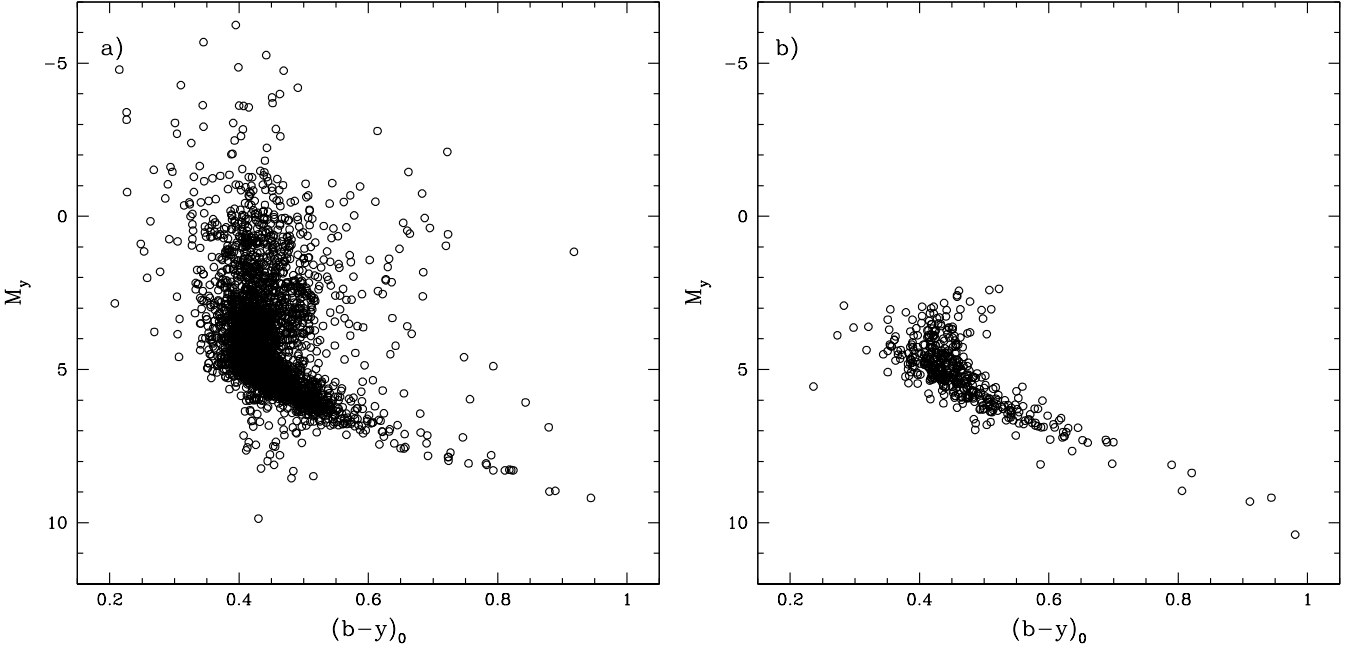


Fig. 4. **a)** HR diagram for the photometric catalogue of dwarf stars (see Sect. 3.2). **b)** HR-diagram for the dwarf stars in the spectroscopic catalogue (see Sect. 3.3).

Table 1. Coefficients for Eq. (2).

Study	Ref.	# of stars	# of stars with ($b - y$) ₀ > 0.6	a	b	c	d	σ
Favata et al. (1997)	2	46	1	1.0608	-0.9662	-0.7918	7.1781	0.07
Feltzing & Gustafsson (1998)	3	23	2	0.7903	-0.8958	-0.1252	3.9841	0.05
Chen et al. (2000)	4	28	1	1.1759	-2.0582	-0.0767	8.2072	0.06
Thorén & Feltzing (2000)	5	12	4	0.9918	0.0163	-0.2020	0.8187	0.08
Santos et al. (2001)	6	61	1	1.0405	-0.9088	-0.0586	3.6431	0.04
Heiter & Luck (2003)	7	75	0	0.8985	0.7027	-0.1373	-2.0303	0.05
Yong & Lambert (2003)	8	6	2	1.1258	2.0980	-0.2534	-6.3255	0.05
Mishenina et al. (2004)	9	93	1	1.1434	-1.8958	-0.0888	7.5583	0.06
Santos et al. (2004)	10	141	1	1.0098	-1.2361	-0.0838	5.0008	0.04
Bonfils et al. (2005)	11	19	0	0.8761	-0.5454	-0.0422	2.2801	0.07
Luck & Heiter (2005)	12	65	6	0.9736	0.7346	-0.0249	-2.6251	0.06
Santos et al. (2005)	13	64	7	1.0495	-1.1400	-0.0204	4.3450	0.04
Woolf & Wallerstein (2005)	14	8	6	1.0192	0.0846	-0.4226	1.5298	0.04
Sousa et al. (2006)	15	57	1	0.9360	-0.9590	-0.0805	3.9268	0.02

Column 1 lists the study that is being moved onto the Valenti & Fischer (2005) system and Col. 2 the reference number used in Table B.1. Column 3 lists the number of stars in common with Valenti & Fischer (2005). These are used to obtain the coefficients. Column 4 lists the number of stars redder than $(b - y)_0 = 0.6$. Columns 5 to 8 list the coefficients used in Eq. (2), and Col. 9 lists the σ for the difference between $[\text{Fe}/\text{H}]$ in the study listed in Col. 1 and the $[\text{Fe}/\text{H}]$ derived once the data have been put on to the Valenti & Fischer (2005) system. The difference is calculated in the sense $[\text{Fe}/\text{H}]_{\text{original}}$ minus $[\text{Fe}/\text{H}]_{\text{corrected}}$.

$y) > 0.6$., and found such stars in four studies: Olsen (1984), Schuster & Nissen (1988), Olsen (1993), and Olsen (1994a).

As discussed above, in both Olsen (1993) and Olsen (1994a) the stars were classified according to their evolutionary stages. In these two papers, we found 97 and 29 dwarfs stars, respectively, that are redder than $(b - y) = 0.6$. Olsen (1984) and Schuster & Nissen (1988) do not provide stellar classifications, we therefore used the c_1 vs. $(b - y)$ diagram, compare Fig. 2, to exclude any obvious giant or early type stars. We found 37 and 27 stars, respectively, in these two papers which are likely dwarf stars with $(b - y) > 0.6$.

In total, we found 190 probable dwarf stars with $(b - y) > 0.6$. Upon further inspection, it was found that 44 entries in this list were duplications. We decided to keep the most recent photometric measurements when more than one set of measurements were available for a given star.

Eleven additional stars were excluded (5 stars were marked as binaries in one of the four papers and 6 stars had been observed to be variables during those observing campaigns). Finally, we used the SIMBAD database to identify any additional binaries, variables, or unclassified stars. In total, 37 additional stars were excluded by this check: 5 because they had no identification at all in SIMBAD, being possible miss-identifications,

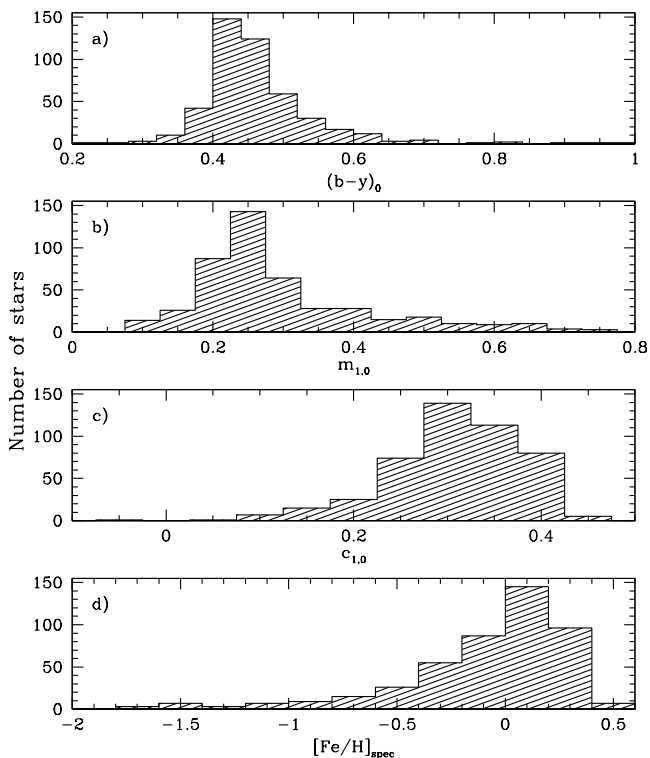


Fig. 5. Histograms showing the distribution of the photometric indices and $[\text{Fe}/\text{H}]$ for the spectroscopic catalogue (Table B.1 and Sect. 3.3). **a)** The number of stars as a function of $(b-y)_0$, **b)** the number of stars as a function of $m_{1,0}$, **c)** the number of stars as a function of $c_{1,0}$, and **d)** the number of stars as a function of $[\text{Fe}/\text{H}]$.

28 stars because they were identified as variable, spectroscopic binaries, carbon stars, T Tauri stars or peculiar; and 4 stars were giants.

For the remaining 98 dwarf stars with $(b-y) > 0.6$, we searched the literature for metallicity determinations using the SIMBAD and VizieR databases (Ochsenbein et al. 2000). Fifty-seven of the stars had no previous metallicity determinations at all. Thirteen stars had only metallicities derived from photometry. We were thus left with 28 stars with $(b-y) > 0.6$ and $[\text{Fe}/\text{H}]$ derived from high-resolution spectroscopy.

The 28 red dwarf stars were found in 15 studies using high-resolution spectroscopy to determine $[\text{Fe}/\text{H}]$: Valenti & Fischer (2005), Favata et al. (1997), Feltzing & Gustafsson (1998), Chen et al. (2000), Thorén & Feltzing (2000), Santos et al. (2001), Heiter & Luck (2003), Yong & Lambert (2003), Santos et al. (2004), Mishenina et al. (2004), Woolf & Wallerstein (2005), Santos et al. (2005), Luck & Heiter (2005), Bonfils et al. (2005), and Sousa et al. (2006).

Several of these 15 studies also include large numbers of dwarf stars bluer than $(b-y) = 0.6$. This is especially true for Valenti & Fischer (2005), which includes $[\text{Fe}/\text{H}]$ for 1040 stars. Our aim is to use this compilation to test available calibrations for, mainly, F- and G-type dwarf stars. We therefore decided that Valenti & Fischer (2005) should be the baseline for our compilation.

Following Twarog et al. (2007), the $[\text{Fe}/\text{H}]$ determined in the 15 spectroscopic studies (referred to as the ‘original studies’ below) were moved onto the system of Valenti & Fischer (2005) in the following way. For each study, we took all stars (i.e., in-

cluding stars with $(b-y) < 0.6$) in common between the study and Valenti & Fischer (2005) and performed a least squares fit to determine the coefficients of the equation that transforms $[\text{Fe}/\text{H}]$ onto the metallicity-scale by Valenti & Fischer (2005) given by

$$[\text{Fe}/\text{H}]_{\text{VF05}} = a[\text{Fe}/\text{H}] + b \log T_{\text{eff}} + c \log g + d, \quad (2)$$

where $[\text{Fe}/\text{H}]$ is the iron abundance, T_{eff} is the effective temperature, and $\log g$ is the surface gravity derived in the original study, that is being moved onto the metallicity-scale by Valenti & Fischer (2005). $[\text{Fe}/\text{H}]_{\text{VF05}}$ is the $[\text{Fe}/\text{H}]$ derived in Valenti & Fischer (2005). The coefficients, a , b , c , and d , together with the number of stars in common between Valenti & Fischer (2005) and the original study are listed in Table 1.

These transformations were then used to move all entries in the 15 studies onto the common metallicity scale. We then used the General Catalogue of Photometric Data (Mermilliod et al. 1997) to find $uvby$ photometry for these stars from the catalogues by Olsen and Schuster and collaborators. In total, 451 stars had $[\text{Fe}/\text{H}]$ derived from high-resolution spectroscopy and $uvby$ photometry. As before, if a star had more than one set of $uvby$ measurements the most recent was kept. The spectroscopic catalogue can be found in Table B.1.

Also for this catalogue we dereddened the photometry as described in Sect. 3.1. We recall that, the photometry for stars with $E(B-V) < 0.02$ were not corrected. The implications of this are discussed in Sect. 4.1. Fifty stars in the catalogue have $E(B-V) > 0.02$. The stellar distances are based on the re-analysed Hipparcos parallaxes (van Leeuwen 2007). Five stars HD 23261, HD 69582, HD 180890, HD 192020, and PLX 1219 do not have Hipparcos parallaxes. Their extinction was estimated using the method of Carney (1983) which is based on VJK photometry. These five stars do not have a Hipparcos number in Table B.1.

For two of the 15 studies, we note that no star redder than $(b-y)_0 > 0.6$ remained after the dereddening (see Table 1). These studies were nevertheless kept in the compilation as they provide valuable additional stars close to this border. Figure 4 b. shows the distribution of the stars in the HR-diagram and Fig. 5 shows the distributions of both the Strömgren indices and $[\text{Fe}/\text{H}]$ for the spectroscopic catalogue.

4. Metallicities from $uvby$ photometry - a critical evaluation

The literature contains many calibrations that make it possible to derive metallicities from Strömgren photometry. Most of them are empirical but theoretical investigations also exist (see, e.g., Önehag et al. 2009, for a recent example). The early metallicity calibrations (Strömgren 1964; Crawford 1975; Olsen 1984) were mostly based on how much the colour indices m_1 and c_1 differed from a given standard relation, $\delta m_1 = m_{1,\text{std}} - m_{1,\text{obs}}$ and $\delta c_1 = c_{1,\text{obs}} - c_{1,\text{std}}$. The $m_{1,0} - (b-y)_0$ and $c_{1,0} - (b-y)_0$ relations used in these calibrations are usually derived from observations of stars belonging to the Hyades stellar cluster (for $m_{1,0} - (b-y)_0$) and from field stars that are believed to be on the ZAMS (for $c_{1,0} - (b-y)_0$). Olsen (1984) provides an example of how the preliminary standard sequences were derived.

More recent calibrations for dwarf stars have abandoned the use of standard relations (with the exception of Haywood 2002) and derive $[\text{Fe}/\text{H}]$ directly from the colour indices $(b-y)_0$, $m_{1,0}$, and $c_{1,0}$ (Schuster & Nissen 1989b; Malyuto 1994;

Table 2. Metallicity calibrations evaluated in Sect 4.

Reference	$(b-y)_0$		[Fe/H]		$\langle [\text{Fe}/\text{H}] - [\text{M}/\text{H}] \rangle$	\pm	σ	Comment
	min	max	min	max				
Olsen (1984)	0.29	1.00	-2.60	0.39	0.11	\pm	0.34	Their Eq. (15)
	0.514	1.000	-2.60	0.39	0.04	\pm	0.39	Their Eq. (15)
	0.514	1.000	-0.25	0.60	0.02	\pm	0.17	Their Eq. (16)
Schuster & Nissen (1989b)	0.22	0.38	-3.5	0.2	0.06	\pm	0.16	F-type dwarfs G-type dwarfs
	0.37	0.59	-2.6	0.4				
Haywood (2002)	0.22	0.59	-2.0	0.5	0.00	\pm	0.18	
Martell & Laughlin (2002)	0.288	0.591	-2.0	0.5	0.05	\pm	0.13	
Martell & Smith (2004)	0.288	0.591	-2.0	0.5	0.06	\pm	0.21	
Nordström et al. (2004)	0.18	0.38	-2.0	0.8	-0.17	\pm	0.52	
	0.44	0.59	-2.0	0.8				
Ramírez & Meléndez (2005a)	0.19	0.35	-3.5	0.4	0.04	\pm	0.14	F-type dwarfs G-type dwarfs
	0.35	0.80	-2.5	0.4				
Holmberg et al. (2007)	0.24	0.63	-1.00	0.37	0.08	\pm	0.16	
Önehag et al. (2008)	0.22	0.59	-3.5	0.4	0.33	\pm	0.30	

Column 1 lists the reference for the calibration. In Cols. 2 to 5 we quote the ranges, for for $(b-y)_0$ and [Fe/H], within which the calibrations is valid. Column 6 gives the mean difference between [Fe/H] and [M/H] and the associated σ . Column 7 provides additional comments.

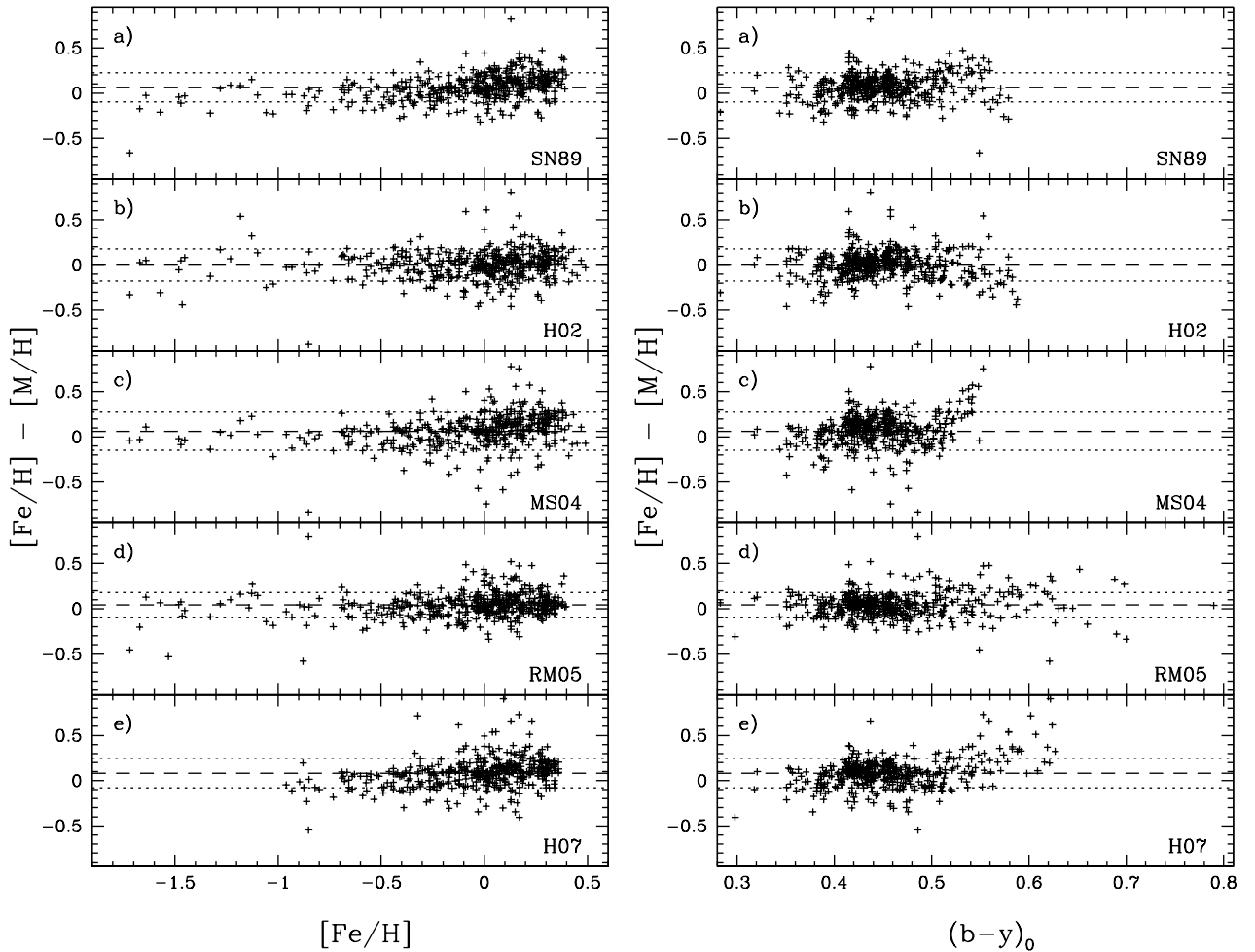


Fig. 6. The difference between [Fe/H] and [M/H], derived from the calibrations listed in Table 2, as a function of [Fe/H] (left hand panels) and $(b-y)_0$ (right hand panels). The metallicity calibrations used are labelled as follows: SN89 for Schuster & Nissen (1989b), MS04 for Martell & Smith (2004), H07 for Holmberg et al. (2007), H02 for Haywood (2002), and RM05 for Ramírez & Meléndez (2005a). The mean differences (dashed lines) and the σ (dotted lines) are listed in Table 2.

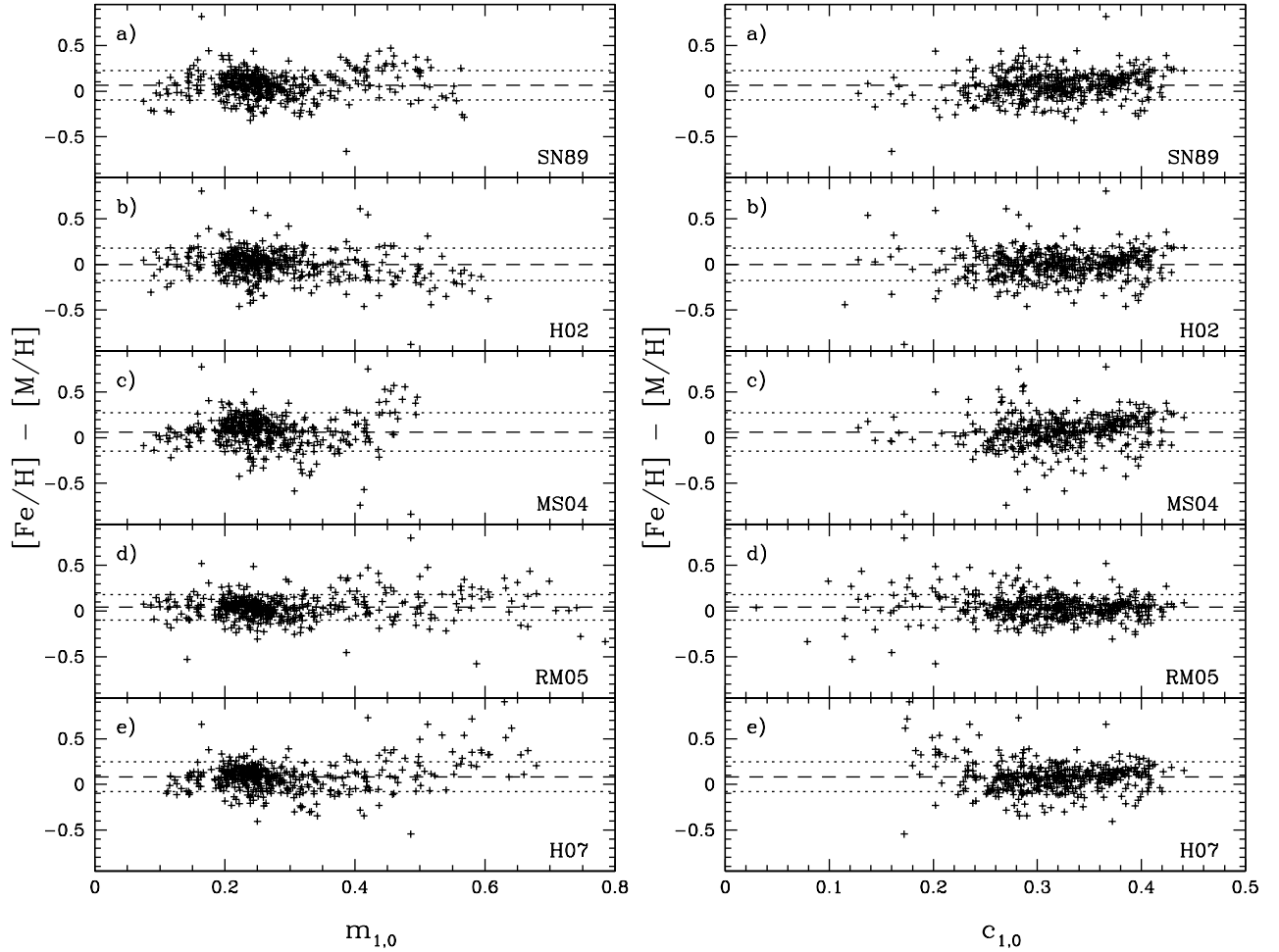


Fig. 7. The difference between $[\text{Fe}/\text{H}]$ and $[\text{M}/\text{H}]$, derived from the calibrations listed in Table 2, as a function of $m_{1,0}$ (left-hand panels) and $c_{1,0}$ (right-hand panels). The metallicity calibrations used are labelled as follows: SN89 for Schuster & Nissen (1989b), MS04 for Martell & Smith (2004), H07 for Holmberg et al. (2007), H02 for Haywood (2002), and RM05 for Ramírez & Meléndez (2005a). The mean differences (dashed lines) and the σ (dotted lines) are listed in Table 2.

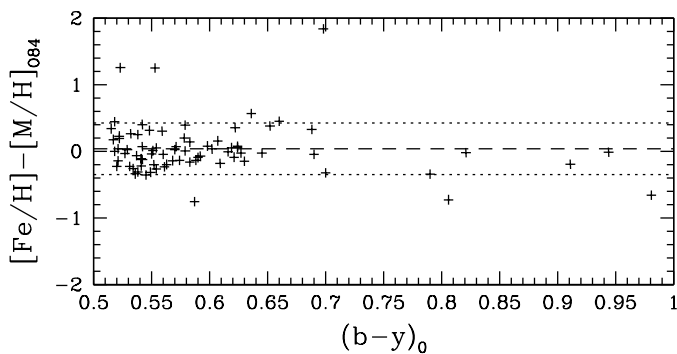


Fig. 8. The difference between $[\text{Fe}/\text{H}]$ and $[\text{M}/\text{H}]$ calculated using the calibration by Olsen (1984) ($[\text{M}/\text{H}]_{084}$). The comparison is made in the colour interval $0.514 < (b-y)_0 < 1.000$. The mean difference is 0.03 dex (dashed line) with a σ of 0.39 dex (dotted lines).

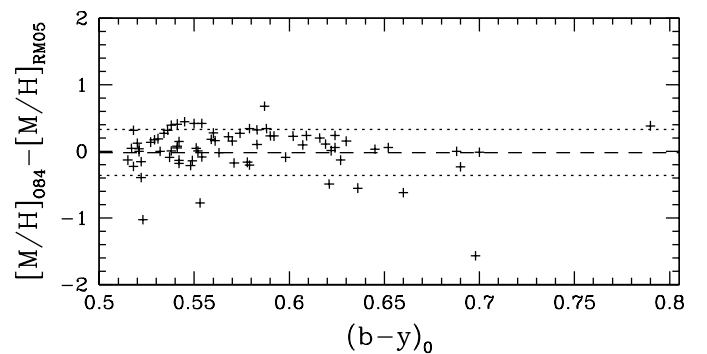


Fig. 9. A comparison of the $[\text{M}/\text{H}]$ calculated using the calibration by Olsen (1984) ($[\text{M}/\text{H}]_{084}$) and the calibration by Ramírez & Meléndez (2005a) ($[\text{M}/\text{H}]_{\text{RM05}}$). The comparison is made in the colour interval $0.514 < (b-y)_0 < 0.800$. The mean difference is -0.02 dex (dashed line) with a σ of 0.39 dex (dotted lines).

Haywood 2002; Martell & Laughlin 2002; Martell & Smith 2004; Nordström et al. 2004; Ramírez & Meléndez 2005a; Holmberg et al. 2007). The metallicity calibration by Olsen

(1984) is the only calibration that extends all the way to $(b-y)_0 =$

1.0. No calibration exists for dwarf stars redder than $(b - y)_0 = 1.0$.

In addition, some metallicity calibrations for dwarf stars require the use of the β index (e.g., Nissen 1981; Twarog et al. 2007) or additional broadband photometry (Kotoneva et al. 2002; Bonfils et al. 2005; Flynn & Morell 1997). These will be not be investigated here.

Already Bond (1980) found tentative evidence of a metallicity dependence in the Strömgren indices for red giant stars in the field, which was further investigated by Anthony-Twarog & Twarog (1994), who also derived metallicity dependent standard sequences of red giants in the $c_{1,0}$ vs. $(b - y)_0$ diagram. Theoretical studies of the stellar colours of red giant stars found that the colours show clear dependencies on both metallicity and the amount of CNO in the atmospheres of the stars (Gustafsson & Bell 1979). Hilker (2000) provided an updated calibration based on both field stars and red giant branch stars in globular clusters. However, the number of metallicity calibrations derived directly for red giant stars is limited. The list includes Bond (1980), Grebel & Richtler (1992), Anthony-Twarog & Twarog (1998), Hilker (2000), and Calamida et al. (2007).

4.1. A test of metallicity calibrations for dwarf stars

We now use our compilation of dwarf stars in Table B.1 to evaluate how well various metallicity calibrations can reproduce $[\text{Fe}/\text{H}]$. We investigate the calibrations by Olsen (1984), Schuster & Nissen (1989b), Haywood (2002), Martell & Laughlin (2002), Martell & Smith (2004), Nordström et al. (2004), Ramírez & Meléndez (2005a), and Holmberg et al. (2007). The common aspect of these calibrations is that they are relatively recent and/or have been influential. In Sect. 6.2, we discuss the ability of model atmospheres to reproduce the observed Strömgren indices (Önehag et al. 2009).

We note that there are two metallicity calibrations in Olsen (1984). Both calibrations depend on δm_1 , but while Eq. (16) in Olsen (1984) is a linear equation in δm_1 , Eq. (15) includes a quadratic term in δm_1 . We investigate both calibrations.

Each calibration was applied only to stars with photometric indices in the range where the calibration is valid (as indicated in the original study). In Table 2, we list the mean difference between $[\text{Fe}/\text{H}]$ and $[\text{M}/\text{H}]$. As can be seen, the mean offset is, in most of the cases, smaller than 0.1 dex. Two calibrations yield larger offsets, Olsen (1984) (full range of Eq. (15)) and Nordström et al. (2004). These calibrations also have some of the largest scatters (compare Table 2 and Figs. 6 and 7).

Figure 6 compares the differences between $[\text{Fe}/\text{H}]$ and $[\text{M}/\text{H}]$ as a function of $[\text{Fe}/\text{H}]$. There is a tendency for some of the calibrations (notably Schuster & Nissen 1989b; Martell & Smith 2004; Holmberg et al. 2007) to show a declining trend towards lower $[\text{Fe}/\text{H}]$. The second and third of these calibrations also show obvious trends with $(b - y)_0$ when $(b - y)_0 \geq 0.5$. Hence, even if these calibrations formally extend all the way to about 0.6, it is clear that there are shortcomings for the redder colours.

A comparison of the difference as a function of $m_{1,0}$ (Fig. 7) indicates that two of the calibrations (Martell & Smith 2004; Holmberg et al. 2007) fall short at the redder end of the distribution. Finally, studying the difference as function of $c_{1,0}$ we note that Holmberg et al. (2007) appears to show some real trend for the lower $c_{1,0}$ and that Martell & Smith (2004), and possibly Haywood (2002), show an overall trend such that the metallicity is underestimated at low $c_{1,0}$ and overestimated at high $c_{1,0}$.

In summary, we find that both Schuster & Nissen (1989b) and Ramírez & Meléndez (2005a) perform very well in all four comparisons. However, as Ramírez & Meléndez (2005a) covers a much larger parameter space we would recommend it over Schuster & Nissen (1989b), but again recall that in the regions where the two calibrations overlap they perform equally well.

However, Ramírez & Meléndez (2005a) extends only to $(b - y)_0 = 0.8$. We therefore investigated the redder calibration of Olsen (1984). In Fig. 8, we compare the $[\text{Fe}/\text{H}]$ with the resulting $[\text{M}/\text{H}]$ from that calibration, finding good agreement. In Fig. 9, we compare the results from Olsen (1984) with the results from Ramírez & Meléndez (2005a) as a function of $(b - y)_0$, and again find close agreement. From these tests, we conclude that Olsen (1984) provides an adequate extension of Ramírez & Meléndez (2005a) for stars redder than $(b - y)_0 = 0.8$.

As discussed in Sect. 3.1, if the reddening towards a star is less than 0.02 we do not apply a reddening correction (Table B.1). The effect of this omission is small. For example, if we use the calibration of Ramírez & Meléndez (2005a) to calculate $[\text{M}/\text{H}]$ and assume that stars with $E(B - V) < 0.02$, have an $E(B - V) = 0.02$ the mean difference between $[\text{Fe}/\text{H}]$ and $[\text{M}/\text{H}]$ changes from 0.041 ± 0.140 to -0.003 ± 0.148 . The trends with $[\text{Fe}/\text{H}]$ and the photometric indices change very little. To the eye, it appears that, e.g., for redder $(b - y)_0$ the scatter increases. Similar trends are seen for the other indices.

4.2. Metallicity calibrations for red giant branch stars

Faria et al. (2007) undertook a detailed investigation of the calibrations then available and found that the calibration of Hilker (2000) was by far the most successful when comparing with high-resolution spectroscopy. However, Faria et al. (2007) only gives a limited comparison of metal-poor, faint red giant stars in the Draco dwarf spheroidal galaxy. Ramírez & Meléndez (2004) undertook a comparison with field giants in the Milky Way ranging from solar all the way down to -2.5 dex. They found that the Hilker (2000) calibration underestimated the intermediate metallicities but overestimated the lowest metallicities when compared to the spectroscopically derived iron abundances. Solar metallicities were well reproduced. Ramírez & Meléndez (2004) provide a correction formula to place the calibrations of Hilker (2000) onto the spectroscopic scale. Since then, Calamida et al. (2007) presented a new, and very comprehensive, study of metallicities of red giant stars and their iron abundance. This study used giant stars in globular clusters as a reference for their calibration. Calamida et al. (2007) used the more metallicity sensitive index $(v - y)_0$, rather than $(b - y)_0$ used in Hilker (2000). As discussed already by Strömgren (1963), the position of the v filter provides a measure of the total decrement due to the presence of metallicity lines. We refer the reader to Calamida et al. (2007) and Calamida et al. (2009) (which provides an update to Calamida et al. 2007) for an extended discussion of the derivation of their metallicity calibration for red giant stars.

Figure 10 compares the different calibrations applied to metal-poor red giant branch stars in three nearby dwarf spheroidal galaxies (Draco, Sextans, and Hercules). For this comparison, we use the calibration by Calamida et al. (2007) as reference. Data for Draco and Sextans are taken from Adén et al. (in prep.) and data for Hercules from Adén et al. (2009a). The data in Adén et al. (in prep.) will supersede those of Faria et al. (2007).

The comparison between Calamida et al. (2007) and Hilker (2000) shows the same banana shape noted by Ramírez & Meléndez (2004). This is most prominently seen for

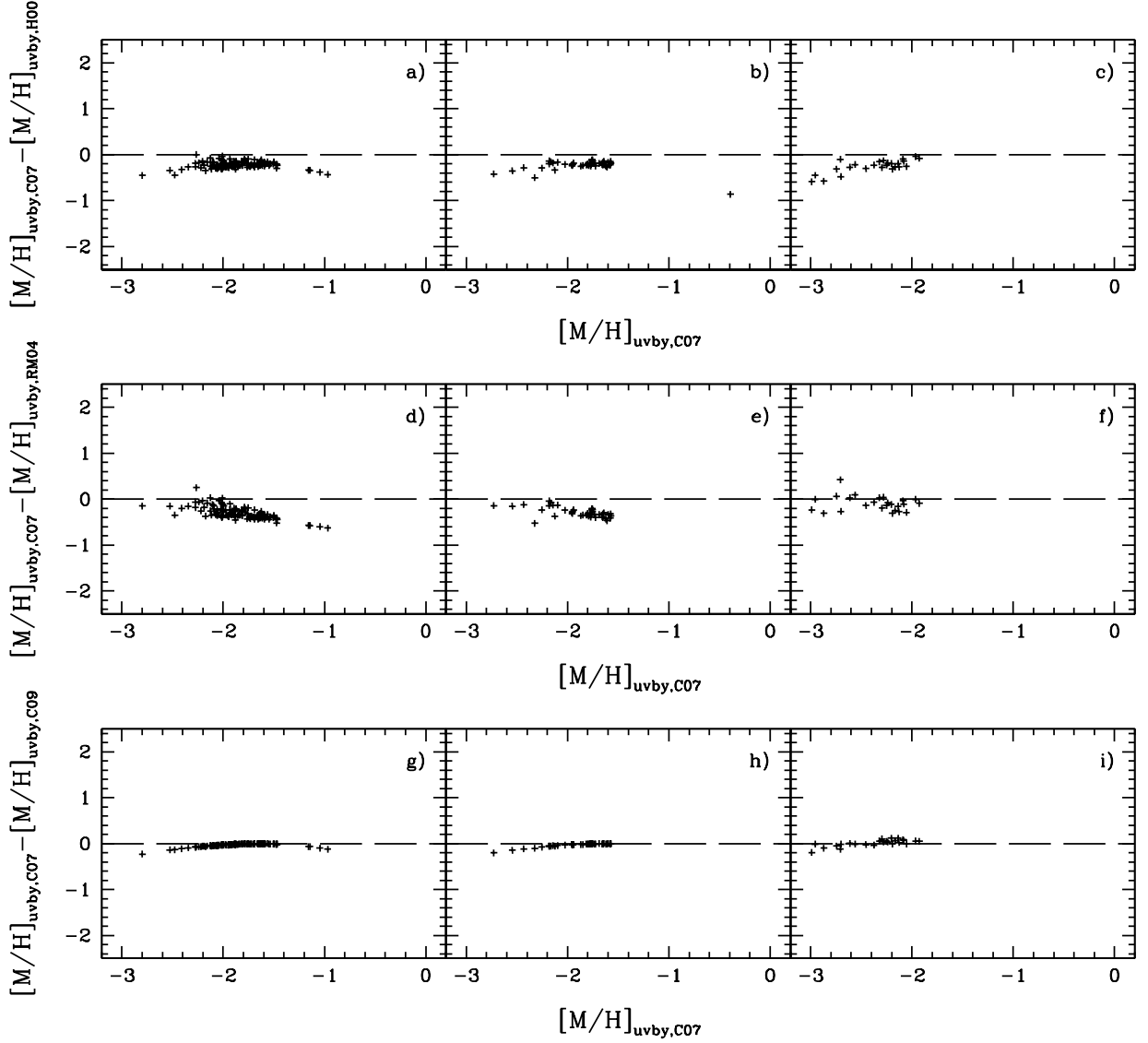


Fig. 10. A comparison of $[M/H]$ derived for giant stars using the four most recent metallicity calibrations for $uvby$ photometry. We use the calibration of Calamida et al. (2007) as the reference for all comparisons. Panels a, d, and g shows the data for stars in the Draco dwarf spheroidal galaxy, panels b, e, and h the data for stars in the Sextans dwarf spheroidal galaxy, and panels c, f, and i data for giant stars in the Hercules dwarf spheroidal galaxy.

stars in the Draco dwarf spheroidal galaxy. The difference between Calamida et al. (2007) and Calamida et al. (2009) is, as expected, very small, the major difference being at the most metal-poor end. Comparing Calamida et al. (2007) and the corrected Hilker (2000) calibration by Ramírez & Meléndez (2004) indicates that the calibration by Ramírez & Meléndez (2004) would produce a more metal-poor as well as more concentrated metallicity distribution function for the three galaxies than if we used the calibration by Calamida et al. (2007). Calamida et al. (2009) use $(v - y)$ and $(u - v)$ for their calibrations; although these colours are more sensitive to metallicity than $(b - y)$ they

are also sensitive to CH and CN. It appears, however, from the comparison carried out here, that the choice of colours to use in the calibration might not be very sensitive to the presence of molecules (at least for the giant stars in the dwarf spheroidal galaxies). This should, however, be further studied.

We note that all of these calibrations are poorly constrained at the metal-poor end and more calibration data are required to improve the calibrations. Many studies currently target stars in the metal-poor dwarf spheroidal galaxies and these data will thus become available soon. We also note that to date only the calibration by Ramírez & Meléndez (2004) extends to solar metal-

licity, which is an important property for investigations where more metal-rich stars can be expected.

Calibrations of *uvby* photometry for red giant stars with metallicities below -2 dex have not been rigorously tested because *uvby* photometry and iron abundances based on high-resolution spectroscopy for metal-poor field red giant have been largely unavailable. However, a first look at data for Hercules (Adén et al. submitted) indicates that $[\text{Fe}/\text{H}]$ based on high-resolution spectroscopy for about ten red giant branch stars infers lower iron abundances than predicted from photometry using any of the metallicity calibrations discussed here. In addition, preliminary comparisons with data from Kirby et al. (2008) find the same result (Adén et al. 2009a, and Adén et al., submitted). This conclusion is supported by a comparison with the new Draco data by Cohen & Huang (2009), who obtained high-resolution spectroscopy of eight of the brighter red giants in the Draco dwarf spheroidal. We have Strömgren photometry for six of these stars. A comparison with $[\text{M}/\text{H}]$ derived using the calibration of Calamida et al. (2009) gives a mean difference of -0.21 dex and a σ of 0.19 dex. A similar comparison but using the calibration by Ramírez & Meléndez (2004) gives a mean difference of -0.25 dex and a σ of 0.22 dex. Cohen & Huang (2009) noted a similar difference when they compared their spectroscopic $[\text{Fe}/\text{H}]$ with those metallicities derived using the calibration of Hilker (2000). We note that the most metal-poor stars in the sample cause the largest deviations. Above about -2 dex, the comparison is very favourable. As part of our ongoing work on *uvby* photometry for red giant stars in dwarf spheroidal galaxies, we are evaluating the possibilities to extend current metallicity calibrations for *uvby* photometry to metallicities below -2 dex.

We also compared the iron abundances of giant stars in the Draco dwarf spheroidal galaxy determined in Cohen & Huang (2009) with metallicities derived from *ugriz* photometry using the calibration of Ivezić et al. (2008). The scatter is very large and some of the metallicities are clearly incorrect. The differences are such that even with a very large sample and considering, e.g., only the mean metallicity of the sample the conclusions would be at best indicative (see also Sect. 4.3 below).

4.3. A comparison with photometric metallicities from SDSS – both dwarf and giant stars

The SDSS (York et al. 2000) is one of the most influential studies covering a very large portion of the sky. The stellar part contains not only *ugriz* photometry but also spectra for a large fraction of the objects. This and additional spectroscopic campaigns provide $[\text{M}/\text{H}]$ (e.g., Lee et al. 2008). It is of great interest to attempt to derive calibrations to use the *ugriz* photometry to provide stellar parameters and in particular $[\text{M}/\text{H}]$ (Ivezić et al. 2008). If good calibrations can be obtained, much new information about the thick disk and the halo can be obtained (see, e.g., Carollo et al. 2008). Because of the potential impact of SDSS, it remains important to test the calibrations against independent metallicity measures. Our Strömgren photometry provides an opportunity to do so for a large sample of fairly faint dwarf and giant stars.

To perform these comparisons we use *uvby* photometry of dwarf stars from Árnadóttir et al. (in preparation) and data for red giant stars from Faria (2006), Faria et al. (2007), Lagerholm (2008), Adén et al. (2009a), and Adén et al. (in prep.). The identification of dwarfs and giants is unambiguous for the stars we use (see e.g., Faria et al. 2007; Adén et al. 2009a). The *ugriz* photometry is from SDSS DR7 (Abazajian et al. 2009).

For the *uvby* photometry, we use the calibrations of Ramírez & Meléndez (2005a) and Olsen (1984) (for dwarf stars) and Calamida et al. (2007) (for giant stars) to calculate $[\text{M}/\text{H}]_{uvby}$. For the *ugriz* photometry, we use the calibration of Ivezić et al. (2008) to calculate $[\text{M}/\text{H}]_{ugriz}$. The comparisons between $[\text{M}/\text{H}]_{uvby}$ and $[\text{M}/\text{H}]_{ugriz}$ are shown in Figs. 11 and 12.

We first note that for the dwarf stars in Fig. 11 there is good agreement at metallicities around -1 dex, but that agreement quickly deteriorates as we move to higher or lower metallicities. There is some scatter but there is a distinctive linear relation such that $[\text{M}/\text{H}]_{ugriz}$ is higher than $[\text{M}/\text{H}]_{uvby}$ at low metallicities and the opposite is true for solar metallicities. At solar metallicity, the offset is about 0.5 dex and at $[\text{M}/\text{H}]_{uvby} = -2$ the offset is about 1.5 dex. Given the fairly extensive tests that have been performed to compare $[\text{M}/\text{H}]_{uvby}$ to $[\text{Fe}/\text{H}]$ derived from stellar spectroscopy provided both in this study (see Sect. 4 and Figs. 6 and 7) and elsewhere, these differences are a concern.

A comparison for metallicities for giants presented in Fig. 12 is perhaps even less encouraging. For $-3 < [\text{M}/\text{H}]_{uvby} < -2$, there is a trend similar to that for the dwarf stars, but at higher metallicities the relation appears to break down completely. We note that our datasets for the giant stars are small but we believe that the more populated red giant branch of the Draco dwarf spheroidal galaxy provides a fairly unambiguous result. It is beyond the scope of this paper to explain these differences. However, given the very large discrepancies in some cases caution is required when using $[\text{M}/\text{H}]_{ugriz}$ to infer the properties of the halo, where clearly many of the targets will be giants. Given the overall scatter for giant stars of metallicity -2 dex, a typical halo metallicity, in Fig. 12 these inferences must be regarded as only indicative.

The comparison between $[\text{M}/\text{H}]_{uvby}$ and $[\text{Fe}/\text{H}]$ from high resolution spectroscopy indicates that $[\text{M}/\text{H}]_{uvby}$ is overestimated (Sect. 4.2). If $[\text{M}/\text{H}]_{uvby}$ were corrected to more closely match $[\text{Fe}/\text{H}]$, then the difference between $[\text{M}/\text{H}]_{ugriz}$ and $[\text{M}/\text{H}]_{uvby}$ would be even greater.

5. The *uvby* system's ability to distinguish between dwarf, sub-giant, and giant stars – New stellar sequences

The Strömgren *uvby* system has a proven ability to distinguish between dwarf and giant stars for certain colour ranges. We have used this in two studies of dwarf spheroidal galaxies to remove the foreground contamination by Milky Way dwarf stars (Faria et al. 2007; Adén et al. 2009a). In the most recent paper, we showed that about 30% of the stars that would otherwise be assumed to be radial velocity members of the Hercules dwarf spheroidal galaxy are instead foreground dwarf stars. This result has led to a re-evaluation of the minimum common mass for such galaxies (compare, e.g., Strigari et al. 2008; Adén et al. 2009b).

A significant drawback is that the stellar sequences merge around $(b - y)_0 = 0.55$ in the $c_{1,0}$ vs. $(b - y)_0$ diagram. For bluer colours, the lower red giant branch almost meets the main sequence and the subgiant branch and turn-off forms a loop (see Fig. 2). Twarog et al. (2007) investigated whether a new index could be developed to distinguish between dwarf, sub-giant, and giant stars at bluer colours. We also performed fairly extensive tests with our datasets described in Sect. 3 based on our studies of dwarf spheroidal galaxies (Faria et al. 2007; Adén et al. 2009a); we found that for larger datasets the proposed new in-

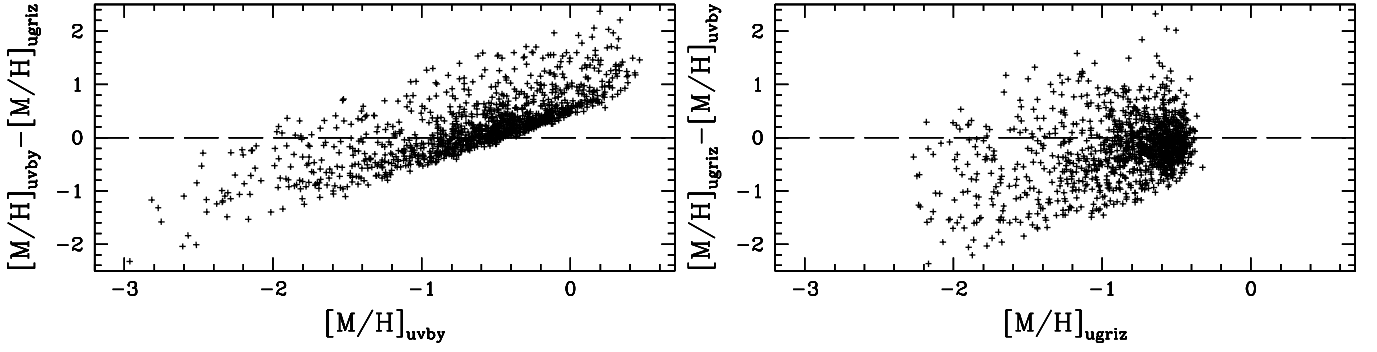


Fig. 11. A comparison of metallicities for dwarf stars derived from $uvby$ photometry ($[M/H]_{uvby}$) using the calibrations by Ramírez & Meléndez (2005a) and Olsen (1984) and metallicities derived from SDSS $ugriz$ photometry ($[M/H]_{ugriz}$) using the calibration of Ivezić et al. (2008). The stars are along the lines-of-sight in the directions of the Hercules, Draco, and Sextans dwarf spheroidal galaxies. A full description of how these stars were selected will be provided in Árnadóttir et al. (in preparation). All stars have $15 < V_0 < 18.5$. The dashed line indicates a metallicity difference of zero. On the abscissa the left-hand panel has $[M/H]_{uvby}$ and the right-hand panel has $[M/H]_{ugriz}$.

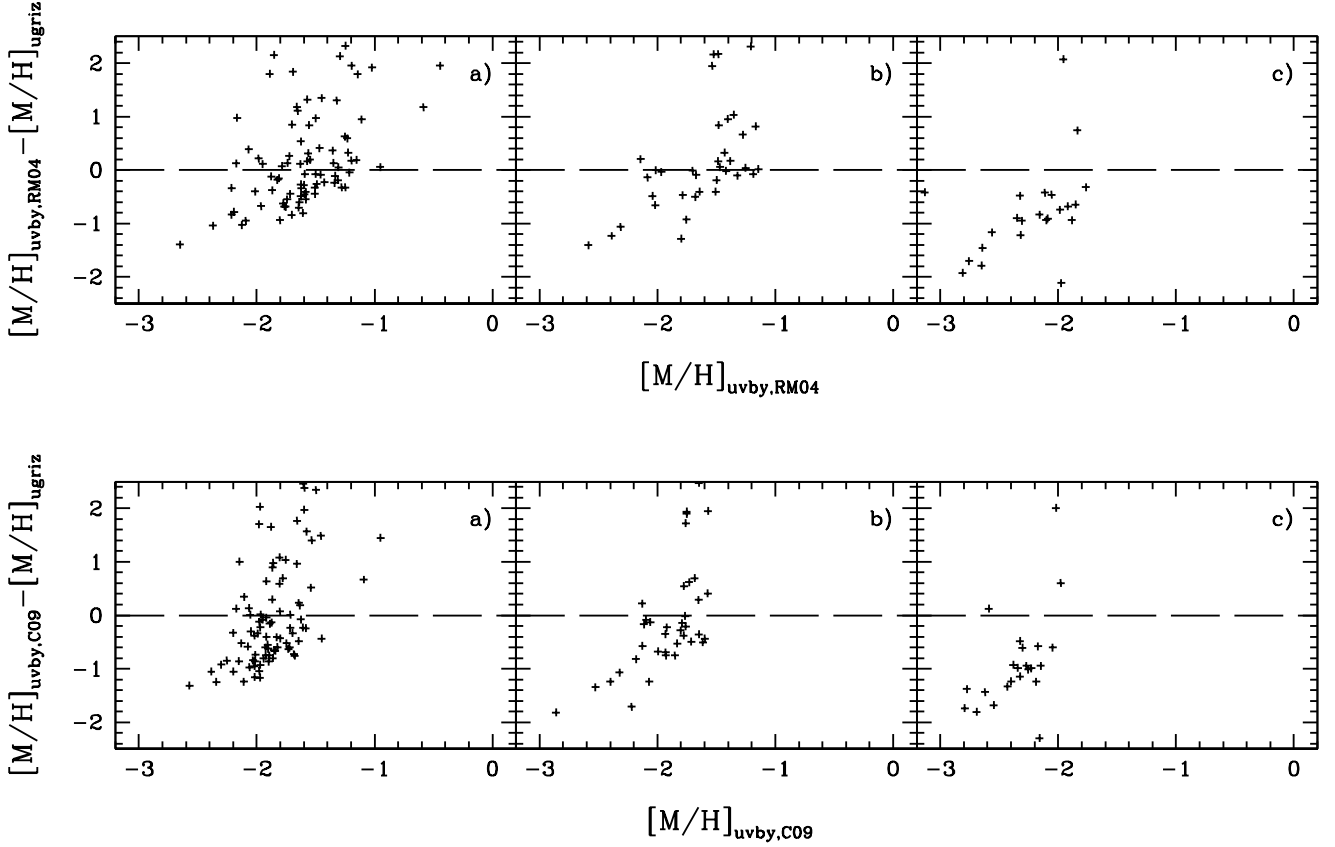


Fig. 12. A comparison of metallicities derived from $uvby$ photometry and $ugriz$ photometry (using the calibration of Ivezić et al. 2008), respectively, for giant stars in dwarf spheroidal galaxies. The top panels use the calibration by Ramírez & Meléndez (2004) and the bottom panels the calibration by Calamida et al. (2009) to obtain metallicities from $uvby$ photometry. **a.** Comparison for red giant branch stars in the Draco dwarf spheroidal galaxy ($uvby$ photometry: Adén et al. in prep.). **b.** Comparison for red giant branch stars in the Sextans dwarf spheroidal galaxy ($uvby$ photometry: Adén et al. in prep. and Lagerholm 2008). **c.** Comparison for red giant branch stars in the Hercules dwarf spheroidal galaxy ($uvby$ photometry: Adén et al. 2009a).

dex does not appear to have the desired ability to distinguish between the bluer dwarf, sub-giant, and giant stars.

5.1. Metallicity-dependent dwarf star sequences

Dwarf star sequences in the Strömgren $c_{1,0} - (b - y_0)$ plane were introduced for F-type dwarf stars by Crawford (1975) and later extended to $(b - y) = 1.0$ by Olsen (1984). These sequences

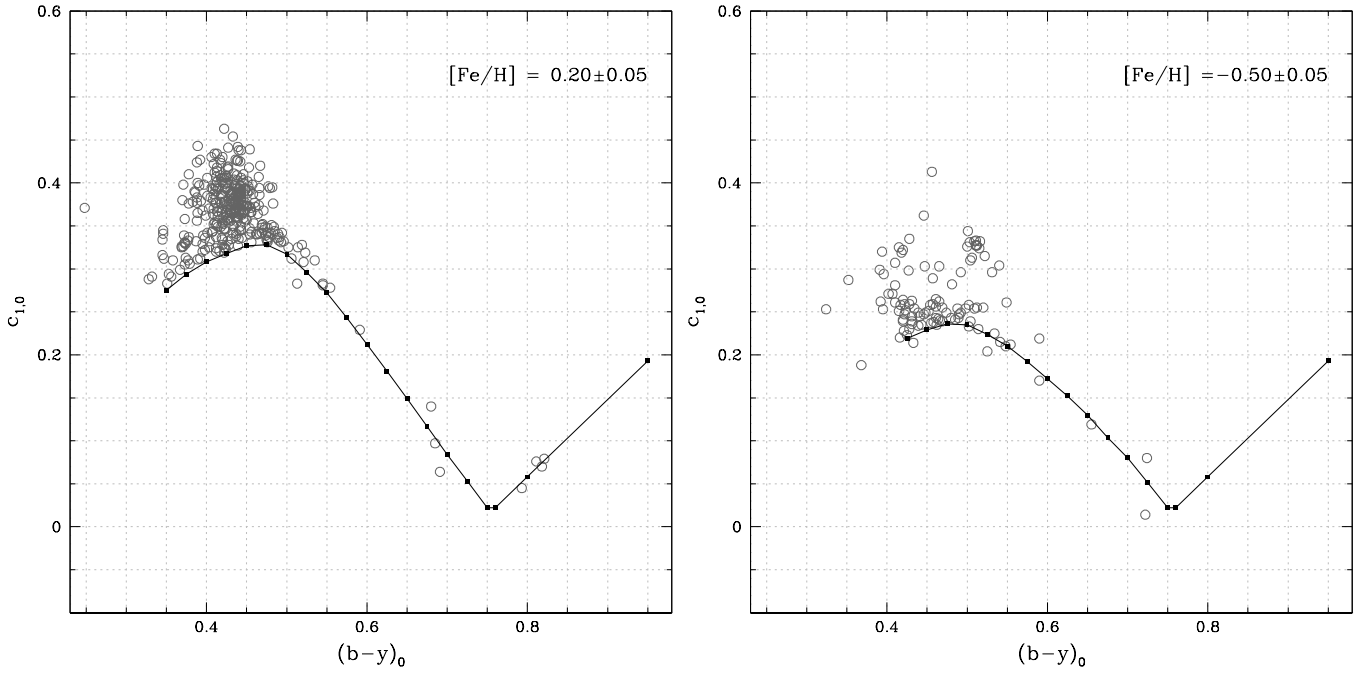


Fig. 13. Two examples of how the dwarf sequences in the $c_{1,0}$ v.s. $(b-y)_0$ diagram, discussed in Sect. 5.1, were established. The left hand panel shows dwarf stars with $0.15 < [M/H] < 0.25$ and the right hand panel dwarf stars with $-0.55 < [M/H] < -0.45$. A complete set of similar plots for all metallicities can be found in Appendix A (available online). The standard relations are listed in Tables 3 and 4.

Table 3. New metallicity-dependent sequences for dwarf stars (see Sect. 5.1 and Figs. 13, and A.1 to A.14). For each range of metallicity (as indicated in the top two rows), we list the $c_{1,0}$ value for each $(b-y)_0$, as listed in the first column.

[M/H]	0.50	0.40	0.30	0.20	0.10	0.00	-0.10	-0.20	-0.30	-0.40	-0.50	-0.60	-0.80	-1.00
±	0.05	0.05	0.05	0.05	0.05	0.05	0.05	0.05	0.05	0.05	0.05	0.10	0.15	0.20
$(b-y)_0$	$c_{1,0}$	$c_{1,0}$	$c_{1,0}$	$c_{1,0}$	$c_{1,0}$	$c_{1,0}$	$c_{1,0}$	$c_{1,0}$	$c_{1,0}$	$c_{1,0}$	$c_{1,0}$	$c_{1,0}$	$c_{1,0}$	$c_{1,0}$
0.400	0.380	0.345	0.326	0.308	0.288	0.271	0.252	0.244	0.242	0.228	-	0.217	-	-
0.425	0.398	0.363	0.338	0.318	0.300	0.284	0.265	0.252	0.242	0.229	0.219	0.211	0.192	0.140
0.450	0.395	0.378	0.347	0.327	0.310	0.293	0.278	0.267	0.249	0.238	0.229	0.217	0.194	0.146
0.475	0.371	0.371	0.347	0.328	0.310	0.298	0.285	0.274	0.256	0.247	0.236	0.227	0.196	0.154
0.500	0.341	0.341	0.336	0.317	0.305	0.292	0.280	0.272	0.259	0.249	0.235	0.228	0.196	0.161
0.525	0.309	0.309	0.307	0.296	0.290	0.276	0.266	0.262	0.254	0.243	0.224	0.220	0.193	0.165
0.550	0.277	0.277	0.276	0.272	0.267	0.258	0.245	0.243	0.238	0.230	0.210	0.207	0.186	0.165
0.575	0.245	0.245	0.245	0.243	0.240	0.235	0.223	0.221	0.219	0.211	0.192	0.190	0.175	0.163
0.600	0.213	0.213	0.213	0.212	0.210	0.209	0.198	0.196	0.195	0.186	0.172	0.172	0.162	0.153
0.625	0.181	0.181	0.181	0.181	0.180	0.180	0.173	0.171	0.171	0.162	0.152	0.152	0.145	0.139
0.650	0.149	0.149	0.149	0.149	0.149	0.149	0.145	0.144	0.144	0.136	0.130	0.130	0.126	0.120
0.675	0.117	0.117	0.117	0.117	0.117	0.117	0.115	0.115	0.115	0.109	0.104	0.104	0.103	0.097
0.700	0.084	0.084	0.084	0.084	0.084	0.084	0.084	0.084	0.084	0.082	0.080	0.080	0.077	0.072
0.725	0.053	0.053	0.053	0.053	0.053	0.053	0.053	0.053	0.053	0.052	0.051	0.051	0.049	0.047
0.750	0.022	0.022	0.022	0.022	0.022	0.022	0.022	0.022	0.022	0.022	0.022	0.022	0.022	0.022
0.760	0.022	0.022	0.022	0.022	0.022	0.022	0.022	0.022	0.022	0.022	0.022	0.022	0.022	0.022
0.800	0.058	0.058	0.058	0.058	0.058	0.058	0.058	0.058	0.058	0.058	0.058	0.058	0.058	0.058
0.950	0.193	0.193	0.193	0.193	0.193	0.193	0.193	0.193	0.193	0.193	0.193	0.193	0.193	0.193

were drawn by hand tracing the lower envelope of field stars in the relevant diagram. No attempts were made to investigate if the stellar sequences were metallicity dependent, although this possibility was discussed already by Strömgren (1964). It is clear, in the $c_{1,0}$ vs. $(b-y)_0$ diagram, when we compare the dwarf star sequence of Olsen (1984) to the dwarf region for metal-poor stars, given by Schuster et al. (2004), that the metal-poor dwarf stars have lower $c_{1,0}$ indices than the, mainly, solar metallicity stars

used to define the sequence in Olsen (1984). This can be seen, e.g., in Fig. 2.

We are now in a position to extend the study of Olsen (1984) and investigate the metallicity dependence of dwarf star sequences in both the $c_{1,0}$ vs. $(b-y)_0$ diagram and the $c_{1,0}$ vs $(v-y)_0$ diagram. For stars in our photometric catalogue $[M/H]$ were calculated (see Sect. 3.2) using the metallicity calibrations by Ramírez & Meléndez (2005a) for dwarf and subgiant stars

Table 4. New metallicity-dependent sequences for dwarf stars (see Sect. 5.1). For each range of metallicity (as indicated in the top two rows), we list the $c_{1,0}$ value for each $(v - y)_0$, as listed in the first column.

[M/H]	0.50	0.40	0.30	0.20	0.10	0.00	-0.10	-0.20	-0.30	-0.40	-0.50	-0.60	-0.80	-1.00
\pm	0.05	0.05	0.05	0.05	0.05	0.05	0.05	0.05	0.05	0.05	0.05	0.10	0.15	0.20
$(v - y)_0$	$c_{1,0}$	$c_{1,0}$	$c_{1,0}$	$c_{1,0}$	$c_{1,0}$	$c_{1,0}$	$c_{1,0}$	$c_{1,0}$	$c_{1,0}$	$c_{1,0}$	$c_{1,0}$	$c_{1,0}$	$c_{1,0}$	$c_{1,0}$
1.100	0.381	0.336	0.321	0.308	0.292	0.273	0.260	0.254	0.245	0.231	0.226	0.211	0.190	0.140
1.150	0.393	0.349	0.332	0.315	0.299	0.281	0.271	0.260	0.247	0.237	0.230	0.215	0.195	0.147
1.200	0.400	0.359	0.339	0.322	0.306	0.289	0.278	0.265	0.253	0.241	0.233	0.219	0.198	0.152
1.250	0.395	0.365	0.342	0.327	0.309	0.294	0.283	0.271	0.257	0.245	0.236	0.227	0.201	0.156
1.300	0.385	0.367	0.345	0.328	0.310	0.297	0.285	0.274	0.260	0.247	0.237	0.233	0.202	0.159
1.350	0.375	0.364	0.345	0.326	0.308	0.296	0.284	0.272	0.261	0.248	0.237	0.234	0.203	0.162
1.400	0.363	0.358	0.340	0.322	0.305	0.294	0.282	0.271	0.260	0.247	0.236	0.232	0.202	0.164
1.450	0.350	0.348	0.332	0.314	0.298	0.288	0.276	0.266	0.255	0.246	0.232	0.228	0.200	0.166
1.500	0.337	0.335	0.323	0.304	0.288	0.281	0.268	0.259	0.249	0.243	0.225	0.222	0.196	0.166
1.550	0.324	0.322	0.312	0.293	0.279	0.271	0.260	0.251	0.242	0.238	0.219	0.215	0.192	0.165
1.600	0.309	0.308	0.301	0.282	0.268	0.261	0.250	0.242	0.232	0.229	0.211	0.207	0.186	0.163
1.650	0.296	0.294	0.289	0.270	0.257	0.250	0.239	0.232	0.221	0.219	0.202	0.198	0.177	0.161
1.700	0.279	0.278	0.275	0.258	0.245	0.239	0.227	0.221	0.208	0.207	0.192	0.188	0.168	0.155
1.750	0.264	0.263	0.261	0.245	0.232	0.227	0.215	0.210	0.195	0.194	0.181	0.177	0.159	0.148
1.800	0.246	0.246	0.245	0.231	0.218	0.214	0.202	0.198	0.183	0.181	0.170	0.166	0.150	0.140
1.850	0.229	0.229	0.228	0.215	0.203	0.200	0.188	0.185	0.170	0.168	0.158	0.154	0.140	0.130
1.900	0.211	0.211	0.210	0.198	0.187	0.185	0.174	0.172	0.157	0.154	0.146	0.141	0.129	0.120
1.950	0.191	0.191	0.190	0.181	0.171	0.169	0.159	0.158	0.143	0.140	0.133	0.128	0.118	0.110
2.000	0.169	0.169	0.169	0.162	0.154	0.152	0.143	0.142	0.129	0.126	0.120	0.115	0.107	0.099
2.050	0.146	0.146	0.146	0.142	0.136	0.135	0.126	0.125	0.116	0.111	0.106	0.102	0.095	0.088
2.100	0.122	0.122	0.122	0.120	0.116	0.115	0.108	0.107	0.101	0.095	0.091	0.087	0.083	0.076
2.150	0.097	0.098	0.098	0.097	0.097	0.094	0.090	0.089	0.085	0.080	0.077	0.074	0.070	0.064
2.200	0.074	0.074	0.074	0.073	0.073	0.072	0.070	0.069	0.067	0.063	0.061	0.059	0.056	0.051
2.250	0.050	0.050	0.050	0.050	0.050	0.050	0.049	0.049	0.048	0.044	0.042	0.041	0.040	0.037
2.310	0.022	0.022	0.022	0.022	0.022	0.022	0.022	0.022	0.022	0.022	0.022	0.022	0.022	0.022
2.350	0.120	0.120	0.120	0.120	0.120	0.120	0.120	0.120	0.120	0.120	0.120	0.120	0.120	0.120
2.380	0.200	0.200	0.200	0.200	0.200	0.200	0.200	0.200	0.200	0.200	0.200	0.200	0.200	0.200

Table 5. The upper envelope for dwarf stars in the solar neighbourhood.

$c_{1,0}$	$(b - y)_0$	$(v - y)_0$
0.396	0.350	0.895
0.423	0.375	0.947
0.448	0.400	1.010
0.458	0.410	1.044
0.461	0.430	1.085
0.450	0.450	1.131
0.424	0.470	1.205
0.385	0.490	1.305

with $(b - y)_0 < 0.80$ and the calibration by Olsen (1984) for dwarf stars with $0.80 < (b - y)_0 < 1.00$.

To trace the stellar (standard) sequences, we plotted $c_{1,0}$ vs. $(b - y)_0$ and $c_{1,0}$ vs. $(v - y)_0$ for the dwarf stars, but each time only for a narrow range in metallicity. Following the procedure in Olsen (1984), we trace the lower envelope of the stellar distribution in both the $c_{1,0}$ vs. $(b - y)_0$ and $c_{1,0}$ vs. $(v - y)_0$ diagrams. This lower envelope is sensitive to metallicity. For $(b - y)_0 > 0.7$, all dwarf stars fall on a tight relation without any dependence on metallicity. We used all stars redder than $(b - y)_0 \sim 0.7$ to define the sequence up to $(b - y)_0 = 1.0$. Our data set has no stars redder than 1.0. Figure 13 shows two examples of how these tracings were done. Figures A.1 to A.14 in Appendix A show all tracings. The sequences are tabulated in Tables 3 and 4.

Although we have extended the tracings to as blue colours as possible in Figs. A.1 to A.14, it is clear that for colours bluer

than $(b - y)_0 = 0.4$ the data are not substantial enough in quantity at any metallicity to provide a secure tracing. Moreover, we use only stars classified as GKV in Olsen (1993), Olsen (1994a), and Olsen (1994b), and therefore exclude bluer main sequence stars. This exclusion is also colour dependent because it depends on the metallicity of the stars. Because of these limitations we refrain from showing the tracings bluer than $(b - y)_0 = 0.4$ and $(v - y)_0 = 1.1$.

We also traced a global upper envelope for all dwarf stars. This upper envelope is listed in Table 5.

5.2. The ability of the *ugriz* photometric system to identify giant stars

Helmi et al. (2003) used *ugriz* photometry to identify metal-poor giant stars. We test this method using stars in the direction of the Draco dwarf spheroidal galaxy. The field contains both foreground dwarf stars in the Milky Way as well as metal-poor giant stars in the dwarf spheroidal galaxy (Faria 2006; Faria et al. 2007; Árnadóttir et al. in prep.; Adén et al. in prep.).

Helmi et al. (2003) define a new colour index, $s = -0.249u + 0.794g - 0.555r + 0.24$ which is used to identify the metal-poor giant stars. They find that metal-poor giant stars in general have larger s -indices than the dwarf stars and define a giant star as a star with an s -index more than 0.05 magnitudes above the median s -index for the field.

We use metal-poor giant stars in the Draco dwarf spheroidal galaxy and foreground stars along the same line-of-sight to test the ability of the s -index to distinguish dwarf from giant stars. The *ugriz* colour-magnitude diagram for the field used is shown

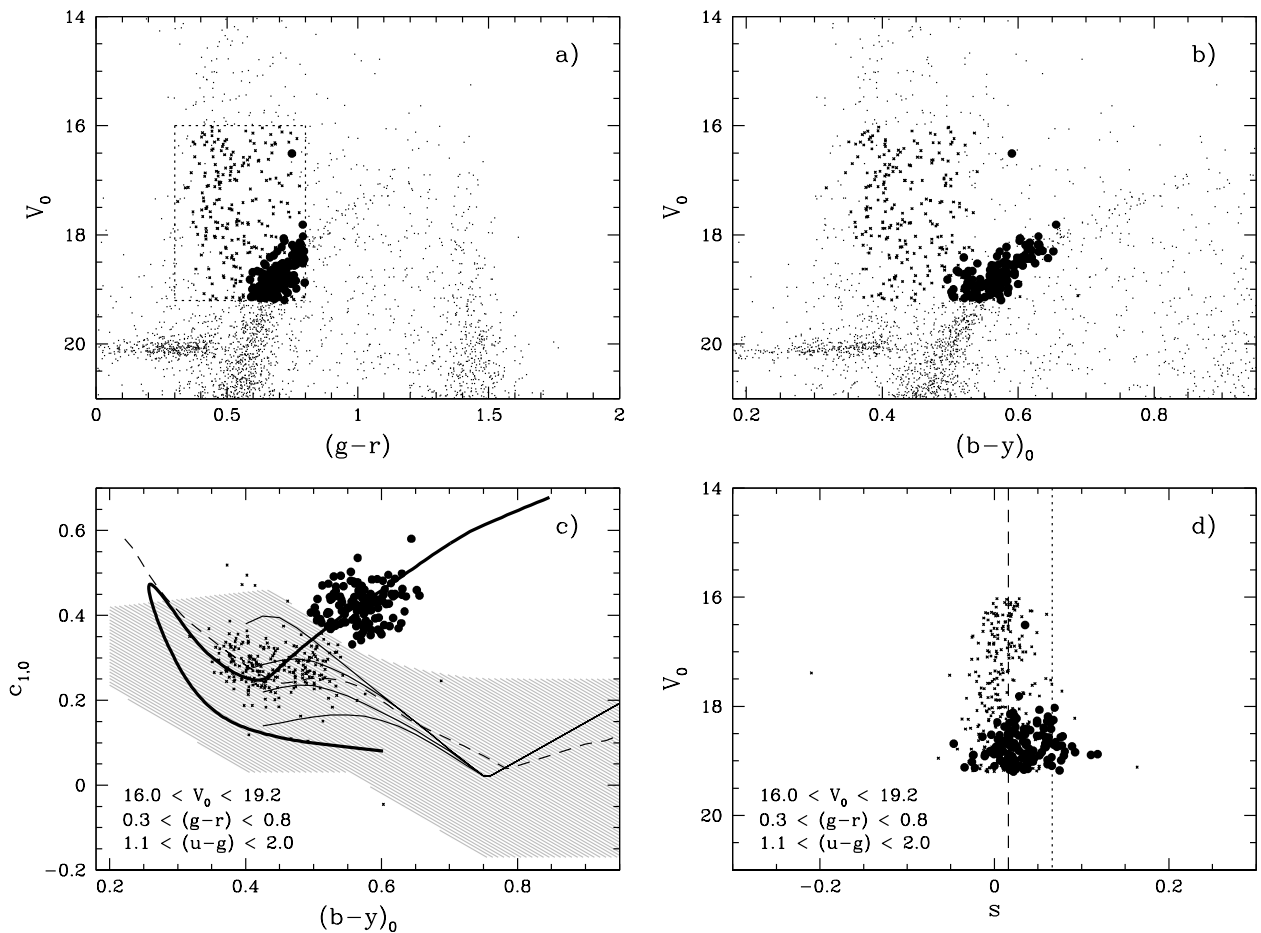


Fig. 14. **a)** Colour–magnitude diagram showing the selection of stars along the line of sight towards the Draco dSph galaxy used for testing the giant star identification of Helmi et al. (2003). These have $16.0 < V_0 < 19.2$, $1.1 < (u - g) < 2.0$ and $0.3 < (g - r) < 0.8$ (marked with a box). Stars identified as giant stars in the $c_{1,0}$ vs. $(b - y)_0$ plane are shown as filled dots. **b)** The same stars but in a colour-magnitude diagram based on Strömgen photometry. Same symbols as in panel a. The box indicated by a dotted line in a. is not included as it is a non-square area once mapped into this colour-magnitude plane. **c)** Identification of giant stars (filled dots) in the $c_{1,0}$ vs. $(b - y)_0$ plane. Grey hashed area shows the dwarf region used in Árnadóttir et al. (in prep.). Our new dwarf star sequences (solid lines) are shown along with the preliminary relations by Olsen (1984) and Crawford (1975) (dashed line), and an isochrone with an age of 12 Gyr and $[\text{Fe}/\text{H}] = -2.3$ (thick solid line, Vandenberg & Bell 1985; Clem et al. 2004). **d)** The distribution of identified giant stars (filled dots) in the s -index of Helmi et al. (2003). Dashed line indicates the median s of the selected stars (0.016) and the dotted line indicates the limit above which metal-poor giant stars are identified according to Helmi et al. (2003).

in Fig. 14a. For the comparison, we only use stars in the colour range $1.1 < (u - g) < 2.0$ and $0.3 < (g - r) < 0.8$, where the s -index is defined (Helmi et al. 2003). We identify metal-poor giant stars in the direction of the Draco dwarf spheroidal galaxy with $16.0 < V_0 < 19.2$ using the Strömgen $c_{1,0} - (b - y)_0$ diagram (see Fig. 14c). In Fig. 14c, the dwarf region is indicated as a shaded region (Árnadóttir et al., in prep.).

Figure 14d shows the $V_0 - s$ diagram for stars selected as dwarf and giant stars using the Strömgen $c_{1,0} - (b - y)_0$ diagram. The metal-poor giant stars that we identify in the $c_{1,0}$ vs. $(b - y)_0$ plane have a wide range of s -index values. The dotted line indicates the s -value above which metal-poor giant stars should be found. Figure 14d shows that metal-poor giant stars can not be distinguished from the dwarf stars using the s -index. Although the stars identified using the s -index are pre-dominantly metal-poor giant stars, the s -index is unable to reliably differentiate between metal-poor giant stars and the foreground dwarf stars to good accuracy. More importantly, the majority of the giant stars can not be identified by the s -index.

6. A comparison of stellar sequences and model predictions

The stellar sequences for dwarf stars constructed in Sect. 5.1 can be compared with model predictions based on stellar evolutionary tracks and stellar model atmospheres. Such comparisons are important for two reasons, they help us to understand the physical processes occurring inside stars (stellar evolution) and the processes in the stellar photospheres (e.g., how well we can model the lines in the resulting stellar spectra). Additionally, after ensuring that we understand these processes (to a certain level), we may utilise the resulting stellar isochrones and theoretically calculate indices to infer, e.g., the age of a globular cluster.

In Fig. 15, we compare our new stellar sequences for dwarf stars with the preliminary relations of Olsen (1984) and Crawford (1975). As can be seen, the metallicity dependence is significant and the lower envelope changes by about 0.1 in c_1 as we change the metallicity with 0.5 dex. For the reddest part, we

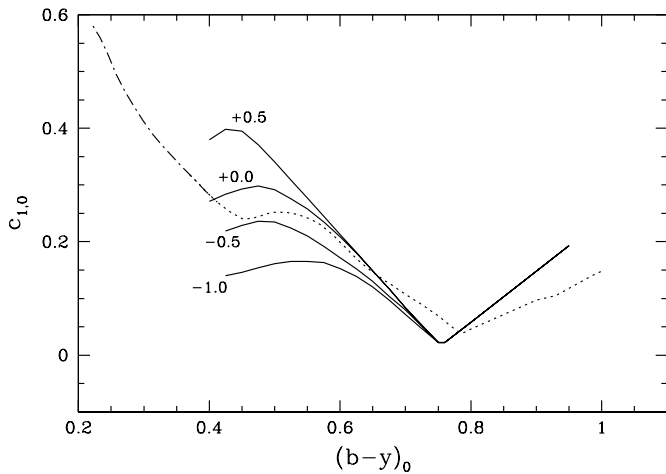


Fig. 15. Comparison of the new dwarf star sequences (solid lines), metallicities as indicated, to the preliminary relations by Olsen (1984) (dotted line) and by Crawford (1975) (dot-dashed line).

agree with the preliminary sequences in that there is only a single relation (see discussion in Sect. 5.1), although the slopes of the sequences differ.

6.1. A comparison with stellar isochrones

Few isochrones have been calculated for the Strömgren photometric system, the most important set is probably that provided by Vandenberg & Bell (1985) and derivations from that work. To convert theoretical stellar evolutionary sequences into stellar isochrones, a colour-temperature relation is required (e.g., Lester et al. 1986; Clem et al. 2004). The empirical calibration of Clem et al. (2004) is the most recent and is used to convert, e.g., the isochrones of Vandenberg & Bell (1985) and their derivatives onto the observed plane. Clem et al. (2004) performed a detailed comparison between stellar isochrones produced using their colour-temperature relation and sequences of, e.g., red giant branches for globular clusters with different metallicities, finding a good agreement.

Faria et al. (2007) performed an additional comparison of the stellar isochrones produced using the colour-temperature relation by Clem et al. (2004) with *uvby* photometry for field stars for which $[\text{Fe}/\text{H}]$ had been determined by high-resolution spectroscopy. Their dataset is essentially identical to that used by Clem et al. (2004) to obtain the, interpolated, colour-temperature relation for metallicities between -2 dex and super-solar metallicities. The comparison found some (still) unexplained discrepancies between the data and the isochrones. However, it was confirmed that the isochrones for about -2 dex and solar metallicity fit the field stars, with those metallicities, very well. Hence, there might be some problems with the empirical calibration needed for the colour transformation at intermediate metallicities. Here, we therefore repeat the comparison, this time as a comparison between our stellar sequences for dwarf stars and the isochrones derived using the colour-temperature relation by Clem et al. (2004).

The comparison is shown in Fig. 16. The stellar sequences and the isochrones in general agree well with our sequences for dwarf stars at $0.45 < (b-y)_0 < 0.7$. We note, however, that the stellar sequences trace the *lower* envelope of all stars that have a narrow range of metallicities (see Table 3) and the

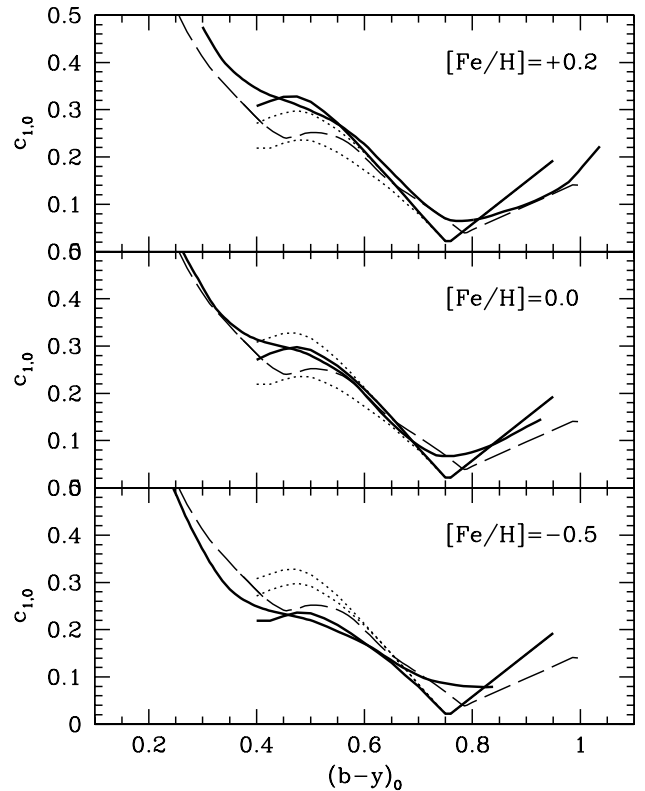


Fig. 16. A comparison of dwarf star sequences, as derived in this paper with stellar isochrones. In each panel, we show three of our sequences for dwarf stars for $[\text{Fe}/\text{H}] = +0.20, 0.0,$ and -0.5 . In each panel, the sequence with the metallicity indicated in the panel is shown with a thick solid line, the other two sequences are shown with dotted lines. The preliminary sequences by Olsen (1984) and by Crawford (1975) are shown with long dashes. An isochrone with the correct metallicity is also shown in each panel (thin, solid line). These isochrones are indicated with thick lines and all have an age of 1 Gyr (Vandenberg & Bell 1985; Clem et al. 2004).

isochrones should reproduce the mean metallicity. Hence, there might be some offset with respect to the $c_{1,0}$ index, but otherwise the agreement is good for this fairly narrow magnitude range of dwarf stars. This comparison spans the main sequence from the turn-off, late F-type dwarf stars to three magnitudes down the main sequence to $M_V \sim 8$ (compare with Fig. 4 b).

We performed a comparison between our sequences for dwarf stars, the stellar isochrones, and the calculated indices in the $c_{1,0}$ vs. $(b-y)_0$ diagram. This makes for an easy comparison with earlier works that often used $(b-y)_0$ as the colour along the x -axis. However, the $(v-y)_0$ colour is more sensitive to metallicity, as shown, e.g., by Calamida et al. (2007). This is true for both giant and dwarf stars. Although the $(v-y)_0$ is more sensitive to metallicity than $(b-y)_0$, it has the disadvantage that it is also sensitive to the presence of CH and CN molecules in the stellar atmosphere.

6.2. A note about calculated indices

Theoretical indices in the Strömgren system have been studied in several articles, including Lester et al. (1986),

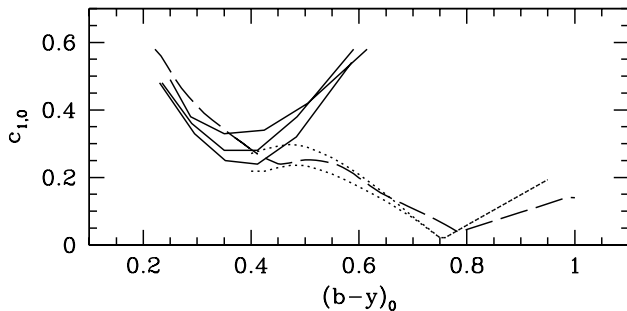


Fig. 17. A comparison of dwarf star sequences, as derived in this paper, for $[\text{Fe}/\text{H}]$ of 0, and -0.5 dex (dotted lines) with stellar indices, for stars with $\log g = 4.5$ and $[\text{Fe}/\text{H}]$ of 0, -0.5 , and -1.0 dex, from Önehag et al. (2009) (solid lines). The preliminary sequences by Olsen (1984) and by Crawford (1975) are also shown (long dashed line).

Gustafsson & Bell (1979), and Önehag et al. (2009). In Fig. 17, we perform a non-exhaustive comparison between our stellar sequences for dwarf stars and indices calculated by Önehag et al. (2009) for stars with $\log g = 4.5$. We show stellar sequences for 0 and -0.5 dex because we believe that the sequence for -1 dex is less robust (compare Fig. A.14). It is clear from this comparison that the calculated indices do not reproduce the colours found for field dwarf stars in the solar neighbourhood for $(b - y)_0 > 0.45$.

Based on the calculated indices, Önehag et al. (2009) derive a metallicity calibration that is nominally valid for stars with $0.22 < (b - y)_0 < 0.59$. In Table 2, we compare this calibration with the spectroscopic catalogue, in the same way as for the empirically derived metallicity calibrations. We find an offset of 0.33 dex with a scatter of 0.3 dex. This calibration clearly reproduces the spectroscopically derived iron abundances more poorly than the empirical calibrations available in the literature. This shortcoming of the theoretical calibrations was already noted and discussed by Önehag et al. (2009).

6.3. $\log g$ from $uvby$ photometry - a critical evaluation

Although the Strömgren system is clearly capable of distinguishing between dwarf and giant stars for colours redder than $(b - y)_0 \sim 0.55$, the situation is far less clear when we consider the turn-off and sub-giant region. To separate, e.g., field dwarf stars from field sub-giants, we need a measure of their surface gravity for which any metallicity dependence has been taken into account, before being able to distinguish between the dwarf, sub-giant, and giant stars in this narrow colour space (compare Fig. 2).

Hence, it would be desirable to derive $\log g$ directly from the photometry itself. To our knowledge, the only $\log g$ calibration based only on $uvby$ photometry is that of Olsen (1984). If β were to be included, additional calibrations would be available (including van Leeuwen 2009; Edvardsson et al. 1993, where the calibration is only shown graphically).

Using the stars in Table B.1 with $\log g$ determinations from Valenti & Fischer (2005), we test the calibration of Olsen (1984). Figure 18 shows the $\log g$ derived in the spectroscopic study of Valenti & Fischer (2005) ($\log g_{\text{spec}}$) minus the $\log g$ derived from the photometry ($\log g_{\text{phot}}$). As can be seen, the calibration has a strong dependence on $[\text{Fe}/\text{H}]$.

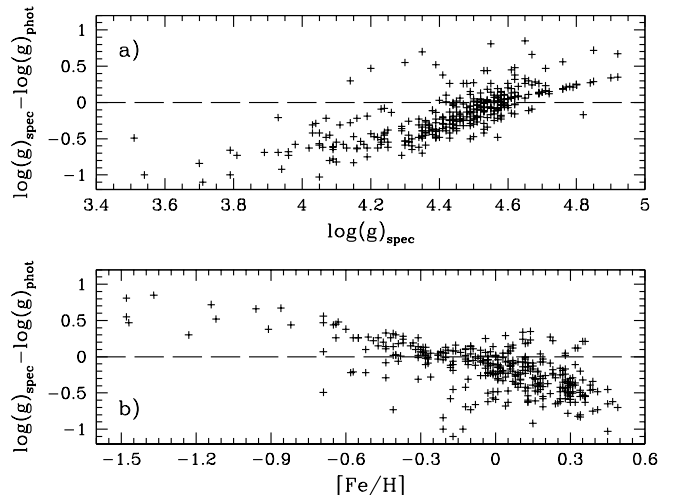


Fig. 18. A comparison of $\log g$ determined using the photometric calibration by Olsen (1984) and $\log g$ determined from an abundance analysis based on high resolution spectroscopy (Valenti & Fischer 2005). **a)** The difference as a function of $\log g$ determined in the spectroscopic analysis. **b)** The difference as a function of $[\text{Fe}/\text{H}]$.

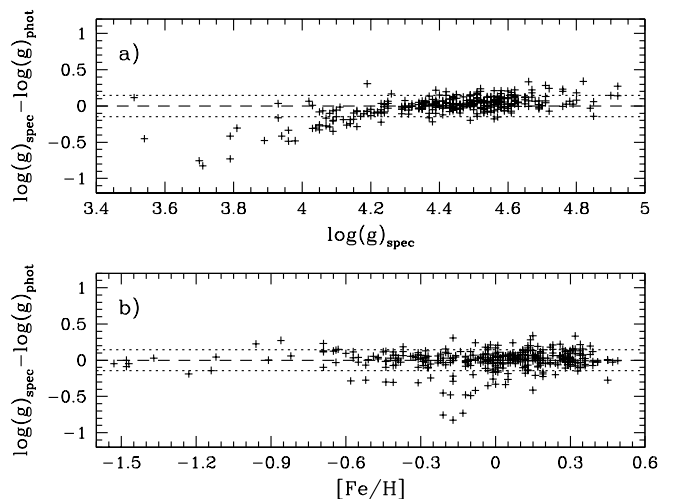


Fig. 19. We show our best attempt at deriving a new $\log g$ calibration from $uvby$ photometry. **a)** A comparison of $\log g$ determined using Eq. (3) and $\log g$ determined from abundance analysis based on high resolution spectroscopy (Valenti & Fischer 2005), plotted as a function of spectroscopically determined $\log g$. The mean difference (dashed line) is 0.00 with a $\sigma = 0.15$ (dotted line). **b)** A comparison of $\log g$ determined using Eq. (3) and $\log g$ determined from high resolution spectroscopy (Valenti & Fischer 2005) as a function of $[\text{Fe}/\text{H}]$. The mean difference (dashed line) is 0.00 with a $\sigma = 0.15$ (dotted line).

We now attempt the construction of a new calibration to derive $\log g$ directly from dereddened $uvby$ photometry, using the spectroscopic catalogue in Table B.1. We start with a third order polynomial in $(b - y)_0$, $m_{1,0}$, and $c_{1,0}$. We note that some calibrations include terms in $[\text{Fe}/\text{H}]$, which we do not because we derive $[\text{M}/\text{H}]$ from the same photometry and hence adding $[\text{M}/\text{H}]$ terms

would only mean adding yet more terms to the equation without gaining any further knowledge.

After removing terms that do not contribute significantly, we obtain the fifteenth order polynomial

$$\begin{aligned}
\log g = & -178.0420(b-y)_0 + 109.7056m_{1,0} \\
& +47.4263c_{1,0} + 615.0911(b-y)_0^2 \\
& +47.0152m_{1,0}^2 - 114.8399c_{1,0}^2 \\
& -525.0138(b-y)_0m_{1,0} - 112.5602m_{1,0}c_{1,0} \\
& -598.8569(b-y)_0^3 + 674.8341(b-y)_0^2m_{1,0} \\
& -267.7717(b-y)_0^2c_{1,0} - 147.5764m_{1,0}^2(b-y)_0 \\
& +265.3608c_{1,0}^2(b-y)_0 + 266.5860(b-y)_0m_{1,0}c_{1,0} \\
& +14.3503.
\end{aligned} \tag{3}$$

If we were to include [Fe/H] terms the result was a ninth order polynomial. However, as we want to derive both metallicity and surface gravity from the photometry itself, the 15th order polynomial presented above is a better choice.

Figure 19 shows a comparison with $\log g$ from Table B.1. The comparison is good for stars with $\log g \gtrsim 4.0$ but is progressively poorer towards more evolved star, including the regime where we would most need a good calibration to separate dwarf and sub-giant stars with similar colours! Hence, the use of our new calibration is limited to $\log g > 4.0$. Equation 3 is calibrated using dwarf stars in the parameter ranges $0.236 < (b-y)_0 < 0.616$, $0.122 < c_{1,0} < 0.441$, $0.075 < m_{1,0} < 0.679$, and $-1.64 < [\text{Fe}/\text{H}] < 0.49$.

We also considered restricting ourselves to the region of the $c_{1,0} - (b-y)_0$ plane where we most need a calibration ($(b-y)_0 < 0.55$, $0.24 < c_{1,0} < 0.44$, and $c_{1,0} < -1.504 * (b-y)_0 + 1.147$). This also failed in the same way as described for the wider parameter ranges, i.e. we were not able to reliably determine the $\log g$ for subgiant stars. We also attempted to make a calibration that would retrieve the original $\log g$ in a synthetic stellar population, this also failed. Hence, there does not appear to be an easy, straightforward way to derive $\log g$ directly from the Strömgren *uvby* photometry for turn-off and subgiant stars.

Based on their theoretical investigation, Önehag et al. (2009) find that for dwarf stars cooler than the Sun $c_{1,0}$ is not a good measure of stellar gravity. However, from our empirical comparison of $\log g$ derived using the calibration by Olsen (1984) and from spectroscopy we find that for stars redder than $(b-y)_0 \sim 0.5$ the spectroscopic $\log g$ compares very well with the photometric $\log g$. For stars with $\log g \sim 4.5$, the comparison is also good. It thus seems that for main sequence, cool dwarf stars the Strömgren system is able to predict the surface gravity of the star.

7. Summary

As part of our studies of the properties of the Milky Way disk system we have undertaken a critical evaluation of the Strömgren system's ability to provide accurate stellar parameters and to distinguish between dwarf, sub-giant, and giant stars.

We have found that the metallicity calibration for dwarf stars by Ramírez & Meléndez (2005a) is the most widely applicable calibration for determining metallicities for dwarf and subgiant stars. The calibration of Olsen (1984) provides an extension from $(b-y)_0 = 0.8$ to $(b-y)_0 = 1.0$. We also note that the older calibration of Schuster & Nissen (1989b) performs almost

equally well, but it does not extend to as red colours as the calibration of Ramírez & Meléndez (2005a).

Although we have found that *uvby* photometry can readily distinguish between giant and dwarf stars for redder colours, it is disconcerting that no calibration of $\log g$, for dwarf and subgiant stars, is able to reproduce $\log g$ derived from either spectra or Hipparcos parallaxes. In his provisional calibration van Leeuwen (2009) also notes the same.

Using the catalogues of Olsen (1993), Olsen (1994a), and Olsen (1994b) and the metallicity calibration of Ramírez & Meléndez (2005a), we have traced new, improved standard sequences for dwarf stars. These new sequences are metallicity dependent and provide crucial calibrations for, e.g., stellar isochrones.

Even though we have found that stellar isochrones in the *uvby* system reasonably well reproduce empirical stellar sequences it is clear that the disagreement between theoretically calculated Strömgren indices and observed ones can be large. This appears somewhat surprising as stellar isochrones employ the same type of model atmospheres to get the predicted colours as is often used for the elemental abundance studies. This state of affairs is unsatisfactory and we encourage future theoretical studies to resolve these problems.

As part of this work, we have compiled a catalogue of dwarf stars with *uvby* photometry as well as [Fe/H] derived from high-resolution, high S/N spectroscopy. The iron abundances have been homogenised to the scale provided by Valenti & Fischer (2005). This catalogue is provided in full (in electronic form) with this paper.

Acknowledgements. We would like to thank the anonymous referee for pointing out the work done by Ramírez & Meléndez (2004) on the metallicity calibration of Strömgren photometry for giant stars. Bengt Gustafsson is thanked for a careful reading of the penultimate manuscript and the provision of numerous detailed comments and discussions that improved both the content and the style of the paper. SF is a Royal Swedish Academy of Sciences Research Fellow supported by a grant from the Knut and Alice Wallenberg Foundation. This research has made use of the SIMBAD database, operated at CDS, Strasbourg, France.

References

- Abazajian, K. N., Adelman-McCarthy, J. K., Agüeros, M. A., et al. 2009, *ApJS*, 182, 543
- Adén, D., Feltzing, S., Koch, A., et al. 2009a, *A&A*, 506, 1147
- Adén, D., Wilkinson, M. I., Read, J. I., et al. 2009b, *ApJ*, 706, L150
- Alonso, A., Arribas, S., & Martínez-Roger, C. 1996, *A&AS*, 117, 227
- Alonso, A., Arribas, S., & Martínez-Roger, C. 1999, *A&AS*, 140, 261
- Anthony-Twarog, B. J. & Twarog, B. A. 1994, *AJ*, 107, 1577
- Anthony-Twarog, B. J. & Twarog, B. A. 1998, *AJ*, 116, 1922
- Arce, H. G. & Goodman, A. A. 1999, *ApJ*, 512, L135
- Arellano Ferro, A. & Mendoza V., E. E. 1993, *AJ*, 106, 2516
- Beers, T. C., Drilling, J. S., Rossi, S., et al. 2002, *AJ*, 124, 931
- Bell, R. A. & Gustafsson, B. 1978, *A&AS*, 34, 229
- Bensby, T., Feltzing, S., Lundström, I., & Ilyin, I. 2005, *A&A*, 433, 185
- Bond, H. E. 1970, *ApJS*, 22, 117
- Bond, H. E. 1980, *ApJS*, 44, 517
- Bonfils, X., Delfosse, X., Udry, S., et al. 2005, *A&A*, 442, 635
- Bonifacio, P., Caffau, E., & Molaro, P. 2000, *A&AS*, 145, 473
- Calamida, A., Bono, G., Stetson, P. B., et al. 2007, *ApJ*, 670, 400
- Calamida, A., Bono, G., Stetson, P. B., et al. 2009, *ApJ*, 706, 1277
- Carney, B. W. 1983, *AJ*, 88, 623
- Carollo, D., Beers, T. C., Lee, Y. S., et al. 2008, *Nature*, 451, 216
- Chen, Y. Q., Nissen, P. E., Zhao, G., Zhang, H. W., & Benoni, T. 2000, *A&AS*, 141, 491
- Clausen, J. V., Larsen, S. S., Garcia, J. M., Gimenez, A., & Storm, J. 1997, *A&AS*, 122, 559
- Clem, J. L., VandenBerg, D. A., Grundahl, F., & Bell, R. A. 2004, *AJ*, 127, 1227
- Cohen, J. G. & Huang, W. 2009, *ApJ*, 701, 1053
- Cousins, A. W. J. 1987, *South African Astronomical Observatory Circular*, 11, 93
- Crawford, D. L. 1975, *AJ*, 80, 955

- Crawford, D. L. & Barnes, J. V. 1970, *AJ*, 75, 978
- Edvardsson, B., Andersen, J., Gustafsson, B., et al. 1993, *A&A*, 275, 101
- ESA. 1997, *VizieR Online Data Catalog*, 1239, 0
- Faria, D. 2006, *Photometry of resolved stellar populations in local group galaxies* (PhD thesis), *Lund Observatory*, ISBN: 978-91-628-6905-2.
- Faria, D., Feltzing, S., Lundström, I., et al. 2007, *A&A*, 465, 357
- Favata, F., Micela, G., & Sciortino, S. 1997, *A&A*, 323, 809
- Feltzing, S. & Gustafsson, B. 1998, *A&AS*, 129, 237
- Ferguson, A. M. N., Johnson, R. A., Faria, D. C., et al. 2005, *ApJ*, 622, L109
- Flynn, C. & Morell, O. 1997, *MNRAS*, 286, 617
- Gilmore, G. & Reid, N. 1983, *MNRAS*, 202, 1025
- Golay, M., ed. 1974, *Astrophysics and Space Science Library*, Vol. 41, Introduction to astronomical photometry
- Grebel, E. K. & Richtler, T. 1992, *A&A*, 253, 359
- Grønbech, B., Olsen, E. H., & Strömgren, B. 1976, *A&AS*, 26, 155
- Grundahl, F., Stetson, P. B., & Andersen, M. I. 2002, *A&A*, 395, 481
- Gustafsson, B. & Ardeberg, A. 1978, in *Astronomical Papers Dedicated to Bengt Strömgren*, ed. A. Reiz & T. Andersen, 145–152
- Gustafsson, B. & Bell, R. A. 1979, *A&A*, 74, 313
- Gustafsson, B. & Nissen, P. E. 1972, *A&A*, 19, 261
- Haywood, M. 2002, *MNRAS*, 337, 151
- Heiter, U. & Luck, R. E. 2003, *AJ*, 126, 2015
- Helmi, A., Ivezić, Z., Prada, F., et al. 2003, *ApJ*, 586, 195
- Hilker, M. 2000, *A&A*, 355, 994
- Holmberg, J., Nordström, B., & Andersen, J. 2007, *A&A*, 475, 519
- Ibata, R., Irwin, M., Lewis, G., Ferguson, A. M. N., & Tanvir, N. 2001, *Nature*, 412, 49
- Ivezić, Ž., Sesar, B., Jurić, M., et al. 2008, *ApJ*, 684, 287
- Johnson, H. L. & Morgan, W. W. 1953, *ApJ*, 117, 313
- Jönch-Sørensen, H. 1995, *A&A*, 298, 799
- Kirby, E. N., Simon, J. D., Geha, M., Guhathakurta, P., & Grebel, A. 2008, *ApJ*, 685, L43
- Kotoneva, E., Flynn, C., Chiappini, C., & Matteucci, F. 2002, *MNRAS*, 336, 879
- Lagerholm, C. 2008, *An investigation of metallicity and memberships of the Sextans dSph galaxy*
- Landolt, A. U. 1992, *AJ*, 104, 340
- Lee, Y. S., Beers, T. C., Sivarani, T., et al. 2008, *AJ*, 136, 2050
- Lester, J. B., Gray, R. O., & Kurucz, R. L. 1986, *ApJS*, 61, 509
- Luck, R. E. & Heiter, U. 2005, *AJ*, 129, 1063
- Malyuto, V. 1994, *A&AS*, 108, 441
- Martell, S. & Laughlin, G. 2002, *ApJ*, 577, L45
- Martell, S. L. & Smith, G. H. 2004, *PASP*, 116, 920
- Mermilliod, J.-C., Mermilliod, M., & Hauck, B. 1997, *A&AS*, 124, 349
- Mishenina, T. V., Soubiran, C., Kovtyukh, V. V., & Korotin, S. A. 2004, *A&A*, 418, 551
- Nissen, P. E. 1981, *A&A*, 97, 145
- Nordström, B., Mayor, M., Andersen, J., et al. 2004, *A&A*, 418, 989
- Ochsenbein, F., Bauer, P., & Marcout, J. 2000, *A&AS*, 143, 23
- Olsen, E. H. 1983, *A&AS*, 54, 55
- Olsen, E. H. 1984, *A&AS*, 57, 443
- Olsen, E. H. 1993, *A&AS*, 102, 89
- Olsen, E. H. 1994a, *A&AS*, 104, 429
- Olsen, E. H. 1994b, *A&AS*, 106, 257
- Olsen, E. H. 1995, *A&A*, 295, 710
- Önehag, A., Gustafsson, B., Eriksson, K., & Edvardsson, B. 2009, *A&A*, 498, 527
- Perry, C. L., Olsen, E. H., & Crawford, D. L. 1987, *PASP*, 99, 1184
- Perryman, M. A. C., Lindegren, L., Kovalevsky, J., et al. 1997, *A&A*, 323, L49
- Ramírez, I. & Meléndez, J. 2004, *A&A*, 417, 301
- Ramírez, I. & Meléndez, J. 2005a, *ApJ*, 626, 446
- Ramírez, I. & Meléndez, J. 2005b, *ApJ*, 626, 465
- Santos, N. C., Israelian, G., & Mayor, M. 2001, *A&A*, 373, 1019
- Santos, N. C., Israelian, G., & Mayor, M. 2004, *A&A*, 415, 1153
- Santos, N. C., Israelian, G., Mayor, M., et al. 2005, *A&A*, 437, 1127
- Schlegel, D. J., Finkbeiner, D. P., & Davis, M. 1998, *ApJ*, 500, 525
- Schuster, W. J., Beers, T. C., Michel, R., Nissen, P. E., & García, G. 2004, *A&A*, 422, 527
- Schuster, W. J., Moitinho, A., Márquez, A., Parrao, L., & Covarrubias, E. 2006, *A&A*, 445, 939
- Schuster, W. J. & Nissen, P. E. 1988, *A&AS*, 73, 225
- Schuster, W. J. & Nissen, P. E. 1989a, *A&A*, 222, 69
- Schuster, W. J. & Nissen, P. E. 1989b, *A&A*, 221, 65
- Schuster, W. J., Nissen, P. E., Parrao, L., Beers, T. C., & Overgaard, L. P. 1996, *A&AS*, 117, 317
- Sousa, S. G., Santos, N. C., Israelian, G., Mayor, M., & Monteiro, M. J. P. F. G. 2006, *A&A*, 458, 873
- Strigari, L. E., Bullock, J. S., Kaplinghat, M., et al. 2008, *Nature*, 454, 1096
- Strömgren, B. 1963, *QJRAS*, 4, 8
- Strömgren, B. 1964, *Astrophysica Norvegica*, 9, 333
- Thorén, P. & Feltzing, S. 2000, *A&A*, 363, 692
- Twarog, B. A., Anthony-Twarog, B. J., & De Lee, N. 2003, *AJ*, 125, 1383
- Twarog, B. A., Vargas, L. C., & Anthony-Twarog, B. J. 2007, *AJ*, 134, 1777
- Valenti, J. A. & Fischer, D. A. 2005, *ApJS*, 159, 141
- van Leeuwen, F. 2007, *Hipparcos, the New Reduction of the Raw Data* (Hipparcos, the New Reduction of the Raw Data. By Floor van Leeuwen, Institute of Astronomy, Cambridge University, Cambridge, UK Series: Astrophysics and Space Science Library, Vol. 350 20 Springer Dordrecht)
- van Leeuwen, F. 2009, *A&A*, 497, 209
- VandenBerg, D. A. & Bell, R. A. 1985, *ApJS*, 58, 561
- VandenBerg, D. A., Bergbusch, P. A., & Dowler, P. D. 2006, *ApJS*, 162, 375
- von Hippel, T. & Bothun, G. D. 1993, *ApJ*, 407, 115
- von Hippel, T. A. 1992, *AJ*, 104, 1765
- Wolf, V. M. & Wallerstein, G. 2005, *MNRAS*, 356, 963
- Yasuda, N., Fukugita, M., & Schneider, D. P. 2007, *AJ*, 134, 698
- Yong, D. & Lambert, D. L. 2003, *PASP*, 115, 22
- York, D. G., Adelman, J., Anderson, Jr., J. E., et al. 2000, *AJ*, 120, 1579

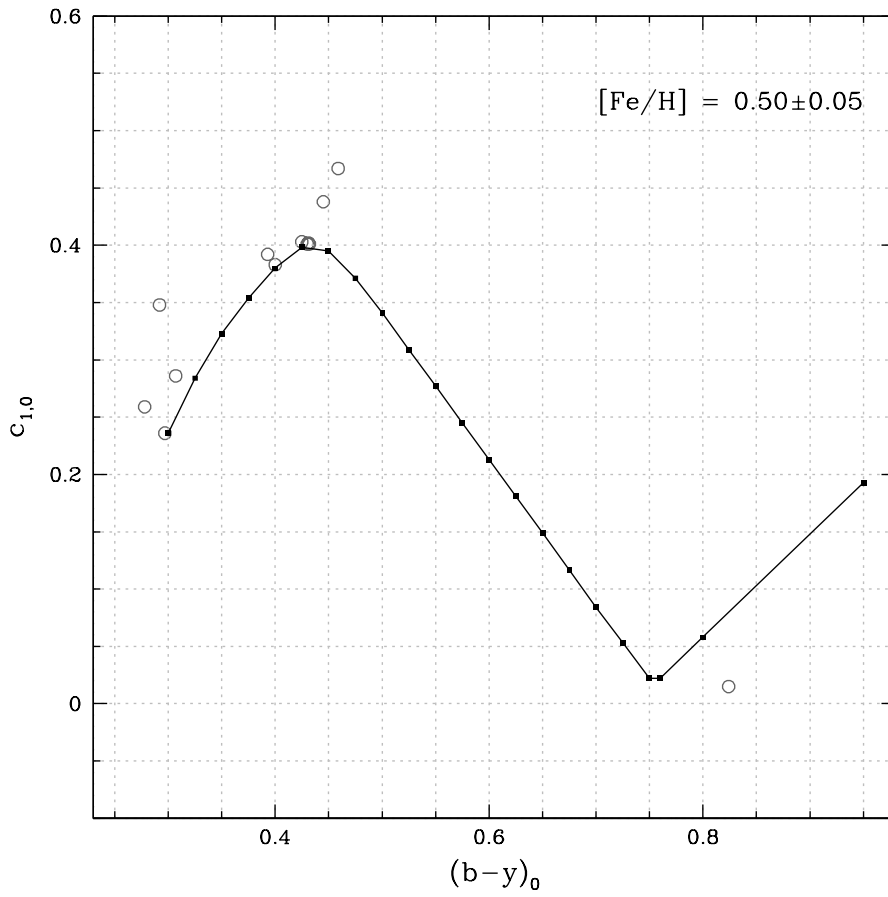


Fig. A.1. The figure shows how the dwarf star sequence was traced from nearby dwarf stars with $[Fe/H] = 0.50 \pm 0.05$ plotted in the $c_{1,0}$ vs $(b-y)_0$ diagram.

Appendix A: Stellar sequences

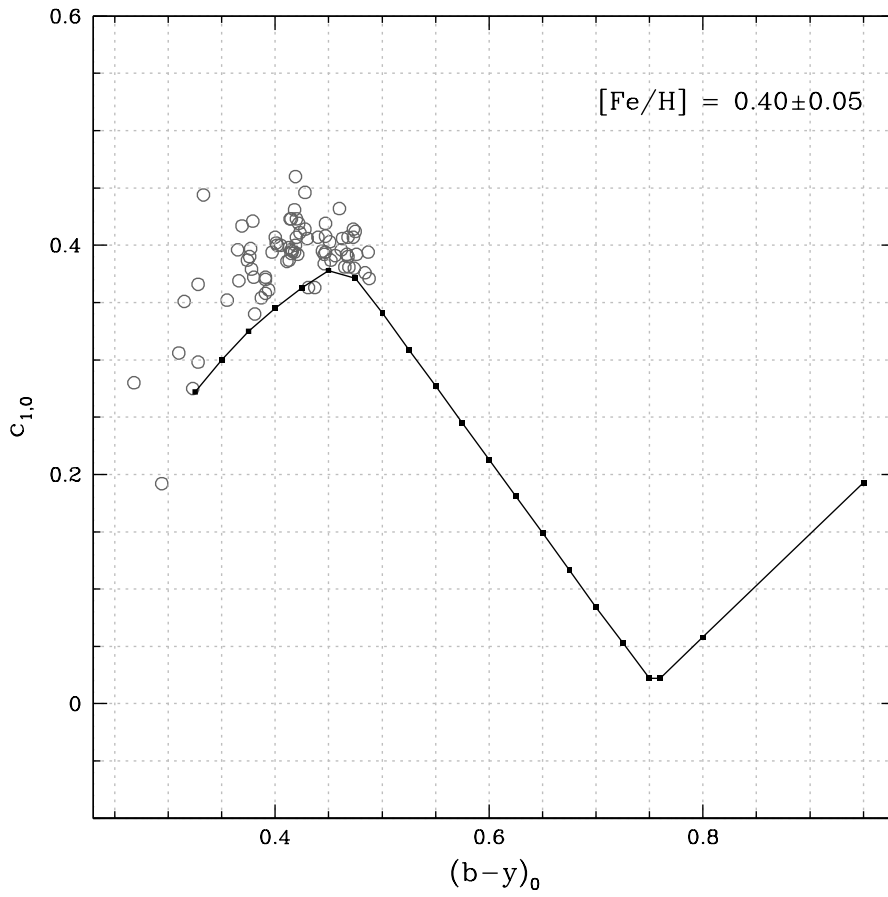


Fig. A.2. The figure shows how the dwarf star sequence was traced from nearby dwarf stars with $[Fe/H] = 0.40 \pm 0.05$ plotted in the $c_{1,0}$ vs $(b-y)_0$ diagram.

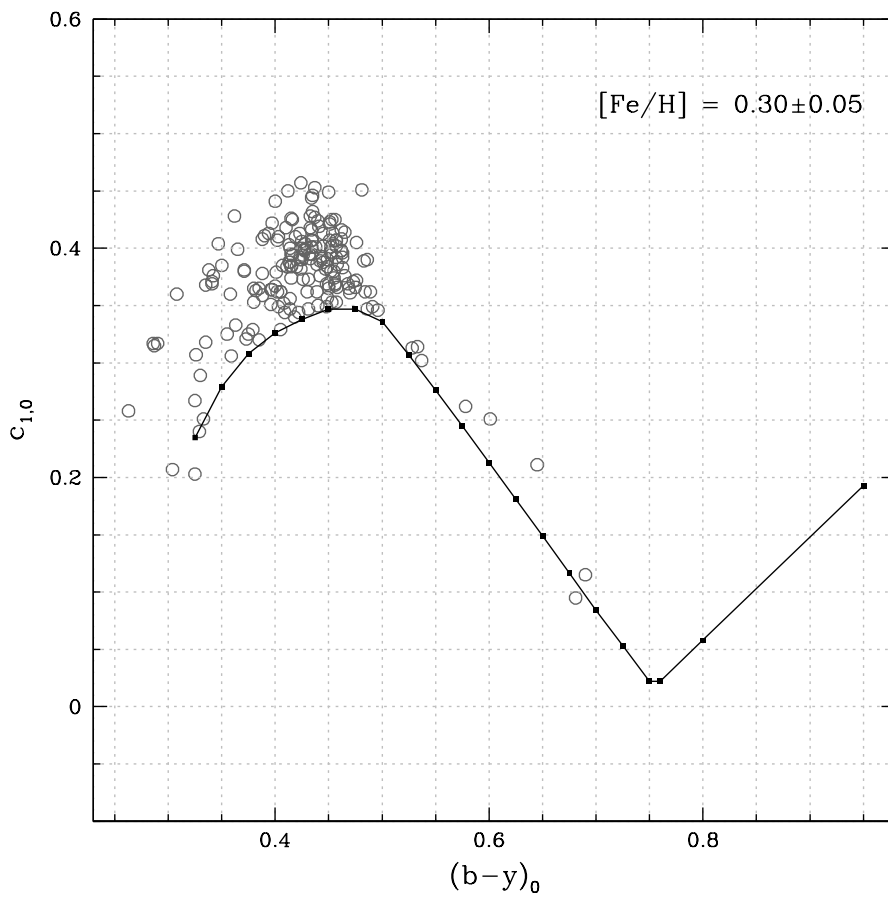


Fig. A.3. The figure shows how the dwarf star sequence was traced from nearby dwarf stars with $[Fe/H] = 0.30 \pm 0.05$ plotted in the $c_{1,0}$ vs $(b-y)_0$ diagram.

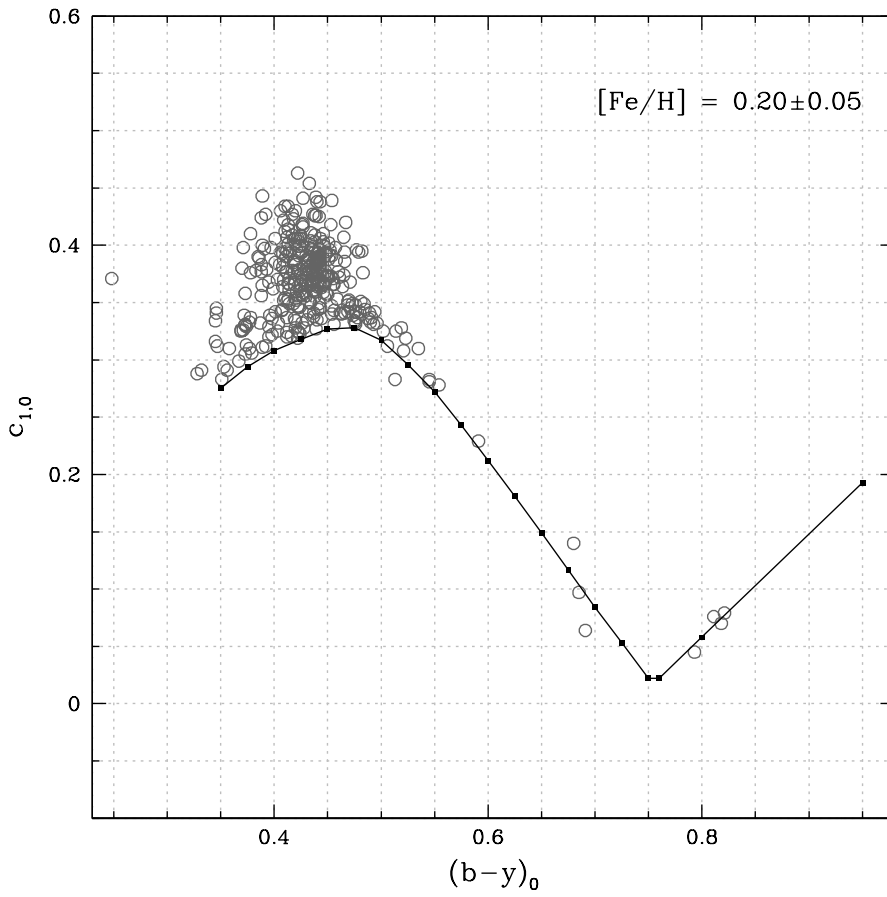


Fig. A.4. The figure shows how the dwarf star sequence was traced from nearby dwarf stars with $[Fe/H] = 0.20 \pm 0.05$ plotted in the $c_{1,0}$ vs $(b-y)_0$ diagram.

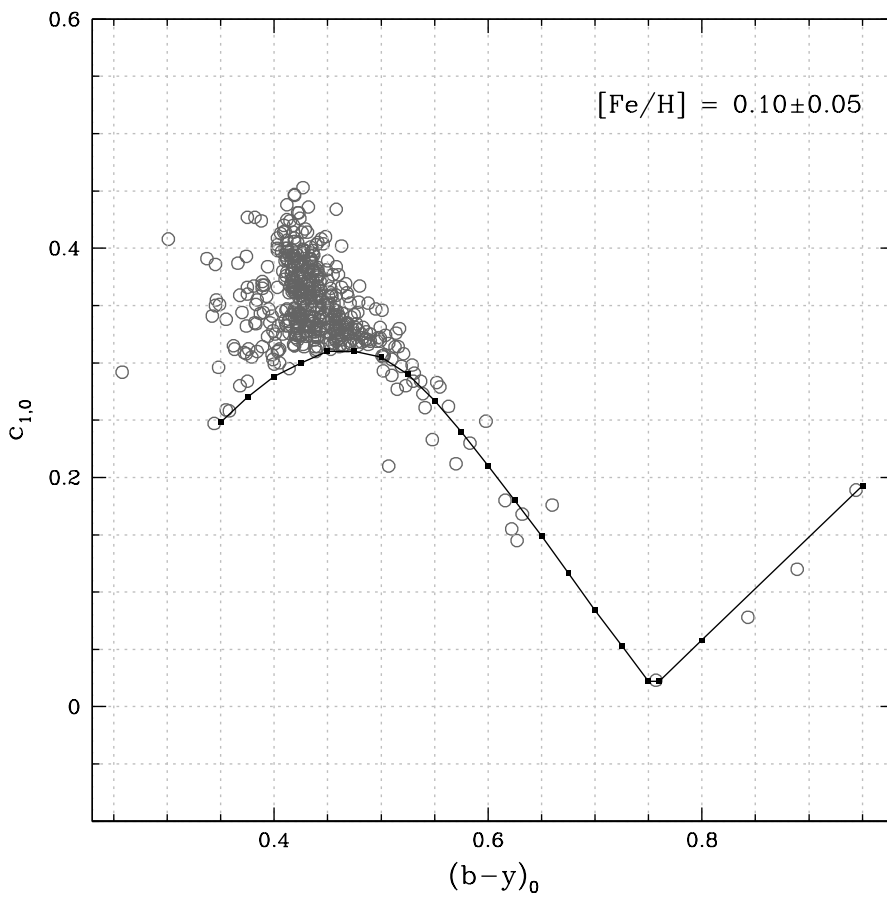


Fig. A.5. The figure shows how the dwarf star sequence was traced from nearby dwarf stars with $[Fe/H] = 0.10 \pm 0.05$ plotted in the $c_{1,0}$ vs $(b-y)_0$ diagram.

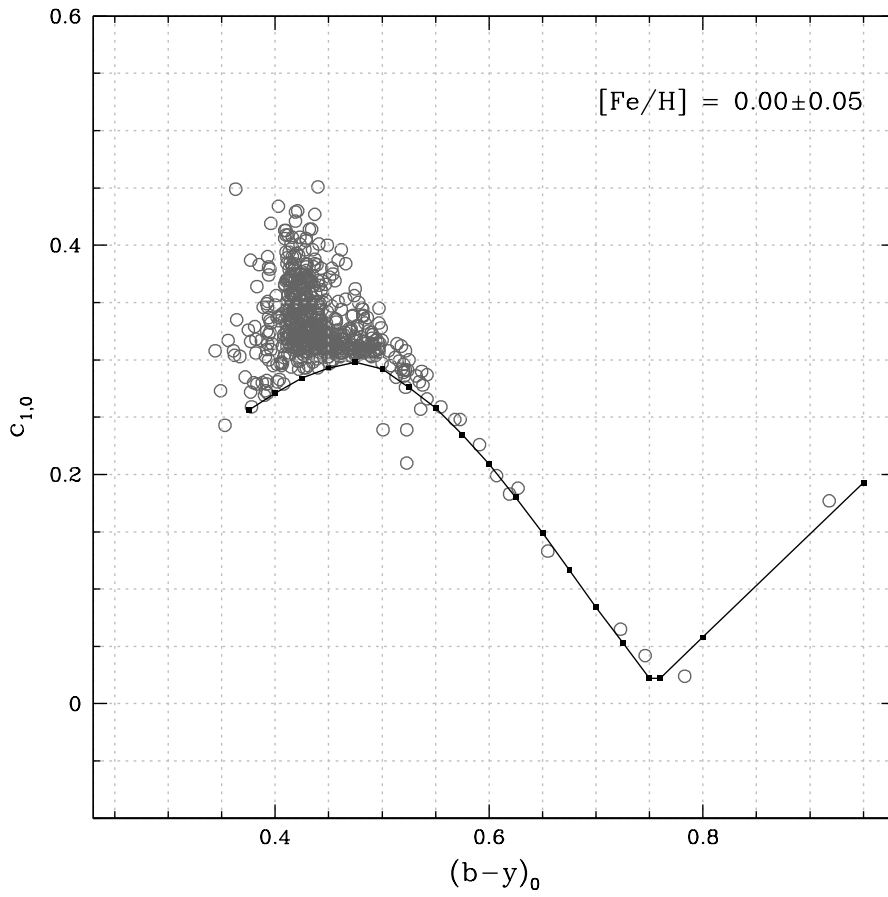


Fig. A.6. The figure shows how the dwarf star sequence was traced from nearby dwarf stars with $[Fe/H] = 0.00 \pm 0.05$ plotted in the $c_{1,0}$ vs $(b-y)_0$ diagram.

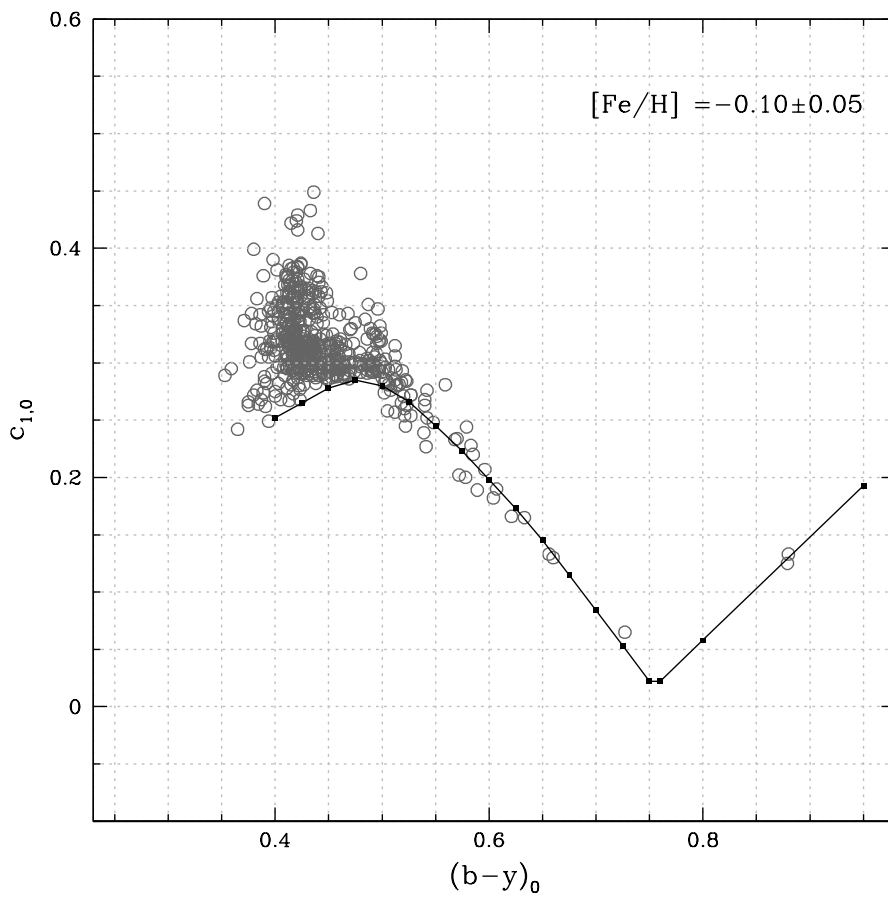


Fig. A.7. The figure shows how the dwarf star sequence was traced from nearby dwarf stars with $[Fe/H] = -0.10 \pm 0.05$ plotted in the $c_{1,0}$ vs $(b-y)_0$ diagram.

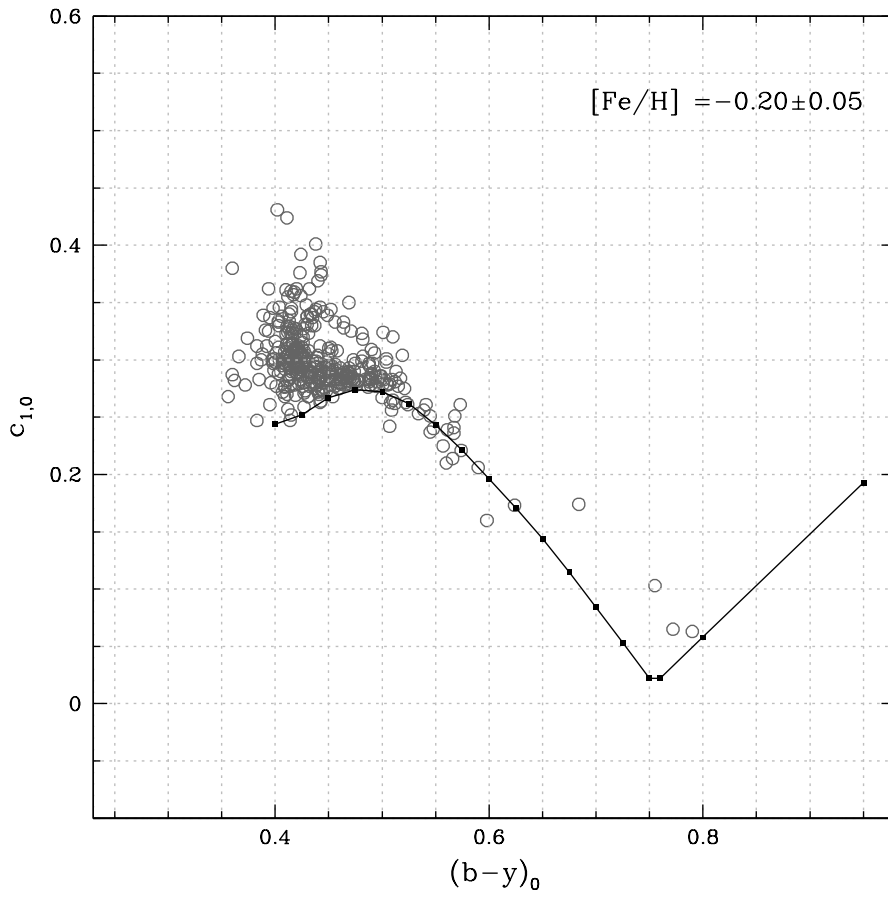


Fig. A.8. The figure shows how the dwarf star sequence was traced from nearby dwarf stars with $[Fe/H] = -0.20 \pm 0.05$ plotted in the $c_{1,0}$ vs $(b-y)_0$ diagram.

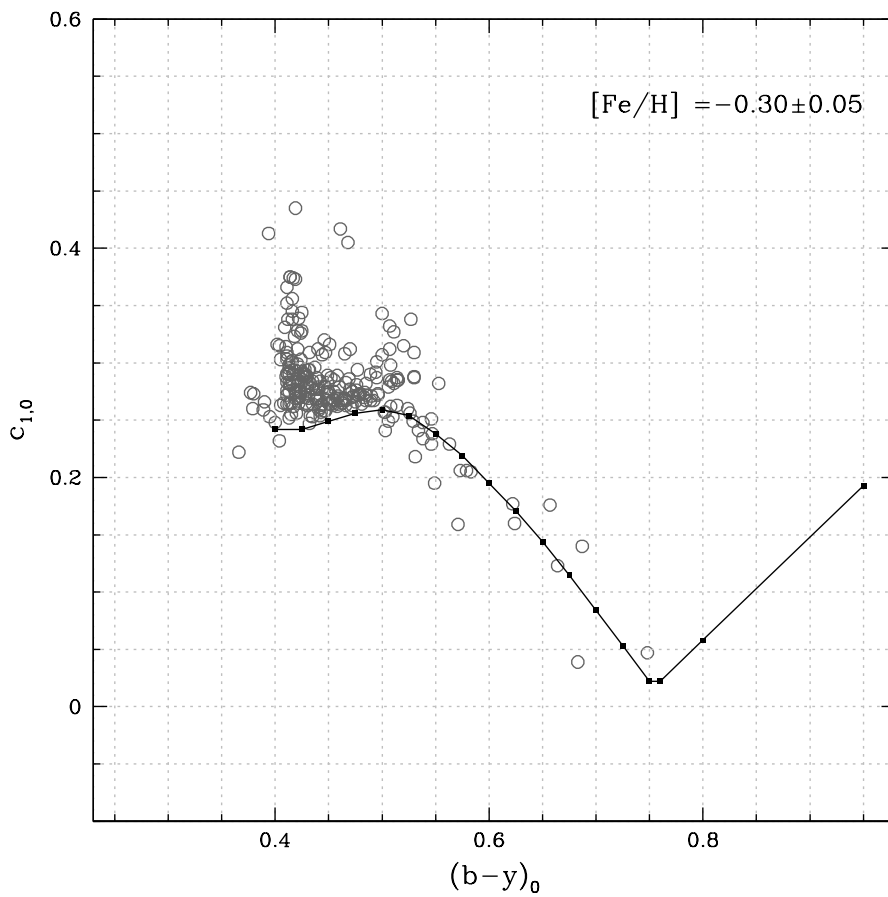


Fig. A.9. The figure shows how the dwarf star sequence was traced from nearby dwarf stars with $[Fe/H] = -0.30 \pm 0.05$ plotted in the $c_{1,0}$ vs $(b-y)_0$ diagram.

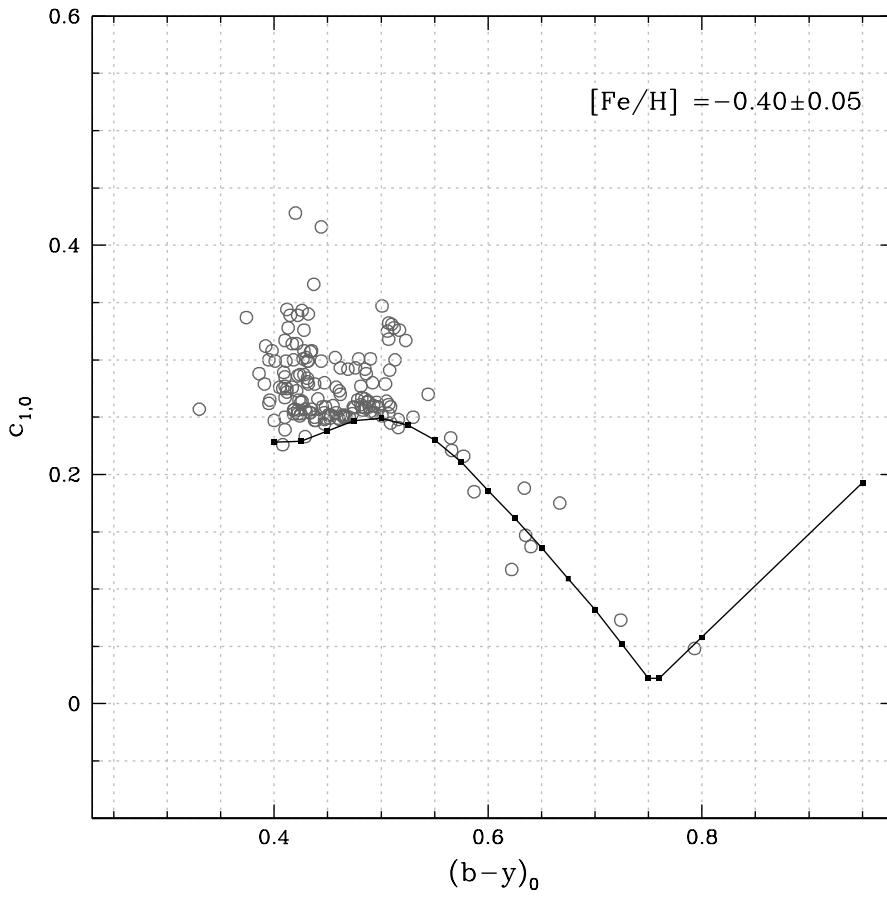


Fig. A.10. The figure shows how the dwarf star sequence was traced from nearby dwarf stars with $[Fe/H] = -0.40 \pm 0.05$ plotted in the $c_{1,0}$ vs $(b-y)_0$ diagram.

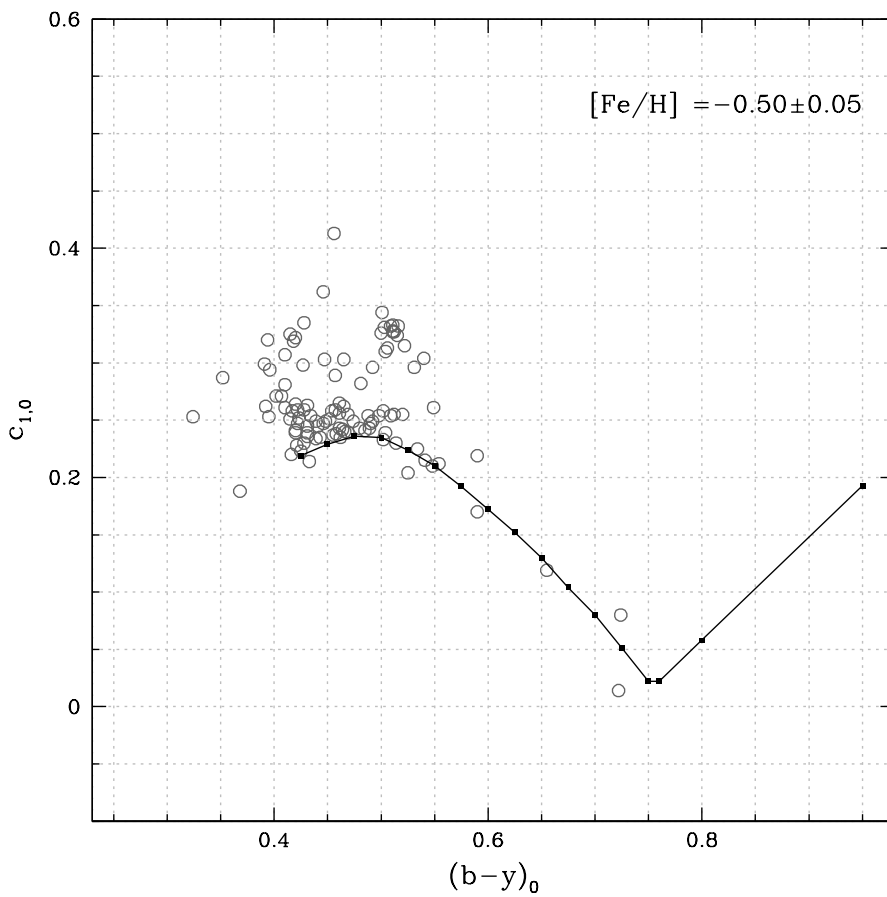


Fig. A.11. The figure shows how the dwarf star sequence was traced from nearby dwarf stars with $[Fe/H] = -0.50 \pm 0.05$ plotted in the $c_{1,0}$ vs $(b-y)_0$ diagram.

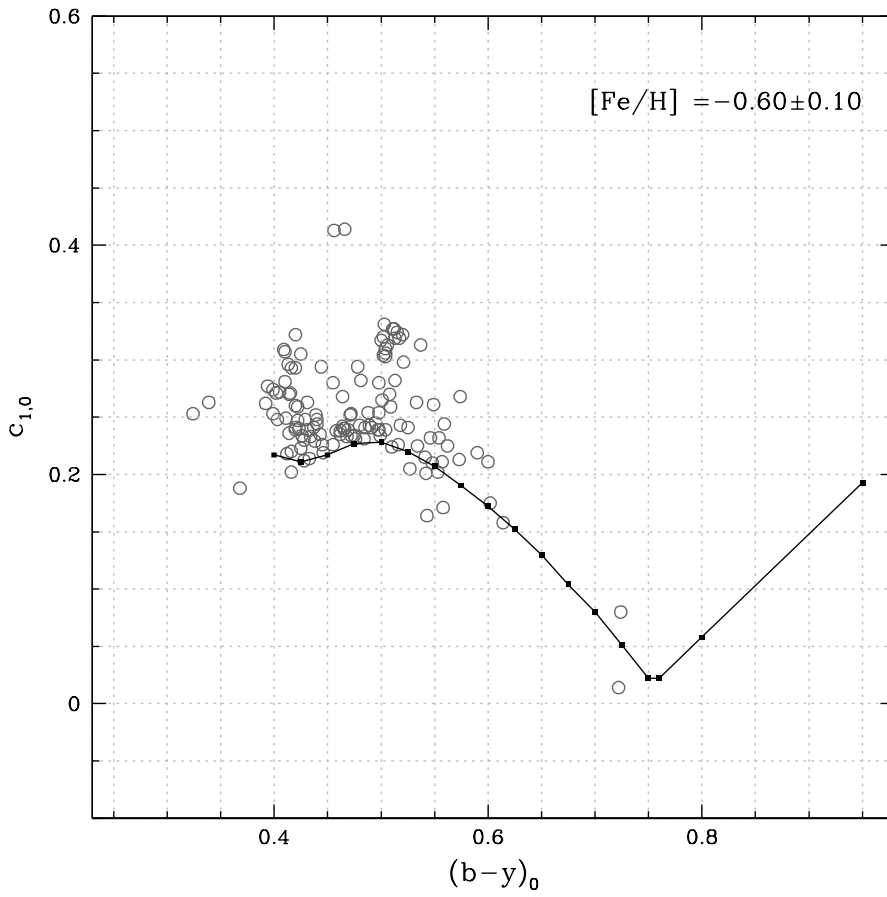


Fig. A.12. The figure shows how the dwarf star sequence was traced from nearby dwarf stars with $[Fe/H] = -0.60 \pm 0.10$ plotted in the $c_{1,0}$ vs $(b-y)_0$ diagram.

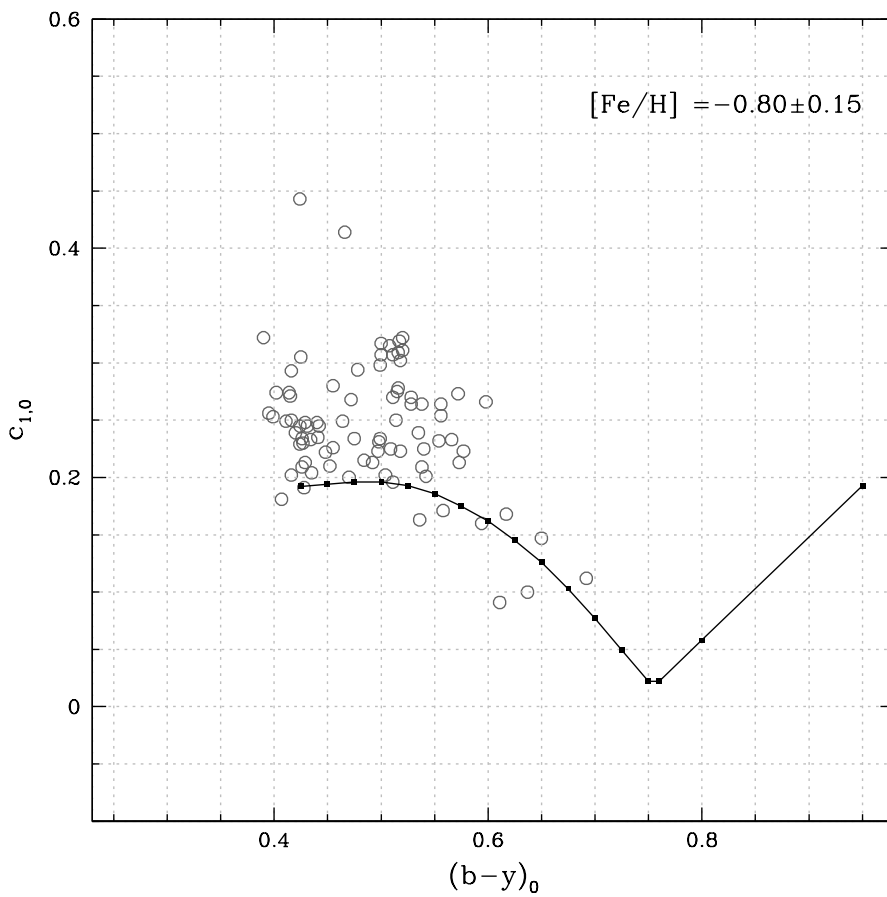


Fig. A.13. The figure shows how the dwarf star sequence was traced from nearby dwarf stars with $[Fe/H] = -0.80 \pm 0.15$ plotted in the $c_{1,0}$ vs $(b-y)_0$ diagram.

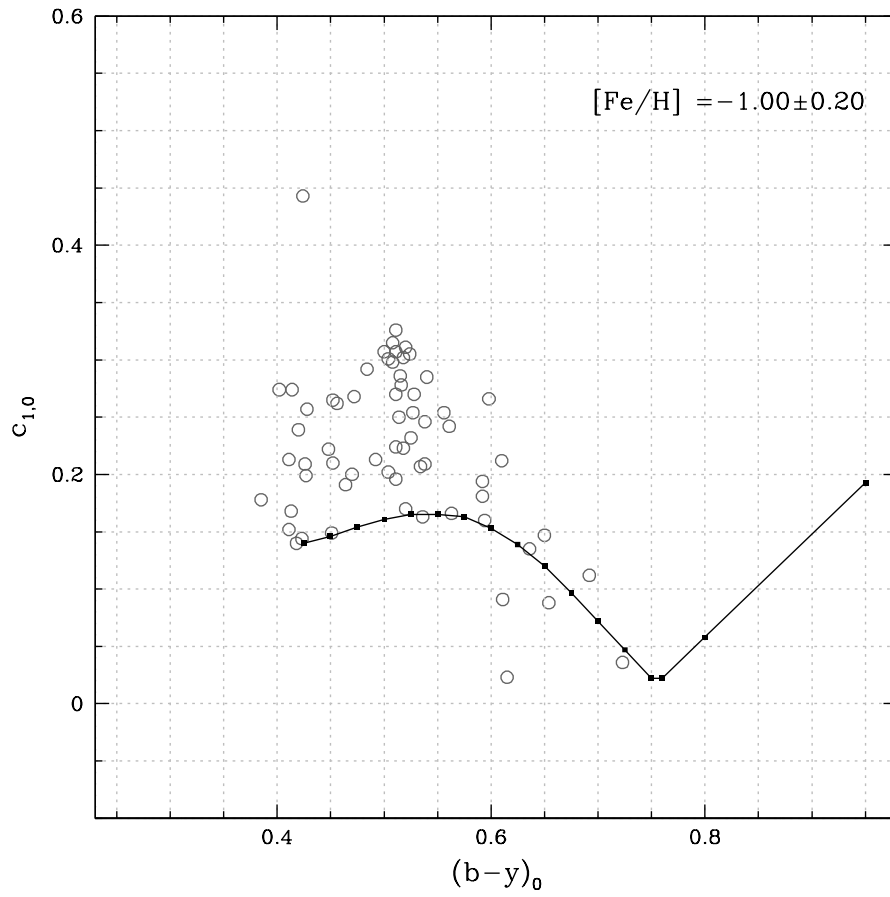


Fig. A.14. The figure shows how the dwarf star sequence was traced from nearby dwarf stars with $[\text{Fe}/\text{H}] = -1.00 \pm 0.20$ plotted in the $c_{1,0}$ vs $(b-y)_0$ diagram.

Appendix B: Table containing the data collected to test calibrations of [Fe/H] in Sect.

How the catalogue is constructed is explained in detail in Sect. 3.

Column 1 lists the Hipparcos number of the star and Col. 2 gives an alternative stellar name. Column 3 gives the photometry reference (SN88 for Schuster & Nissen (1988), O84 for Olsen (1984), O93 for Olsen (1993), and O94 for Olsen (1994a)) and Columns 4 to 7 give the *uvby* photometry. Column 8 gives the colour excess of the star. Columns 9 to 12 give the dereddened *uvby* photometry. Column 13 and 14 give the average [Fe/H] (on the Valenti & Fischer 2005, scale) and the full range of [Fe/H] (on the same scale as in column 13) if the star was found in more than one study. Columns 15 and 16 give the number of references for the [Fe/H] and lists them (1: Valenti & Fischer (2005), 2: Favata et al. (1997), 3: Feltzing & Gustafsson (1998), 4: Chen et al. (2000), 5: Thorén & Feltzing (2000), 6: Santos et al. (2001), 7: Heiter & Luck (2003), Yong & Lambert (2003), 9: Mishenina et al. (2004), 10: Santos et al. (2004), 11: Bonfils et al. (2005), 12: Luck & Heiter (2005), 13: Santos et al. (2005), 14: Woolf & Wallerstein (2005), and 15: Sousa et al. (2006)). The data will be made publicly available through CDS.

dwarf stars with both Strömgren photometry and [Fe/H] based on high resolution, high S/N spectroscopy.

HIP	Name	Ref. <i>uvby</i>	<i>V</i>	<i>(b - y)</i>	<i>m</i> ₁	<i>c</i> ₁	<i>E(B - V)</i>	<i>V</i> ₀	<i>(b - y)</i> ₀	<i>m</i> _{1,0}	<i>c</i> _{1,0}	<[Fe/H]>	[Fe/H] range	N	Ref. [Fe/H]
400	HD 225261	O93	7.824	0.453	0.271	0.252	< 0.02	7.824	0.453	0.271	0.252	-0.44	...	1	1
544	HD 166	O93	6.089	0.459	0.286	0.311	< 0.02	6.089	0.459	0.286	0.311	0.14	0.08	3	1,7,12
1499	HD 1461	O93	6.471	0.421	0.244	0.360	< 0.02	6.471	0.421	0.244	0.360	0.18	...	1	1
1931	HD 2039	O93	9.008	0.412	0.218	0.394	< 0.02	9.008	0.412	0.218	0.394	0.30	0.04	2	1,10
1936	HD 2025	O93	7.884	0.538	0.473	0.234	< 0.02	7.884	0.538	0.473	0.234	-0.25	0.07	2	1,2
2282	HD 2587	O93	8.462	0.462	0.268	0.398	< 0.02	8.462	0.462	0.268	0.398	0.26	...	1	1
2790	HD 3277	O93	7.451	0.453	0.247	0.295	< 0.02	7.451	0.453	0.247	0.295	-0.07	...	1	1
3170	HD 3823	SN88	5.907	0.363	0.146	0.353	< 0.02	5.907	0.363	0.146	0.353	-0.27	...	1	1
3185	HD 3795	O93	6.148	0.443	0.217	0.282	< 0.02	6.148	0.443	0.217	0.282	-0.59	0.02	2	1,2
3206	HD 3765	O93	7.353	0.537	0.494	0.302	< 0.02	7.353	0.537	0.494	0.302	0.17	0.02	2	1,9
3497	HD 4308	SN88	6.552	0.408	0.190	0.307	< 0.02	6.552	0.408	0.190	0.307	-0.32	0.02	2	1,15
3502	HD 4203	O93	8.708	0.467	0.288	0.392	< 0.02	8.708	0.467	0.288	0.392	0.43	0.04	2	1,10
3765	HD 4628	O93	5.728	0.509	0.423	0.256	< 0.02	5.728	0.509	0.423	0.256	-0.25	0.04	3	1,7,12
3850	HD 4747	O93	7.151	0.460	0.295	0.275	< 0.02	7.151	0.460	0.295	0.275	-0.22	0.01	2	1,13
4148	HD 5133	O93	6.931	0.531	0.466	0.269	< 0.02	6.931	0.531	0.466	0.269	-0.09	0.08	4	1,2,6,10
5054	HD 6434	SN88	7.729	0.386	0.160	0.272	< 0.02	7.729	0.386	0.160	0.272	-0.57	0.08	3	2,6,10
5315	HD 6734	O93	6.458	0.511	0.315	0.327	< 0.02	6.458	0.511	0.315	0.327	-0.41	...	1	1
5799	HD 7438	O93	7.840	0.465	0.320	0.263	< 0.02	7.840	0.465	0.320	0.263	-0.26	...	1	2
5842	HD 7693	O93	7.239	0.559	0.512	0.235	< 0.02	7.239	0.559	0.512	0.235	0.23	...	1	1
5938	HD 7661	O93	7.540	0.464	0.295	0.301	< 0.02	7.540	0.464	0.295	0.301	0.06	...	1	1
6197	HD 8038	O93	8.380	0.432	0.251	0.365	< 0.02	8.380	0.432	0.251	0.365	0.18	...	1	1
6442	HD 8331	O93	7.475	0.423	0.202	0.371	< 0.02	7.475	0.423	0.202	0.371	-0.01	...	1	1
6498	HD 8328	O93	8.288	0.434	0.234	0.411	< 0.02	8.288	0.434	0.234	0.411	0.36	...	1	1
6653	HD 8648	O93	7.394	0.418	0.220	0.384	< 0.02	7.394	0.418	0.220	0.384	0.18	0.02	2	1,9
6712	HD 8765	O93	8.143	0.433	0.266	0.342	< 0.02	8.143	0.433	0.266	0.342	0.19	...	1	1
6978	HD 9070	O93	7.940	0.430	0.265	0.406	< 0.02	7.940	0.430	0.265	0.406	0.30	...	1	1
7080	HD 9280	O93	8.035	0.456	0.248	0.425	< 0.02	8.035	0.456	0.248	0.425	0.38	...	1	1
7221	HD 9331	O93	8.418	0.437	0.255	0.398	0.020	8.352	0.421	0.260	0.394	0.13	...	1	1
7235	HD 9540	O93	6.971	0.451	0.291	0.294	< 0.02	6.971	0.451	0.291	0.294	-0.02	...	1	1
7539	HD 10002	O94	8.130	0.502	0.370	0.344	< 0.02	8.130	0.502	0.370	0.344	0.22	0.04	2	1,15
7733	HD 10126	O93	7.736	0.445	0.267	0.312	< 0.02	7.736	0.445	0.267	0.312	0.02	...	1	1
7734	HD 10086	O93	6.617	0.419	0.237	0.339	< 0.02	6.617	0.419	0.237	0.339	0.12	...	1	1
7751	HD 10360	O94	5.739	0.500	0.392	0.267	< 0.02	5.739	0.500	0.392	0.267	-0.21	0.03	3	1,6,10
7751	HD 10361	O94	5.863	0.512	0.421	0.262	< 0.02	5.863	0.512	0.421	0.262	-0.22	...	1	1
7902	HD 10145	O93	7.713	0.421	0.232	0.326	0.035	7.597	0.394	0.242	0.320	0.01	0.05	2	1,9
8102	HD 10700	O93	3.503	0.435	0.263	0.238	< 0.02	3.503	0.435	0.263	0.238	-0.53	0.05	5	1,7,12,6,10
8159	HD 10697	O93	6.284	0.442	0.235	0.377	< 0.02	6.284	0.442	0.235	0.377	0.18	0.02	2	1,10
8346	HD 11020	O94	8.970	0.474	0.316	0.305	< 0.02	8.970	0.474	0.316	0.305	-0.28	...	1	1
8362	HD 10780	O93	5.627	0.468	0.316	0.327	< 0.02	5.627	0.468	0.316	0.327	0.06	0.12	4	1,7,12,9
9073	HD 11850	O93	7.863	0.435	0.248	0.314	< 0.02	7.863	0.435	0.248	0.314	0.09	...	1	1
9094	HD 11964	SN88	6.427	0.504	0.294	0.372	< 0.02	6.427	0.504	0.294	0.372	0.15	0.04	3	1,15,11
9269	HD 12051	O93	7.151	0.475	0.309	0.372	< 0.02	7.151	0.475	0.309	0.372	0.26	...	1	1
9381	HD 12387	SN88	7.376	0.410	0.196	0.316	< 0.02	7.376	0.410	0.196	0.316	-0.23	...	1	1
10117	HD 13386	O94	8.894	0.514	0.418	0.325	< 0.02	8.894	0.514	0.418	0.325	0.26	...	1	15
10138	HD 13445	O94	6.113	0.483	0.337	0.286	< 0.02	6.113	0.483	0.337	0.286	-0.23	0.06	3	1,6,10
10449	BD-01 306	SN88	9.086	0.387	0.133	0.231	< 0.02	9.086	0.387	0.133	0.231	-0.96	...	1	1
10505	HD 13825	O93	6.801	0.434	0.251	0.353	< 0.02	6.801	0.434	0.251	0.353	0.19	...	1	1
10629	HD 13783	O93	8.311	0.420	0.200	0.241	< 0.02	8.311	0.420	0.200	0.241	-0.73	...	1	9
10798	HD 14412	O93	6.342	0.438	0.258	0.229	< 0.02	6.342	0.438	0.258	0.229	-0.49	0.06	4	1,12,6,10
11983	BD +4 415	SN88	9.788	0.534	0.437	0.233	< 0.02	9.788	0.534	0.437	0.233	-0.46	...	1	8
12048	HD 16141	SN88	6.832	0.421	0.213	0.381	< 0.02	6.832	0.421	0.213	0.381	0.15	0.04	3	1,6,10
12114	HD 16160	O93	5.794	0.552	0.515	0.271	< 0.02	5.794	0.552	0.515	0.271	-0.09	0.04	4	1,7,12,11
12186	HD 16417	O93	5.774	0.414	0.210	0.383	< 0.02	5.774	0.414	0.210	0.383	0.14	0.03	2	1,15
12198	HD 16275	O93	8.656	0.419	0.226	0.414	0.038	8.533	0.390	0.236	0.407	0.34	...	1	1
12306	HD 16397	SN88	7.361	0.387	0.157	0.279	< 0.02	7.361	0.387	0.157	0.279	-0.51	...	1	1
13513	GJ 118.1A	O94	8.240	0.553	0.420	0.282	< 0.02	8.240	0.553	0.420	0.282	0.17	...	1	2
13601	HD 18144	O93	7.409	0.452	0.275	0.320	< 0.02	7.409	0.452	0.275	0.320	0.07	...	1	1
13769	HD 18445	O93	7.792	0.550	0.500	0.222	< 0.02	7.792	0.550	0.500	0.222	0.00	...	1	1
14086	HD 18907	O93	5.880	0.498	0.250	0.299	< 0.02	5.880	0.498	0.250	0.299	-0.57	...	1	1
14241	HD 19034	O93	8.087	0.416	0.214	0.263	< 0.02	8.087	0.416	0.214	0.263	-0.49	...	1	1
14286	HD 18757	SN88	6.652	0.408	0.202	0.313	< 0.02	6.652	0.408	0.202	0.313	-0.23	...	1	11
14623	HD 19632	O93	7.292	0.421	0.230	0.329	< 0.02	7.292	0.421	0.230	0.329	0.13	...	1	1
15099	HD 20165	O93	7.812	0.503	0.404	0.296	0.036	7.695	0.476	0.414	0.290	-0.03	...	1	1
15234	LHS 170	SN88	10.629	0.715	0.557	0.125	0.022	10.557	0.698	0.563	0.121	-1.12	0.12	2	8,14
15510	HD 20794	O93	4.256	0.439	0.235	0.285	< 0.02	4.256	0.439	0.235	0.285	-0.40	0.04	3	1,6,10
15904	BD+11 468	SN88	10.755	0.395	0.087	0.158	0.206	10.080	0.236	0.142	0.122	-1.53	...	1	1
15919	HD 21197	O93	7.841	0.645	0.729	0.149	< 0.02	7.841	0.645	0.729	0.149	0.25	0.10	3	2, 15,5
16115	HD 22104	O93	8.311	0.423	0.229	0.403	< 0.02	8.311	0.423	0.229	0.403	0.34	...	1	1
16209	LHS 173	SN88	11.060	0.822	0.615	-0.038	0.021	10.991	0.806	0.621	-0.042	-1.47	...	1	14
16405	HD 21774	O93	8.092	0.426	0.247	0.372	0.045	7.945	0.391	0.259	0.364	0.26	...	1	1
16537	HD 22049	O93	3.716	0.498	0.436	0.257	< 0.02	3.716	0.498	0.436	0.257	-0.05	0.05	5	1,12,9,6,10
16727	HD 22282	O93	8.531	0.469	0.309	0.351	0.037	8.408	0.440	0.319	0.344	0.16	...	1	1
17054	HD 23127	O93	8.574	0.435	0.249	0.424	0.022	8.501	0.418	0.255	0.420	0.34	...	1	1
17147	HD 22879	SN88	6.687	0.370	0.115	0.277	< 0.02	6.687	0.370	0.115	0.277	-0.90	0.03	2	1,9
	HD 23261	O93	8.977	0.512	0.418	0.302	< 0.02	8.977	0.512	0.418	0.302	0.04	...	1	5
17439	HD 23484	O93	6.968	0.508	0.400	0.295	< 0.02	6.968	0.508	0.400	0.295	0.11	0.02	3	1,6,10
18082	BD -4 680	SN88	9.977	0.388	0.049	0.288	0.136	9.530	0.283	0.086	0.264	-1.57	...	1	8
18208	HD 24365	O93	7.885	0.506	0.294	0.303	0.036	7.765	0.478	0.304	0.297				

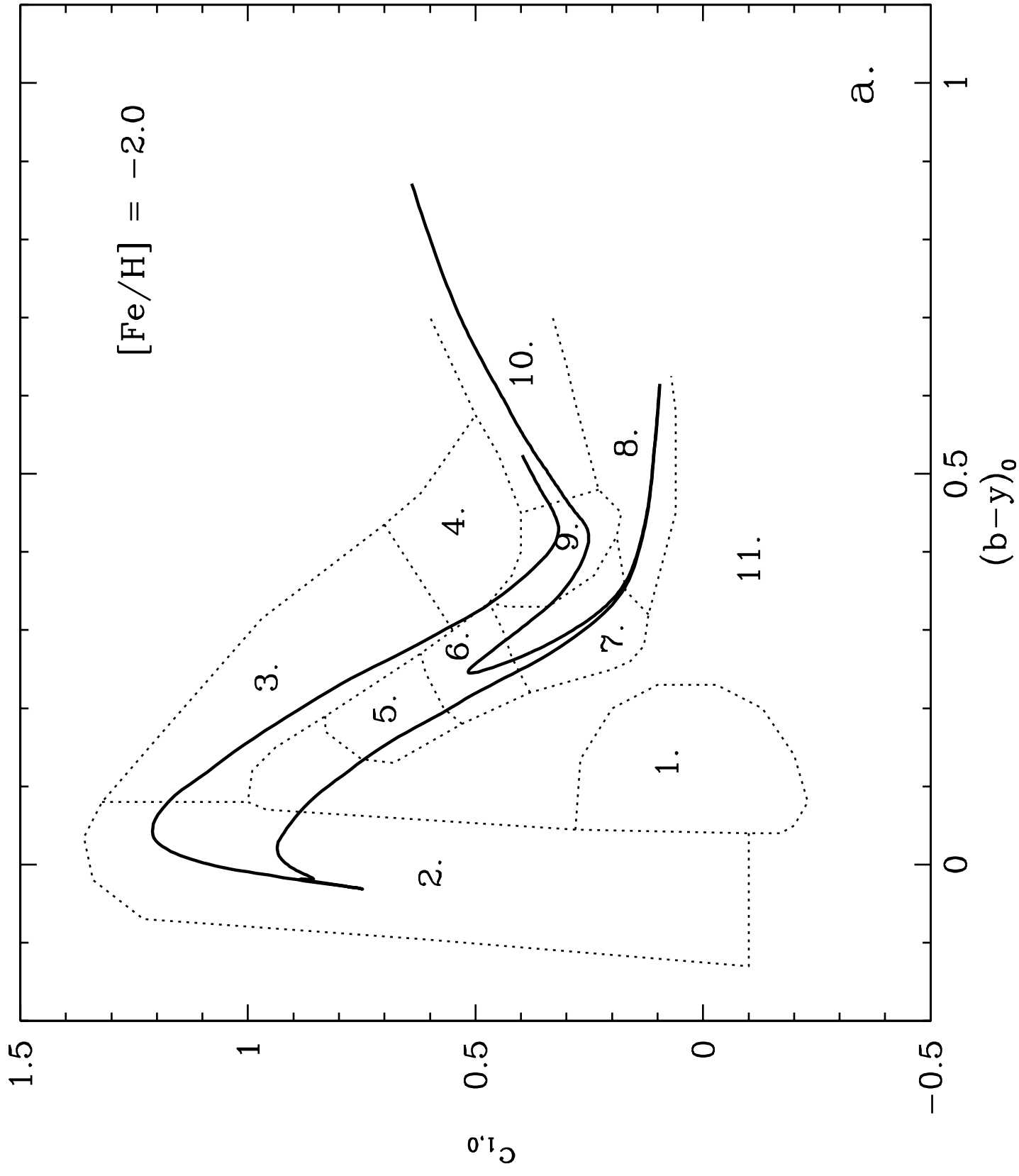
19301	HD 25918	O93	7.730	0.440	0.242	0.319	< 0.02	7.730	0.440	0.242	0.319	-0.05	...	1	1
19422	HD 25665	O93	7.703	0.541	0.497	0.238	< 0.02	7.703	0.541	0.497	0.238	-0.03	...	1	1
19849	HD 26965	O93	4.416	0.477	0.341	0.288	< 0.02	4.416	0.477	0.341	0.288	-0.26	0.06	6	1,7,12,6,10,11
20723	HD 28185	O93	7.808	0.443	0.258	0.366	0.023	7.733	0.425	0.264	0.362	0.22	0.06	4	7,6,10,15
21010	HD 28447	O93	6.527	0.441	0.221	0.347	0.067	6.307	0.389	0.239	0.335	-0.02	0.02	2	1,9
21436	HD 29150	O93	7.590	0.414	0.235	0.305	0.033	7.482	0.389	0.244	0.299	0.02	0.06	2	1,9
21731	HD 30306	O93	7.743	0.460	0.264	0.377	< 0.02	7.743	0.460	0.264	0.377	0.23	...	1	15
21850	HD 30177	O93	8.397	0.476	0.294	0.392	< 0.02	8.397	0.476	0.294	0.392	0.40	0.01	2	1,10
21889	HD 30295	O93	8.856	0.489	0.338	0.362	< 0.02	8.856	0.489	0.338	0.362	0.28	...	1	1
21923	HD 29836	O93	7.124	0.427	0.225	0.408	0.053	6.950	0.386	0.239	0.399	0.26	...	1	1
21988	HD 29883	O93	7.985	0.526	0.431	0.282	0.024	7.908	0.508	0.437	0.278	-0.18	...	1	1
22122	HD 30501	O93	7.582	0.506	0.414	0.281	< 0.02	7.582	0.506	0.414	0.281	0.04	...	1	5
22319	HD 30508	O93	6.521	0.496	0.300	0.335	< 0.02	6.521	0.496	0.300	0.335	-0.08	...	1	1
22336	HD 30562	SN88	5.770	0.395	0.216	0.409	< 0.02	5.770	0.395	0.216	0.409	0.26	0.01	4	1,3,9,15
22451	HD 30876	O94	7.479	0.513	0.418	0.280	< 0.02	7.479	0.513	0.418	0.280	-0.06	...	1	1
22576	HD 30708	O93	6.780	0.427	0.224	0.375	0.028	6.689	0.406	0.231	0.370	0.19	...	1	1
22633	HD 30825	O93	6.726	0.517	0.311	0.320	0.072	6.489	0.461	0.330	0.307	-0.17	...	1	1
22646	HD 33214	O94	8.589	0.518	0.437	0.265	< 0.02	8.589	0.518	0.437	0.265	0.17	...	1	15
22787	HD 31392	O93	7.592	0.473	0.318	0.327	< 0.02	7.592	0.473	0.318	0.327	0.05	...	1	5
22953	HD 31827	O93	8.257	0.468	0.306	0.390	< 0.02	8.257	0.468	0.306	0.390	0.41	...	1	1
23311	HD 32147	O93	6.208	0.598	0.637	0.231	< 0.02	6.208	0.598	0.637	0.231	0.33	0.10	9	1,2, 3,7,12,9,13,15
23884	HD 32963	O93	7.606	0.410	0.228	0.335	0.029	7.510	0.387	0.236	0.330	0.08	...	1	1
24110	HD 33811	O93	8.711	0.465	0.283	0.409	< 0.02	8.711	0.465	0.283	0.409	0.28	0.01	2	1,2
25094	HD 34575	O93	7.095	0.458	0.264	0.404	< 0.02	7.095	0.458	0.264	0.404	0.32	...	1	1
25220	HD 35171	O93	7.929	0.624	0.650	0.160	< 0.02	7.929	0.624	0.650	0.160	-0.00	...	1	12
25421	HD 35854	O94	7.694	0.536	0.501	0.257	< 0.02	7.694	0.536	0.501	0.257	-0.04	...	1	1
25623	HD 36003	O93	7.623	0.627	0.655	0.188	< 0.02	7.623	0.627	0.655	0.188	-0.12	...	1	12
25873	HD 36308	O93	8.363	0.465	0.312	0.303	0.112	7.995	0.378	0.342	0.283	0.15	...	1	1
25963	HD 36889	O93	7.368	0.419	0.210	0.387	< 0.02	7.368	0.419	0.210	0.387	0.16	...	1	1
26273	HD 37213	O93	8.215	0.446	0.201	0.291	< 0.02	8.215	0.446	0.201	0.291	-0.44	...	1	1
26779	HD 37394	O93	6.210	0.495	0.362	0.317	< 0.02	6.210	0.495	0.362	0.317	0.13	0.10	3	1,12,11
26834	HD 37986	O93	7.357	0.477	0.307	0.369	< 0.02	7.357	0.477	0.307	0.369	0.30	0.01	2	3,15
26935	HD 38110	O93	8.180	0.416	0.209	0.399	0.153	7.678	0.298	0.250	0.372	0.17	...	1	1
27207	HD 38230	O93	7.337	0.493	0.363	0.301	< 0.02	7.337	0.493	0.363	0.301	-0.08	...	1	1
27253	HD 38529	O93	5.941	0.471	0.278	0.437	0.043	5.800	0.438	0.290	0.429	0.43	0.05	4	1,7,6,10
27887	HD 40307	O93	7.135	0.541	0.462	0.261	< 0.02	7.135	0.541	0.462	0.261	-0.25	0.06	3	1,6,10
28393	HD 41004 A	O94	8.639	0.518	0.392	0.312	< 0.02	8.639	0.518	0.392	0.312	0.18	...	1	13
29208	HD 42182	O93	8.434	0.520	0.460	0.295	< 0.02	8.434	0.520	0.460	0.295	0.07	...	1	5
29271	HD 43834	O94	5.073	0.442	0.269	0.329	< 0.02	5.073	0.442	0.269	0.329	0.09	0.01	3	1,6,10
29568	HD 43162	O93	6.364	0.428	0.246	0.303	< 0.02	6.364	0.428	0.246	0.303	-0.04	0.03	2	6,10
29761	HD 42250	O93	7.433	0.469	0.287	0.333	< 0.02	7.433	0.469	0.287	0.333	0.01	...	1	1
29843	HD 43745	SN88	6.062	0.355	0.192	0.418	< 0.02	6.062	0.355	0.192	0.418	0.12	0.02	2	1,15
30104	HD 44594	O93	6.615	0.410	0.212	0.373	< 0.02	6.615	0.410	0.212	0.373	0.15	...	1	1
30243	HD 44420	O93	7.602	0.426	0.252	0.380	< 0.02	7.602	0.426	0.252	0.380	0.29	...	1	1
30344	HD 44821	O93	7.356	0.420	0.238	0.303	< 0.02	7.356	0.420	0.238	0.303	0.11	...	1	1
30476	HD 45289	O93	6.669	0.419	0.213	0.350	< 0.02	6.669	0.419	0.213	0.350	-0.02	...	1	1
30860	HD 45350	O93	7.892	0.457	0.263	0.407	< 0.02	7.892	0.457	0.263	0.407	0.29	...	1	1
31246	HD 46375	O93	7.914	0.502	0.401	0.337	< 0.02	7.914	0.502	0.401	0.337	0.24	0.01	2	1,10
31540	HD 47186	O93	7.619	0.445	0.265	0.365	< 0.02	7.619	0.445	0.265	0.365	0.23	...	1	15
31655	HD 47157	O93	7.613	0.440	0.268	0.407	< 0.02	7.613	0.440	0.268	0.407	0.34	...	1	1
31660	HD 47127	O93	6.834	0.437	0.246	0.369	< 0.02	6.834	0.437	0.246	0.369	0.10	...	1	1
32010	HD 47752	O93	8.064	0.583	0.580	0.205	< 0.02	8.064	0.583	0.580	0.205	-0.10	...	1	1
32984	HD 50281	O93	6.572	0.592	0.607	0.206	< 0.02	6.572	0.592	0.607	0.206	0.04	0.18	8	1,2, 7,12,9,6,10,11
33094	HD 50806	O93	6.056	0.437	0.230	0.371	< 0.02	6.056	0.437	0.230	0.371	0.07	...	1	1
33324	HD 51929	SN88	7.404	0.367	0.146	0.290	< 0.02	7.404	0.367	0.146	0.290	-0.64	...	1	1
33382	HD 51219	O93	7.393	0.432	0.236	0.323	< 0.02	7.393	0.432	0.236	0.323	0.01	...	1	1
33690	HD 53143	O93	6.825	0.482	0.323	0.318	< 0.02	6.825	0.482	0.323	0.318	0.22	...	1	13
33848	HD 52456	O93	8.144	0.502	0.383	0.307	< 0.02	8.144	0.502	0.383	0.307	0.01	...	1	1
34065	HD 53705	SN88	5.557	0.383	0.194	0.319	< 0.02	5.557	0.383	0.194	0.319	-0.17	0.20	4	1,2, 6,10
34069	HD 53706	O93	6.857	0.470	0.297	0.284	< 0.02	6.857	0.470	0.297	0.284	-0.26	0.09	4	1,2, 6,10
34739	HD 55720	O93	7.507	0.437	0.233	0.284	< 0.02	7.507	0.437	0.233	0.284	-0.30	...	1	1
35139	HD 56274	SN88	7.750	0.384	0.157	0.273	< 0.02	7.750	0.384	0.157	0.273	-0.55	...	1	1
35910	HD 58895	O93	6.594	0.442	0.235	0.429	< 0.02	6.594	0.442	0.235	0.429	0.34	...	1	15
36210	HD 59468	O93	6.722	0.433	0.253	0.323	< 0.02	6.722	0.433	0.253	0.323	0.02	...	1	1
36249	HD 58781	O93	7.242	0.434	0.271	0.334	< 0.02	7.242	0.434	0.271	0.334	0.10	...	1	1
36285	HD 58595	O93	7.419	0.427	0.212	0.268	< 0.02	7.419	0.427	0.212	0.268	-0.30	...	1	9
36704	HD 59747	O93	7.697	0.517	0.403	0.284	< 0.02	7.697	0.517	0.403	0.284	0.06	...	1	1
36849	HD 60319	SN88	8.929	0.351	0.112	0.302	< 0.02	8.929	0.351	0.112	0.302	-0.87	...	1	4
37309	HD 61686	O94	8.549	0.419	0.230	0.387	< 0.02	8.549	0.419	0.230	0.387	0.30	...	1	1
37349	HD 61606 A	O93	7.168	0.542	0.496	0.266	< 0.02	7.168	0.542	0.496	0.266	0.03	0.06	6	1,3,12,9,13,5
37789	HD 62301	SN88	6.740	0.361	0.126	0.312	< 0.02	6.740	0.361	0.126	0.312	-0.66	...	1	4
38558	HD 65216	O93	7.973	0.420	0.231	0.272	< 0.02	7.973	0.420	0.231	0.272	-0.14	...	1	10
38625	HD 64606	O93	7.432	0.454	0.211	0.208	< 0.02	7.432	0.454	0.211	0.208	-0.85	0.16	3	2, 9,13
39064	HD 65430	O93	7.667	0.490	0.347	0.299	< 0.02	7.667	0.490	0.347	0.299	-0.12	...	1	1
39157	HD 65583	O93	6.982	0.455	0.220	0.229	< 0.02	6.982	0.455	0.220	0.229	-0.69	...	2	1,9
39298	HD 66221	O93	8.064	0.451	0.250	0.374	< 0.02	8.064	0.451	0.250	0.374	0.17	...	1	15
39342	HD 67199	O93	7.161	0.509	0.415	0.285	< 0.02	7.161	0.509	0.415	0.285	0.06	0.06	2	1,13
39417	HD 66428	O93	8.255	0.445	0.256	0.377	< 0.02	8.255	0.445	0.256	0.377	0.31	...	1	1
40118	HD 68017	O93	6.797	0.420	0.194	0.264	< 0.02	6.797	0.420	0.194	0.264	-0.42	0.03	2	1,9
40283	HD 68978	SN88													

41926	HD 72673	O93	6.379	0.473	0.291	0.258	< 0.02	6.379	0.473	0.291	0.258	-0.36	0.02	4	1,2, 6,10
42011	HD 72769	O93	7.225	0.452	0.284	0.387	< 0.02	7.225	0.452	0.284	0.387	0.30	0.02	2	1,2
42074	HD 72760	O93	7.320	0.483	0.336	0.308	< 0.02	7.320	0.483	0.336	0.308	0.13	0.02	2	1,9
42214	HD 73256	O93	8.061	0.473	0.307	0.349	< 0.02	8.061	0.473	0.307	0.349	0.27	...	1	10
42282	HD 73526	O94	8.972	0.451	0.242	0.421	< 0.02	8.972	0.451	0.242	0.421	0.26	0.02	2	1,10
42499	HD 73667	O93	7.601	0.498	0.337	0.258	< 0.02	7.601	0.498	0.337	0.258	-0.49	0.15	2	1,2
42808	HD 74576	O93	6.562	0.538	0.446	0.263	< 0.02	6.562	0.538	0.446	0.263	0.03	0.01	2	6,10
43686	HD 76700	O93	8.149	0.456	0.250	0.431	< 0.02	8.149	0.456	0.250	0.431	0.38	0.06	2	1,10
43852	HD 76218	O93	7.710	0.473	0.306	0.301	< 0.02	7.710	0.473	0.306	0.301	0.07	...	1	1
44075	HD 76932	SN88	5.801	0.354	0.117	0.297	< 0.02	5.801	0.354	0.117	0.297	-1.02	...	1	9
44089	HD 76752	O93	7.484	0.412	0.208	0.351	< 0.02	7.484	0.412	0.208	0.351	0.03	...	1	1
44097	HD 76780	O93	7.648	0.414	0.234	0.361	< 0.02	7.648	0.414	0.234	0.361	0.17	...	1	3
44137	HD 76909	O93	7.843	0.452	0.263	0.407	< 0.02	7.843	0.452	0.263	0.407	0.38	...	1	1
44892	HD 78418	O93	5.959	0.429	0.215	0.358	< 0.02	5.959	0.429	0.215	0.358	-0.12	...	1	4
46007	HD 81110	O93	8.298	0.435	0.247	0.366	< 0.02	8.298	0.435	0.247	0.366	0.24	...	1	15
46580	HD 82106	O93	7.190	0.570	0.550	0.234	< 0.02	7.190	0.570	0.550	0.234	0.07	0.09	3	1,12,9
48133	GJ 368.1A	O94	7.910	0.522	0.415	0.308	< 0.02	7.910	0.522	0.415	0.308	0.11	...	1	2
48331	HD 85512	O93	7.627	0.660	0.666	0.176	< 0.02	7.627	0.660	0.666	0.176	-0.10	...	1	13
48423	HD 85301	O93	7.746	0.436	0.251	0.320	< 0.02	7.746	0.436	0.251	0.320	0.19	...	1	1
49350	HD 87359	O93	7.495	0.429	0.224	0.340	< 0.02	7.495	0.429	0.224	0.340	0.06	...	1	1
49680	HD 87836	O93	7.516	0.439	0.253	0.401	< 0.02	7.516	0.439	0.253	0.401	0.36	...	1	1
49908	HD 88230	O93	6.553	0.790	0.741	0.030	< 0.02	6.553	0.790	0.741	0.030	-0.10	...	1	14
49942	HD 88371	SN88	8.414	0.407	0.186	0.329	< 0.02	8.414	0.407	0.186	0.329	-0.31	...	1	1
50505	HD 89269	O93	6.656	0.420	0.208	0.292	< 0.02	6.656	0.420	0.208	0.292	-0.21	0.01	2	1,9
51257	HD 90711	O93	7.876	0.482	0.337	0.359	< 0.02	7.876	0.482	0.337	0.359	0.30	...	1	1
51258	HD 90722	O93	7.875	0.445	0.271	0.388	< 0.02	7.875	0.445	0.271	0.388	0.36	...	1	1
52409	HD 92788	O93	7.317	0.439	0.243	0.385	< 0.02	7.317	0.439	0.243	0.385	0.31	0.03	4	1,7,10,13
52462	HD 92945	O94	7.713	0.507	0.387	0.279	< 0.02	7.713	0.507	0.387	0.279	0.13	...	1	1
54035	HD 95735	O93	7.422	0.981	0.419	0.155	< 0.02	7.422	0.981	0.419	0.155	-0.67	...	1	14
54287	HD 96423	O93	7.233	0.427	0.222	0.370	< 0.02	7.233	0.427	0.222	0.370	0.10	...	1	1
54538	GJ 9350	O93	9.728	0.471	0.286	0.286	< 0.02	9.728	0.471	0.286	0.286	-0.34	...	1	2
54651	BD -10 3216	O93	9.192	0.636	0.559	0.135	< 0.02	9.192	0.636	0.559	0.135	-1.14	...	1	8
54704	HD 97343	SN88	7.052	0.460	0.296	0.324	< 0.02	7.052	0.460	0.296	0.324	-0.04	...	1	1
55013	HD 97998	SN88	7.362	0.397	0.185	0.260	< 0.02	7.362	0.397	0.185	0.260	-0.41	...	1	1
55022	HD 97916	SN88	9.209	0.293	0.104	0.407	0.025	9.126	0.273	0.111	0.403	-1.06	...	1	4
55210	HD 98281	O93	7.272	0.457	0.254	0.288	< 0.02	7.272	0.457	0.254	0.288	-0.20	...	1	1
55846	HD 99491	O93	6.488	0.484	0.335	0.362	< 0.02	6.488	0.484	0.335	0.362	0.34	...	1	1
55848	HD 99492	O93	7.550	0.578	0.279	0.262	< 0.02	7.550	0.578	0.279	0.262	0.33	0.05	3	1,2, 13
55900	HD 99610	O93	7.414	0.436	0.239	0.377	< 0.02	7.414	0.436	0.239	0.377	0.23	...	1	1
56242	HD 100180	O93	9.146	0.652	0.669	0.131	< 0.02	9.146	0.652	0.669	0.131	-0.00	0.02	2	1,4
56452	HD 100623	O93	5.955	0.485	0.320	0.241	< 0.02	5.955	0.485	0.320	0.241	-0.38	0.02	2	1,13
56830	HD 101259	O93	6.409	0.508	0.229	0.315	< 0.02	6.409	0.508	0.229	0.315	-0.69	...	1	1
56832	HD 101242	O93	7.611	0.412	0.226	0.327	< 0.02	7.611	0.412	0.226	0.327	0.08	...	1	3
56998	HD 101581	O93	7.751	0.602	0.580	0.175	< 0.02	7.751	0.602	0.580	0.175	-0.32	...	1	13
57001	HD 101563	O94	6.436	0.404	0.212	0.334	< 0.02	6.436	0.404	0.212	0.334	0.04	...	1	7
57271	HD 102071	O94	7.973	0.475	0.315	0.309	< 0.02	7.973	0.475	0.315	0.309	0.01	...	1	1
57291	HD 102117	O93	7.462	0.455	0.246	0.407	< 0.02	7.462	0.455	0.246	0.407	0.30	0.01	2	1,13
57349	HD 102158	SN88	8.066	0.393	0.163	0.309	< 0.02	8.066	0.393	0.163	0.309	-0.47	...	1	1
57443	HD 102365	O93	4.892	0.418	0.199	0.278	< 0.02	4.892	0.418	0.199	0.278	-0.32	0.02	2	1,13
57450	BD+51 1696	SN88	9.912	0.397	0.100	0.180	< 0.02	9.912	0.397	0.100	0.180	-1.48	...	1	1
57507	HD 102438	O93	6.478	0.433	0.210	0.281	< 0.02	6.478	0.433	0.210	0.281	-0.27	0.01	2	1,13
57939	HD 103095	SN88	6.416	0.484	0.219	0.167	< 0.02	6.416	0.484	0.219	0.167	-1.28	0.14	3	1,7,12
58067	HD 103432	O93	8.211	0.420	0.224	0.287	< 0.02	8.211	0.420	0.224	0.287	-0.10	0.05	2	1,2
58345	HD 103932	O93	6.949	0.630	0.709	0.162	< 0.02	6.949	0.630	0.709	0.162	0.15	0.16	4	3,12,13,5
58576	HD 104304	O93	5.546	0.464	0.319	0.335	< 0.02	5.546	0.464	0.319	0.335	0.30	0.09	3	1,12,13
58843	HD 104800	SN88	9.227	0.382	0.141	0.255	< 0.02	9.227	0.382	0.141	0.255	-0.82	...	1	1
59572	HD 106156	O93	7.917	0.471	0.329	0.341	< 0.02	7.917	0.471	0.329	0.341	0.19	0.09	2	1,3
59750	HD 106516	SN88	6.111	0.318	0.110	0.335	< 0.02	6.111	0.318	0.110	0.335	-0.80	0.08	2	4,9
60081	HD 107148	O93	8.022	0.428	0.238	0.404	< 0.02	8.022	0.428	0.238	0.404	0.31	...	1	1
60729	HD 108309	O93	8.231	0.437	0.164	0.366	< 0.02	8.231	0.437	0.164	0.366	0.13	...	1	1
61028	HD 108874	O93	8.764	0.457	0.277	0.356	< 0.02	8.764	0.457	0.277	0.356	0.21	0.05	2	1,10
61291	HD 109200	O93	7.137	0.496	0.351	0.272	< 0.02	7.137	0.496	0.351	0.272	-0.26	0.07	2	1,13
61595	HD 109749	O93	8.176	0.425	0.207	0.395	< 0.02	8.176	0.425	0.207	0.395	0.26	...	1	15
62145	HD 110833	O93	7.014	0.548	0.477	0.286	< 0.02	7.014	0.548	0.477	0.286	0.15	...	1	9
62345	HD 111031	O93	6.890	0.426	0.250	0.376	< 0.02	6.890	0.426	0.250	0.376	0.28	...	1	1
62523	HD 111395	O93	6.288	0.438	0.241	0.334	< 0.02	6.288	0.438	0.241	0.334	0.11	0.04	2	1,7
62534	HD 111232	O93	7.598	0.436	0.211	0.273	< 0.02	7.598	0.436	0.211	0.273	-0.36	...	1	10
62536	HD 111398	O93	7.105	0.425	0.213	0.368	< 0.02	7.105	0.425	0.213	0.368	0.08	...	1	1
62607	HD 111515	O93	8.113	0.437	0.201	0.241	< 0.02	8.113	0.437	0.201	0.241	-0.60	...	1	1
63048	HD 112257	O93	7.809	0.423	0.213	0.336	< 0.02	7.809	0.423	0.213	0.336	-0.03	...	1	1
64150	HD 114174	O93	6.794	0.423	0.217	0.340	< 0.02	6.794	0.423	0.217	0.340	0.07	...	1	1
64219	HD 114260	O93	7.356	0.452	0.248	0.310	< 0.02	7.356	0.452	0.248	0.310	-0.09	...	1	1
64275	BD +68 714	O93	8.868	0.542	0.460	0.287	< 0.02	8.868	0.542	0.460	0.287	0.22	...	1	8
64408	HD 114613	O93	4.848	0.441	0.235	0.390	< 0.02	4.848	0.441	0.235	0.390	0.24	...	1	1
64426	HD 114762	SN88	7.324	0.366	0.123	0.300	< 0.02	7.324	0.366	0.123	0.300	-0.68	0.07	3	1,7,10
64457	HD 114783	O84	7.565	0.521	0.458	0.309	< 0.02	7.565	0.521	0.458	0.309	0.13	0.02	2	1,10
64459	HD 114729	SN88	6.687	0.391	0.163	0.344	< 0.02	6.687	0.391	0.163	0.344	-0.27	0.01	2	1,10
64577	HD 114946	O93	5.321	0.523	0.322	0.317	< 0.02	5.321	0.523	0.322	0.317	-0.21	...	1	1
64924	HD 115617	O93	4.734	0.433	0.256	0.328	< 0.02	4.734	0.433	0.256	0.328	0.03	0.05	3	

65982	HD 117635	O93	7.325	0.474	0.284	0.249	< 0.02	7.325	0.474	0.284	0.249	-0.40	...	1	9
66238	HD 117939	O93	7.284	0.424	0.191	0.303	< 0.02	7.284	0.424	0.191	0.303	-0.22	0.03	2	1,2
66618	HD 118475	SN88	6.976	0.386	0.206	0.372	< 0.02	6.976	0.386	0.206	0.372	0.10	...	1	1
66765	HD 118972	O93	6.922	0.504	0.363	0.287	< 0.02	6.922	0.504	0.363	0.287	0.00	...	2	1,13
67408	HD 120237	SN88	6.584	0.355	0.167	0.364	< 0.02	6.584	0.355	0.167	0.364	-0.03	...	1	1
67487	HD 120467	O93	8.152	0.700	0.785	0.079	< 0.02	8.152	0.700	0.785	0.079	0.02	...	1	12
67620	HD 120690	O93	6.442	0.433	0.236	0.315	< 0.02	6.442	0.433	0.236	0.315	-0.03	0.16	2	1,2
68273	HD 121849	O93	8.155	0.432	0.202	0.294	< 0.02	8.155	0.432	0.202	0.294	-0.29	...	1	2
68634	HD 122676	O93	7.127	0.458	0.242	0.314	< 0.02	7.127	0.458	0.242	0.314	-0.02	...	1	1
68682	HD 122742	O93	6.273	0.452	0.264	0.317	< 0.02	6.273	0.452	0.264	0.317	0.01	...	1	1
69357	HD 124106	O93	7.924	0.515	0.370	0.285	< 0.02	7.924	0.515	0.370	0.285	-0.10	...	1	1
69390	HD 124244	O93	8.467	0.420	0.195	0.379	< 0.02	8.467	0.420	0.195	0.379	0.20	...	1	4
69881	HD 125184	O93	6.466	0.454	0.247	0.413	< 0.02	6.466	0.454	0.247	0.413	0.34	0.12	3	1,9,15
69972	HD 125072	O93	6.642	0.583	0.594	0.230	< 0.02	6.642	0.583	0.594	0.230	0.30	0.03	2	1,13
70016	HD 125455	O93	7.577	0.494	0.374	0.285	< 0.02	7.577	0.494	0.374	0.285	-0.15	0.05	2	1,11
70470	HD 126511	O93	8.365	0.460	0.301	0.321	< 0.02	8.365	0.460	0.301	0.321	0.09	...	1	3
70873	HD 127334	O93	6.362	0.441	0.245	0.366	< 0.02	6.362	0.441	0.245	0.366	0.27	...	1	1
71462	HD 128428	O93	7.803	0.466	0.277	0.412	0.026	7.717	0.446	0.284	0.407	0.47	...	1	1
71735	HD 128674	O93	7.393	0.423	0.204	0.265	< 0.02	7.393	0.423	0.204	0.265	-0.39	...	1	1
71743	HD 128987	O93	7.238	0.439	0.269	0.304	< 0.02	7.238	0.439	0.269	0.304	0.04	...	1	3
72312	HD 130307	O93	7.776	0.521	0.405	0.275	< 0.02	7.776	0.521	0.405	0.275	-0.16	...	1	1
72339	HD 130322	O93	8.036	0.475	0.305	0.316	< 0.02	8.036	0.475	0.305	0.316	0.04	0.07	3	1,7,10
72577	HD 130871	O93	9.060	0.545	0.507	0.231	< 0.02	9.060	0.545	0.507	0.231	-0.16	...	1	1
72688	HD 130992	O93	7.790	0.568	0.556	0.233	< 0.02	7.790	0.568	0.556	0.233	-0.00	0.01	2	1,13
72875	BD +23 2751	O93	8.621	0.554	0.498	0.212	< 0.02	8.621	0.554	0.498	0.212	-0.34	...	1	8
73005	HD 132142	O93	7.756	0.482	0.297	0.267	< 0.02	7.756	0.482	0.297	0.267	-0.45	...	1	1
73182	HD 131976	O93	8.052	0.944	0.486	0.189	< 0.02	8.052	0.944	0.486	0.189	0.07	0.16	6	1,3,12,9,13,5
73184	HD 131977	O93	5.725	0.609	0.660	0.187	< 0.02	5.725	0.609	0.660	0.187	0.07	0.16	6	1,3,12,9,13,5
73241	HD 131923	O93	6.346	0.443	0.228	0.361	< 0.02	6.346	0.443	0.228	0.361	0.11	...	1	1
73869	HD 134319	O93	8.425	0.419	0.222	0.276	< 0.02	8.425	0.419	0.222	0.276	0.03	...	1	1
74135	HD 134474	O93	8.880	0.482	0.376	0.318	< 0.02	8.880	0.482	0.376	0.318	0.14	...	1	3
74235	HIP 74235	O93	9.058	0.487	0.216	0.159	< 0.02	9.058	0.487	0.216	0.159	-1.45	0.06	2	1,8
74432	HD 135101	O93	6.675	0.436	0.217	0.369	< 0.02	6.675	0.436	0.217	0.369	0.08	...	1	1
74434	HD 135101	O93	7.518	0.460	0.251	0.353	< 0.02	7.518	0.460	0.251	0.353	0.08	...	1	1
74500	HD 134987	O93	6.468	0.434	0.256	0.375	< 0.02	6.468	0.434	0.256	0.375	0.31	0.08	4	1,3,7,10
75181	HD 136352	SN88	5.654	0.401	0.198	0.291	< 0.02	5.654	0.401	0.198	0.291	-0.34	0.01	2	1,13
75266	HD 136834	O93	8.255	0.560	0.563	0.241	< 0.02	8.255	0.560	0.563	0.241	0.27	0.03	3	1,3,5
75676	HD 138004 A	O93	7.496	0.415	0.244	0.202	< 0.02	7.496	0.415	0.244	0.202	-0.09	...	1	1
75676	HD 138004 B	O93	9.831	0.688	0.699	0.099	< 0.02	9.831	0.688	0.699	0.099	-0.09	...	1	1
75722	HD 137778	O93	7.567	0.532	0.455	0.286	< 0.02	7.567	0.532	0.455	0.286	0.28	...	1	1
75829	HD 139813	O93	7.356	0.481	0.298	0.292	< 0.02	7.356	0.481	0.298	0.292	0.14	...	1	1
76200	HD 138549	O93	7.962	0.438	0.264	0.310	< 0.02	7.962	0.438	0.264	0.310	0.00	...	1	1
78170	HD 142709	O93	8.026	0.624	0.641	0.173	< 0.02	8.026	0.624	0.641	0.173	-0.12	...	1	13
78241	HD 143291	O93	8.003	0.465	0.274	0.252	< 0.02	8.003	0.465	0.274	0.252	-0.44	...	1	1
78709	HD 144287	O93	7.094	0.470	0.270	0.325	< 0.02	7.094	0.470	0.270	0.325	-0.09	...	1	9
78775	HD 144579	O93	6.665	0.455	0.232	0.226	< 0.02	6.665	0.455	0.232	0.226	-0.68	0.02	3	1,12,9
78843	HD 144253	O93	7.379	0.590	0.595	0.206	< 0.02	7.379	0.590	0.595	0.206	-0.04	...	1	2
79143	HD 144009	O93	7.232	0.450	0.251	0.327	< 0.02	7.232	0.450	0.251	0.327	0.06	...	1	1
79190	HD 144628	O94	7.113	0.494	0.363	0.254	< 0.02	7.113	0.494	0.363	0.254	-0.37	0.06	3	1,2,13
79242	HD 142022	O94	11.054	0.821	0.691	0.079	< 0.02	11.054	0.821	0.691	0.079	0.19	...	1	13
79242	HD 142022	O94	7.725	0.464	0.287	0.364	< 0.02	7.725	0.464	0.287	0.364	0.19	...	1	13
79537	HD 145417	O93	7.522	0.504	0.280	0.162	< 0.02	7.522	0.504	0.280	0.162	-1.13	...	1	13
79619	HD 147231	O93	7.836	0.443	0.217	0.328	< 0.02	7.836	0.443	0.217	0.328	0.00	...	1	1
79967	HD 146481	O93	7.097	0.418	0.159	0.319	< 0.02	7.097	0.418	0.159	0.319	-0.44	...	1	1
81022	HD 149143	O93	7.899	0.415	0.206	0.424	< 0.02	7.899	0.415	0.206	0.424	0.38	...	1	15
81210	HD 149750	O93	8.588	0.418	0.209	0.379	< 0.02	8.588	0.418	0.209	0.379	0.24	...	1	4
81294	BD -14 4454	O93	10.332	0.557	0.461	0.188	0.092	10.031	0.486	0.486	0.172	-0.85	...	1	8
81300	HD 149661	O93	5.766	0.491	0.366	0.297	< 0.02	5.766	0.491	0.366	0.297	0.06	0.04	5	1,7,12,9,13
81347	HD 149724	O93	7.854	0.460	0.267	0.398	0.060	7.657	0.414	0.283	0.387	0.41	...	1	1
81746	HD 150248	O93	7.026	0.418	0.202	0.323	< 0.02	7.026	0.418	0.202	0.323	-0.11	...	1	1
81767	HD 150437	O93	7.853	0.426	0.245	0.389	0.024	7.776	0.408	0.251	0.385	0.30	...	1	1
81813	HD 151541	O93	7.640	0.469	0.280	0.281	< 0.02	7.640	0.469	0.280	0.281	-0.16	0.05	2	1,9
81819	HD 150474	O93	7.162	0.477	0.261	0.364	0.034	7.050	0.451	0.270	0.358	0.05	...	1	1
81935	HD 150689	O94	7.511	0.574	0.565	0.221	< 0.02	7.511	0.574	0.565	0.221	-0.03	...	1	13
82588	HD 152391	O93	6.608	0.456	0.285	0.298	< 0.02	6.608	0.456	0.285	0.298	0.02	0.04	3	1,9,13
82636	HD 152792	O93	6.818	0.415	0.158	0.325	< 0.02	6.818	0.415	0.158	0.325	-0.31	...	1	1
83229	HD 153075	SN88	7.011	0.389	0.144	0.298	< 0.02	7.011	0.389	0.144	0.298	-0.55	...	1	1
83906	HD 154962	O93	6.353	0.440	0.235	0.409	0.048	6.195	0.403	0.248	0.401	0.32	0.03	2	1,15
83990	HD 154577	O94	7.385	0.510	0.391	0.224	< 0.02	7.385	0.510	0.391	0.224	-0.66	0.06	2	1,13
84489	HD 155974	SN88	6.094	0.321	0.143	0.407	< 0.02	6.094	0.321	0.143	0.407	-0.17	...	1	1
84636	HD 156365	O93	6.603	0.418	0.230	0.406	0.051	6.436	0.379	0.244	0.397	0.28	0.03	2	1,15
84801	HD 156826	O93	6.316	0.519	0.296	0.327	0.079	6.056	0.458	0.317	0.313	-0.13	...	1	1
84905	HD 157089	SN88	6.961	0.379	0.139	0.326	0.023	6.886	0.361	0.145	0.322	-0.57	...	1	9
84988	HD 155918	SN88	7.012	0.389	0.145	0.271	< 0.02	7.012	0.389	0.145	0.271	-0.64	...	1	1
85017	HD 157172	O93	7.848	0.466	0.298	0.350	0.028	7.756	0.444	0.306	0.345	0.17	...	1	1
85042	HD 157347	O93	6.293	0.426	0.221	0.349	0.025	6.213	0.407	0.228	0.345	0.08	0.10	2	1,4
85235	HD 158633	O93	6.429	0.466	0.271	0.240	< 0.02	6.429	0.466	0.271	0.240	-0.43	0.06	3	1,12,9
85653	HD 159062	O93	7.215	0.458	0.258	0.238	< 0.02	7.215	0.458	0.258	0.238	-0.36	...	1	9
85969	HD 158783	O93	7.096	0.424	0.209	0.366	< 0.02	7.096	0.424	0.209	0.366	0.13	...	1	

87089	HD 161848	O93	8.900	0.493	0.326	0.285	< 0.024	8.821	0.474	0.333	0.281	-0.39	...	1	1
87116	HD 161612	O93	7.186	0.447	0.246	0.375	< 0.02	7.186	0.447	0.246	0.375	0.14	...	1	1
87330	HD 162020	O94	9.084	0.579	0.534	0.244	< 0.02	9.084	0.579	0.534	0.244	0.06	0.08	3	1,6,10
87710	HD 163153	O93	6.923	0.478	0.281	0.411	0.058	6.732	0.433	0.297	0.401	0.49	...	1	1
88194	HD 164595	O93	7.070	0.411	0.199	0.314	< 0.02	7.070	0.411	0.199	0.314	-0.04	0.05	2	1,11
88217	HD 164507	O93	6.284	0.463	0.230	0.402	< 0.02	6.284	0.463	0.230	0.402	0.19	...	1	1
88348	HD 164922	O93	6.997	0.487	0.307	0.394	< 0.02	6.997	0.487	0.307	0.394	0.16	0.02	2	1,9
88511	HD 165173	O93	7.958	0.459	0.267	0.345	< 0.02	7.958	0.459	0.267	0.345	0.03	...	1	9
88622	HD 165401	SN88	6.804	0.392	0.163	0.293	< 0.02	6.804	0.392	0.163	0.293	-0.38	...	1	9
89215	BD +5 3640	SN88	10.348	0.474	0.261	0.141	0.020	10.282	0.458	0.266	0.137	-1.18	0.08	2	1,8
89844	HD 168443	O93	6.924	0.455	0.233	0.377	< 0.02	6.924	0.455	0.233	0.377	0.08	0.01	2	1,10
89855	HD 168060	O93	7.337	0.463	0.267	0.396	< 0.02	7.337	0.463	0.267	0.396	0.28	...	1	1
90004	HD 168746	O93	7.948	0.442	0.210	0.348	< 0.02	7.948	0.442	0.210	0.348	-0.08	0.01	3	1,6,10
90355	HD 169822	O93	7.832	0.437	0.224	0.294	< 0.02	7.832	0.437	0.224	0.294	-0.12	...	1	1
90593	HD 170469	O93	8.210	0.425	0.243	0.375	< 0.02	8.210	0.425	0.243	0.375	0.30	...	1	1
90656	HD 170493	O93	8.011	0.616	0.679	0.180	< 0.02	8.011	0.616	0.679	0.180	0.28	0.14	2	1,13
90864	HD 171067	O93	7.200	0.424	0.234	0.309	< 0.02	7.200	0.424	0.234	0.309	-0.03	...	1	1
91360	HD 171999	O93	8.331	0.495	0.370	0.315	0.028	8.238	0.473	0.378	0.310	0.39	...	1	3
91381	HD 172310	O93	8.413	0.441	0.227	0.245	< 0.02	8.413	0.441	0.227	0.245	-0.42	...	1	1
91438	HD 172051	O93	5.852	0.418	0.216	0.277	< 0.02	5.852	0.418	0.216	0.277	-0.24	0.05	3	1,12,13
91700	HD 172513	O93	7.941	0.446	0.252	0.319	< 0.02	7.941	0.446	0.252	0.319	-0.01	...	1	1
92283	HD 174080	O93	7.923	0.607	0.632	0.199	< 0.02	7.923	0.607	0.632	0.199	0.22	...	1	1
92918	HD 175518	O93	7.455	0.468	0.292	0.369	< 0.02	7.455	0.468	0.292	0.369	0.28	0.01	2	1,3
93007	HD 176841	O93	7.636	0.408	0.228	0.381	< 0.02	7.636	0.408	0.228	0.381	0.30	...	1	9
93341	HD 230409	O93	10.104	0.440	0.201	0.208	0.034	9.993	0.414	0.210	0.202	-0.86	...	1	1
93518	HD 176982	O93	8.364	0.463	0.224	0.348	0.053	8.189	0.422	0.238	0.339	-0.10	...	1	1
93858	HD 177565	O93	6.148	0.437	0.248	0.336	0.021	6.080	0.421	0.254	0.332	0.10	0.03	3	1,2, 13
93871	HD 178126	SN88	9.194	0.621	0.587	0.202	< 0.02	9.194	0.621	0.587	0.202	-0.88	...	1	14
94075	HD 178911	O93	8.038	0.461	0.288	0.341	< 0.02	8.038	0.461	0.288	0.341	0.28	...	1	1
	HD 180890	O93	8.349	0.451	0.281	0.331	< 0.02	8.349	0.451	0.281	0.331	0.17	...	1	3
94981	HD 181655	O93	6.291	0.420	0.234	0.322	< 0.02	6.291	0.420	0.234	0.322	0.06	...	1	1
95319	HD 182488	O93	6.362	0.480	0.340	0.331	< 0.02	6.362	0.480	0.340	0.331	0.19	0.05	2	1,9
95821	HD 183650	O93	6.946	0.457	0.251	0.398	< 0.02	6.946	0.457	0.251	0.398	0.31	...	1	1
96085	HD 183870	O93	7.517	0.529	0.448	0.266	< 0.02	7.517	0.529	0.448	0.266	0.05	...	1	1
96124	HD 183877	SN88	7.151	0.424	0.222	0.310	< 0.02	7.151	0.424	0.222	0.310	-0.20	...	1	1
96183	HD 184385	O93	6.899	0.454	0.275	0.319	< 0.02	6.899	0.454	0.275	0.319	0.15	...	1	1
96185	HD 184499	SN88	6.637	0.389	0.144	0.315	< 0.02	6.637	0.389	0.144	0.315	-0.66	...	1	9
97219	HD 187055	O93	9.002	0.488	0.389	0.281	< 0.02	9.002	0.488	0.389	0.281	0.15	...	1	3
97420	HD 187237	O93	6.877	0.409	0.205	0.323	< 0.02	6.877	0.409	0.205	0.323	0.07	...	1	1
97769	HD 188015	O93	8.235	0.439	0.266	0.360	< 0.02	8.235	0.439	0.266	0.360	0.28	0.01	2	1,13
98020	HD 188510	O93	8.830	0.417	0.113	0.128	< 0.02	8.830	0.417	0.113	0.128	-1.64	...	1	1
98066	HD 188376	O93	4.700	0.458	0.258	0.359	< 0.02	4.700	0.458	0.258	0.359	0.10	...	1	7
98192	HD 189087	O93	7.886	0.483	0.319	0.298	< 0.02	7.886	0.483	0.319	0.298	-0.04	...	1	9
98505	HD 189733	O93	7.665	0.527	0.442	0.272	< 0.02	7.665	0.527	0.442	0.272	-0.02	...	1	15
98677	HD 190067	O93	7.146	0.452	0.233	0.287	< 0.02	7.146	0.452	0.233	0.287	-0.37	...	1	1
98714	HD 190228	O93	7.311	0.482	0.264	0.306	0.028	7.219	0.460	0.272	0.301	-0.18	0.13	4	1,7,6,10
98767	HD 190360	O93	5.742	0.461	0.275	0.372	< 0.02	5.742	0.461	0.275	0.372	0.22	0.05	3	1,9,10
98921	HD 190771	O93	6.172	0.413	0.222	0.336	< 0.02	6.172	0.413	0.222	0.336	0.17	...	1	1
98959	HD 189567	SN88	6.080	0.407	0.190	0.302	< 0.02	6.080	0.407	0.190	0.302	-0.26	0.05	3	1,6,10
	HD 192020	O93	7.961	0.500	0.393	0.280	0.054	7.783	0.458	0.408	0.270	0.01	...	1	1
99711	HD 192263	O84	7.769	0.541	0.493	0.275	< 0.02	7.769	0.541	0.493	0.275	0.04	0.01	2	1,10
99729	HD 192344	O93	7.721	0.441	0.235	0.404	0.020	7.655	0.425	0.240	0.400	0.30	...	1	1
100500	HD 194035	O93	7.134	0.450	0.229	0.389	< 0.02	7.134	0.450	0.229	0.389	0.27	...	1	1
100568	HD 193901	SN88	8.660	0.383	0.099	0.221	< 0.02	8.660	0.383	0.099	0.221	-1.23	...	1	1
100792	HD 194598	SN88	8.354	0.344	0.091	0.269	< 0.02	8.354	0.344	0.091	0.269	-1.33	...	1	9
101597	HD 196201	O93	8.495	0.456	0.256	0.296	< 0.02	8.495	0.456	0.256	0.296	-0.14	...	1	1
101997	HD 196761	O93	6.376	0.440	0.251	0.269	< 0.02	6.376	0.440	0.251	0.269	-0.27	0.10	4	1,12,6,10
102018	HD 196800	SN88	7.210	0.388	0.196	0.380	< 0.02	7.210	0.388	0.196	0.380	0.16	...	1	1
103077	HD 198802	O93	6.395	0.416	0.196	0.381	< 0.02	6.395	0.416	0.196	0.381	0.04	...	1	1
103096	HD 199305	O93	8.554	0.911	0.518	0.201	< 0.02	8.554	0.911	0.518	0.201	-0.28	...	1	14
103458	HD 199288	SN88	6.523	0.386	0.143	0.269	< 0.02	6.523	0.386	0.143	0.269	-0.63	...	1	1
103654	HD 199190	SN88	6.872	0.397	0.202	0.383	< 0.02	6.872	0.397	0.202	0.383	0.15	...	2	1,15
104092	HD 200779	O93	8.267	0.690	0.747	0.115	< 0.02	8.267	0.690	0.747	0.115	0.02	...	1	12
104318	HD 201219	O93	8.013	0.444	0.256	0.331	< 0.02	8.013	0.444	0.256	0.331	0.15	...	1	1
104436	HD 199509	O94	6.988	0.396	0.179	0.265	< 0.02	6.988	0.396	0.179	0.265	-0.31	...	1	1
104659	HD 201891	SN88	7.386	0.363	0.094	0.261	< 0.02	7.386	0.363	0.094	0.261	-1.10	0.05	3	1,4,9
104809	HD 201989	O93	7.385	0.430	0.237	0.320	< 0.02	7.385	0.430	0.237	0.320	0.12	...	1	1
104903	HD 202206	O93	7.920	0.437	0.249	0.388	< 0.02	7.920	0.437	0.249	0.388	0.34	0.02	3	1,6,10
105038	HD 202575	O93	7.896	0.579	0.568	0.206	< 0.02	7.896	0.579	0.568	0.206	0.04	...	1	1
105152	HD 202751	O93	8.159	0.563	0.540	0.262	< 0.02	8.159	0.563	0.540	0.262	-0.10	...	1	1
105388	HD 202917	O93	8.597	0.435	0.234	0.299	< 0.02	8.597	0.435	0.234	0.299	0.11	...	1	1
106696	HD 205390	O94	7.144	0.514	0.401	0.263	< 0.02	7.144	0.514	0.401	0.263	-0.17	...	1	1
107022	HD 205536	O93	7.057	0.462	0.279	0.318	< 0.02	7.057	0.462	0.279	0.318	-0.03	...	1	1
107070	HD 206374	O93	7.445	0.430	0.245	0.289	< 0.02	7.445	0.430	0.245	0.289	-0.05	...	1	1
108158	HD 207700	SN88	7.437	0.434	0.225	0.368	< 0.02	7.437	0.434	0.225	0.368	0.04	...	1	1
108736	HD 208998	SN88	7.133	0.371	0.149	0.338	< 0.02	7.133	0.371	0.149	0.338	-0.32	...	1	1
108774	HD 209393	O93	7.970	0.417	0.234	0.262	< 0.02	7.970	0.417	0.234	0.262	-0.17	...	1	1
108870	HD 209100	O93	4.682	0.588	0.605	0.202	< 0.02	4.682	0.588	0.605	0.202	0.04	...	2	6,10
109144	HD 209875	SN88	7.244	0.353	0.152	0.393	< 0.02	7.244	0.353	0.152	0.393	-0.11	...	1	1
109169															

110843	HD 212708	O93	7.494	0.451	0.262	0.373	< 0.02	7.494	0.451	0.262	0.373	0.28	0.02	2	1,15
110996	HD 213042	O93	7.621	0.619	0.666	0.183	< 0.02	7.621	0.619	0.666	0.183	0.20	...	1	5
111148	HD 213519	O93	7.702	0.416	0.175	0.338	< 0.02	7.702	0.416	0.175	0.338	0.00	...	1	1
111978	HD 214759	O94	7.415	0.476	0.328	0.331	< 0.02	7.415	0.476	0.328	0.331	0.22	0.10	3	1,2, 15
112229	HD 215257	SN88	7.410	0.357	0.116	0.310	< 0.02	7.410	0.357	0.116	0.310	-0.66	...	1	4
113137	HD 216437	O93	6.056	0.422	0.215	0.394	< 0.02	6.056	0.422	0.215	0.394	0.22	...	1	1
113283	HD 216803	O93	6.450	0.622	0.630	0.177	< 0.02	6.450	0.622	0.630	0.177	0.09	0.01	2	6,10
113421	HD 217107	O93	6.175	0.455	0.295	0.374	< 0.02	6.175	0.455	0.295	0.374	0.38	0.03	4	1,7,6,10
113948	HD 217958	O93	8.041	0.416	0.215	0.408	< 0.02	8.041	0.416	0.215	0.408	0.31	...	1	1
114622	HD 219134	O93	5.545	0.571	0.552	0.268	< 0.02	5.545	0.571	0.552	0.268	0.11	0.23	4	1,7,12,9
114699	HD 219077	O94	6.131	0.478	0.255	0.350	< 0.02	6.131	0.478	0.255	0.350	-0.12	...	1	1
115087	HD 219709	O94	7.502	0.399	0.197	0.326	< 0.02	7.502	0.399	0.197	0.326	-0.01	...	1	2
115445	HD 220339	O93	7.793	0.510	0.416	0.253	< 0.02	7.793	0.510	0.416	0.253	-0.31	...	1	1
116085	HD 221354	SN88	6.750	0.500	0.362	0.342	< 0.02	6.750	0.500	0.362	0.342	0.01	...	1	1
116250	HD 221420	O94	5.818	0.427	0.225	0.441	< 0.02	5.818	0.427	0.225	0.441	0.34	0.01	2	1,15
116421	HD 221830	SN88	6.862	0.397	0.159	0.327	< 0.02	6.862	0.397	0.159	0.327	-0.40	...	1	1
116745	HD 222237	O94	7.068	0.561	0.523	0.239	< 0.02	7.068	0.561	0.523	0.239	-0.24	0.08	3	1,6,10
116763	HD 222335	O94	7.185	0.477	0.327	0.282	< 0.02	7.185	0.477	0.327	0.282	-0.14	0.05	3	1,6,10
116852	HD 222480	O93	7.117	0.423	0.197	0.407	< 0.02	7.117	0.423	0.197	0.407	0.18	0.01	2	1,15
116984	HD 222697	O93	8.675	0.473	0.290	0.371	< 0.02	8.675	0.473	0.290	0.371	0.16	...	1	1
117159	BD +28 4634	SN88	8.382	0.504	0.381	0.290	< 0.02	8.382	0.504	0.381	0.290	-0.04	...	1	8
117320	HD 223171	SN88	6.888	0.414	0.203	0.382	< 0.02	6.888	0.414	0.203	0.382	0.12	...	2	1,15
117427	HD 223315	O93	8.763	0.452	0.263	0.397	< 0.02	8.763	0.452	0.263	0.397	0.30	...	1	1
117526	HD 223498	O93	8.336	0.456	0.272	0.366	< 0.02	8.336	0.456	0.272	0.366	0.23	...	1	1
117668	HD 223691	O93	7.867	0.445	0.228	0.325	< 0.02	7.867	0.445	0.228	0.325	-0.17	...	1	1
117953	HD 224156	O93	7.750	0.458	0.267	0.326	< 0.02	7.750	0.458	0.267	0.326	-0.03	...	1	1
118115	HD 224383	SN88	7.896	0.403	0.200	0.341	< 0.02	7.896	0.403	0.200	0.341	-0.04	...	1	1
	PLX 1219	SN88	11.515	0.522	0.293	0.144	< 0.02	11.515	0.522	0.293	0.144	-1.67	...	1	8



Metal poor regions:

1. SL-BHB
2. BHB
3. HB
4. RHB-AGB
5. BS
6. BS-TO
7. Turn-off
8. Main sequen
9. Sub-giants
10. Red giants
11. SL